

**For Reference**

---

**NOT TO BE TAKEN FROM THIS ROOM**



For Reference

NOT TO BE TAKEN FROM THIS ROOM

Ex LIBRIS  
UNIVERSITATIS  
ALBERTAENSIS





Digitized by the Internet Archive  
in 2019 with funding from  
University of Alberta Libraries

<https://archive.org/details/Johnson1964>











Thesis  
1964  
#14D

THE UNIVERSITY OF ALBERTA

STRESS CORROSION CRACKING OF ALPHA BRASS

A Thesis

Submitted to the Faculty of Graduate Studies  
In Partial Fulfilment of the Requirements  
for the Degree of Doctor of Philosophy

DEPARTMENT OF MINING AND METALLURGY

by

HARLAND EUCLID JOHNSON

EDMONTON, ALBERTA

FEBRUARY, 1964





THE UNIVERSITY OF ALBERTA  
FACULTY OF GRADUATE STUDIES

The undersigned certify that they have read and recommend to  
the Faculty of Graduate Studies for acceptance, a thesis titled

STRESS CORROSION CRACKING OF ALPHA BRASS

submitted by HARLAND EUCLID JOHNSON

in partial fulfilment of the requirements for the degree of Doctor of  
Philosophy.





## ABSTRACT

Studies of the stress corrosion cracking of alpha brass were undertaken in order to determine the reason for the apparent specificity of ammonia as the agent responsible for cracking failures. No cracking was found to occur in stressed wire samples exposed to controlled dry gaseous atmospheres of  $\text{NH}_3$  alone, and in combination with  $\text{O}_2$ ,  $\text{CO}_2$ , or air; or in  $\text{NH}_3$  saturated with water vapor at room temperature in combination with  $\text{O}_2$  or air.

The black tarnish formed as a byproduct during the stress corrosion cracking of brass in copper-ammonia solutions was definitely identified as  $\text{Cu}_2\text{O}$  by X-ray diffraction and polarographic analysis.

Spectrophotometric and polarographic studies on aqueous ammonia solutions in the pH range 5.0 - 8.0 showed that intergranular stress corrosion cracking of brass could be correlated with  $\bar{n}$ , the average number of ammonia ligands per copper ion originally present in solution as the divalent copper(II)-ammine complex,  $\text{Cu}(\text{NH}_3)_n^{++}$ ; the most rapid cracking occurred when  $\bar{n}$  was 1.5 - 3.0; the cracking time increased exponentially with decreasing initial concentration of  $\text{Cu}(\text{NH}_3)_n^{++}$ . The temperature dependence (15 - 65°C) of the cracking time was not of the Arrhenius type.

It was also shown that cracking could take place in other complexing reagents not containing ammonia, viz., citrate and tartrate solutions.





A surface energy mechanism for the intergranular stress corrosion cracking of brass has been proposed. Surface energy lowering is attributed to the adsorption of the copper(I)-diammine complex which is formed by reduction of the copper(II) complexes initially present in solution; the reduction is facilitated by the simultaneous oxidation of zinc especially at grain boundaries; the oxidized zinc ions are replaced by copper(I)-diammine complexes.

A literature survey of stress corrosion cracking in all alloys systems (with an emphasis on brass) is included.





## ACKNOWLEDGMENTS

Studying under the direction of Dr. Jan Leja has been a rewarding experience; I am glad to have this opportunity to acknowledge the guidance and friendship he has given me during the course of the work leading up to this thesis.

I would like to extend my thanks to the other staff members of this department for the helpful interest they have shown.

The assistance of Miss M. Schwerman and Mr. J. Wojno in preparing the manuscript has been appreciated.

The receipt of three scholarships from the National Research Council of Canada is gratefully acknowledged.



## TABLE OF CONTENTS

|  | Page |
|--|------|
| INTRODUCTION   | 1    |
| REVIEW OF STRESS CORROSION CRACKING                  | 8    |
| 1. STRESS  | 8    |
| 2. COMPOSITION OF MATERIAL                           | 12   |
| A. Ferrous Alloys                                    | 12   |
| B. Copper Base Alloys                                | 16   |
| C. Magnesium Alloys                                  | 21   |
| D. Aluminum Alloys                                   | 22   |
| E. Miscellaneous Alloys                              | 25   |
| 3. CHEMICAL ENVIRONMENT                              | 26   |
| A. Ferrous Alloys                                    | 27   |
| B. Copper Base Alloys                                | 32   |
| C. Aluminum and Magnesium Alloys                     | 36   |
| 4. METALLURGICAL FACTORS                             | 39   |
| A. Heat Treatment and Plastic Deformation            | 39   |
| B. Crystallographic Orientation                      | 42   |
| 5. ELECTROCHEMICAL ASPECTS                           | 43   |
| 6. MISCELLANEOUS FACTORS                             | 48   |
| A. Temperature                                       | 48   |
| B. Topography  | 50   |
| C. Wedging Action of Corrosion Products              | 51   |
| 7. STRESS CORROSION CRACKING MECHANISMS              | 52   |
| SURFACE ENERGY CONCEPTS IN STRESS CORROSION CRACKING | 57   |





|   |     |
|---|-----|
| EXPERIMENTAL METHODS  | 62  |
| 1. MATERIALS  | 62  |
| 2. EXPERIMENTS WITH WIRE SPECIMENS                                | 63  |
| A. Vacuum System 'A'  | 63  |
| B. Reaction Vessel Design   | 66  |
| C. Loading Device   | 72  |
| D. Procedure  | 72  |
| 3. EXPERIMENTS WITH STRIP SPECIMENS                               | 73  |
| A. Vacuum System 'B'  | 73  |
| B. Reaction Vessel  | 75  |
| C. Procedure for Experiments in Vacuum System 'B'                 | 77  |
| D. Procedure for Reactions in Aqueous Solutions                   | 79  |
| 4. ANALYTICAL TECHNIQUES  | 80  |
| A. Polarography   | 80  |
| B. Spectrophotometry  | 84  |
| C. X-ray Diffraction  | 84  |
| RESULTS AND DISCUSSION  | 86  |
| 1. PRELIMINARY EXPERIMENTS WITH WIRE SPECIMENS                    | 86  |
| 2. EXPERIMENTS WITH STRIP SPECIMENS                               | 88  |
| A. Effect of Gaseous Environments                                 | 88  |
| B. Composition of Tarnish   | 93  |
| C. Effect of pH   | 94  |
| D. Effect of Initial Complex Concentration                        | 105 |
| E. Effect of Temperature  | 108 |
| F. Other Cracking Media   | 113 |
| 3. GENERAL DISCUSSION   | 115 |
| SUMMARY AND CONCLUSIONS   | 139 |
| BIBLIOGRAPHY  | 142 |
| APPENDIX A - Description of Major Vacuum System Components        | 156 |
| APPENDIX B - Calculation of $\bar{n}$ , the Average Ligand Number | 157 |
| APPENDIX C - Construction of pH/Potential Diagrams                | 159 |



## LIST OF TABLES

|           |   | Page |
|-----------|---|------|
| Table I   | List of observed stress corrosion cracking failures     | 5    |
| Table II  | Spectroscopic analysis of brass                         | 62   |
| Table III | Effect of gaseous environments on cracking times        | 90   |
| Table IV  | Effect of pH on cracking time                           | 100  |
| Table VI  | Effect of initial copper concentration on cracking time | 107  |
| Table VII | Constants used in pH/potential equations                | 161  |

## LIST OF FIGURES

|         |  |    |
|---------|--|----|
| Fig. 1  | Cu-Zn alloys --- effect of zinc content on cracking time   | 17 |
| Fig. 2  | Cu alloys --- effect of P, As, Sb, Si, Al, Ni content on cracking time   | 18 |
| Fig. 3  | Effect of pH on cracking time and type of cracking   | 35 |
| Fig. 4  | Schematic diagram of vacuum system 'A'   | 65 |
| Fig. 5  | Reaction vessel with seal modification I   | 67 |
| Fig. 6  | Details of seal modifications II and III   | 68 |
| Fig. 7  | a) Reaction vessel in operation using seal modification I<br>b) Vacuum system 'B'<br>c) General view of basic pumping system | 70 |
| Fig. 8  | Schematic diagram of vacuum system 'B'   | 74 |
| Fig. 9  | Details of reaction chamber  | 76 |
| Fig. 10 | Stressed brass strip specimens in: a) 'normal' position<br>b) 'inverted' position  | 77 |





|         |   | Page |
|---------|---|------|
| Fig. 11 | Typical polarogram of standard brass solution   | 83   |
| Fig. 12 | Absorbance (at $\lambda = 630 \text{ m}\mu$ ) vs. copper concentration  | 85   |
| Fig. 13 | Absorption spectra of copper(II)-ammine complexes   | 85   |
| Fig. 14 | Cracking time vs. pH and the average number of complex-bound $\text{NH}_3$ groups per Cu atom                                   | 95   |
| Fig. 15 | Absorption peaks of the copper(II)-ammine complexes   | 99   |
| Fig. 16 | Photomicrographs of brass failures in copper-ammonia solutions; a) pH 5.0, b) pH 6.0-7.5, c) pH 8.0                             | 103  |
| Fig. 17 | Photomicrograph of brass failure at pH 7.1  | 104  |
| Fig. 18 | Photomicrograph of tarnish penetration into brass   | 104  |
| Fig. 19 | Effect of initial copper concentration on cracking time   | 106  |
| Fig. 20 | Effect of temperature on cracking time  | 109  |
| Fig. 21 | Log rate ( $\log 1/t_c$ ) vs. $1/T$ , and rate ( $1/t_c$ ) vs. $1/T$ for cracking of brass in copper-ammonia solutions, pH 7.1  | 111  |
| Fig. 22 | Log rate ( $\log 1/t_c$ ) vs. $1/T$ , and rate ( $1/t_c$ ) vs. $1/T$ for cracking of brass in copper-ammonia solutions, pH 6.80 | 112  |
| Fig. 23 | Photomicrograph of brass failure in copper-citrate solution   | 114  |
| Fig. 24 | Photomicrographs of brass failures in copper-tartrate solutions; a) pH 13.0, b) pH 13.5   | 114  |
| Fig. 25 | pH/potential diagrams for the homogeneous system $\text{Cu-NH}_3\text{-H}_2\text{O}$  | 119  |
| Fig. 26 | pH/potential diagrams for the heterogeneous system $\text{Cu-NH}_3\text{-H}_2\text{O}$  | 120  |
| Fig. 27 | pH/potential diagrams for the heterogeneous system $\text{Zn-NH}_3\text{-H}_2\text{O}$  | 122  |
| Fig. 28 | Effect of initial copper concentration on cracking time   | 131  |



## INTRODUCTION

Of the many phenomena that cause the deterioration or destruction of engineering materials, one of the most intriguing is stress corrosion cracking, the rapid, often catastrophic failure of metals or alloys under the influence of a unique combination of tensile stress and chemical environment. The practical aspects of this problem have caused concern for many years, and although the incidence of stress corrosion fracture is not high, the severity of individual failures has made its prevention a prime objective in those industries using susceptible materials.

Apart from the obvious practical problems of stress corrosion cracking, its study is of fundamental interest since it involves a unique interplay of surface chemistry, electrochemistry and metallurgy. None of the many investigations that have been carried out in these various disciplines has led to a theory or mechanism which would successfully encompass all known forms of stress corrosion cracking, and indeed, it may well be that no single theory can accomplish this feat. However, there are some common features in all of the known stress corrosion cracking systems, and many of these have been studied in detail. One facet of the problem has not received much attention: the specific nature of the chemical species causing cracking (with the possibility of specific adsorption leading to reduction of the surface free energy of the solid

# THE UNIVERSITY OF CHICAGO

THE UNIVERSITY OF CHICAGO LIBRARY

1100 EAST 58TH STREET, CHICAGO, ILL. 60637

TEL: 773-936-5000 FAX: 773-936-5001

WWW.CHICAGO.LIBRARY.EDU

CHICAGO LIBRARY

CHICAGO LIBRARY

CHICAGO LIBRARY

CHICAGO LIBRARY

CHICAGO LIBRARY

CHICAGO LIBRARY

CHICAGO LIBRARY

CHICAGO LIBRARY

CHICAGO LIBRARY

CHICAGO LIBRARY

CHICAGO LIBRARY

CHICAGO LIBRARY

CHICAGO LIBRARY

CHICAGO LIBRARY

CHICAGO LIBRARY

CHICAGO LIBRARY



surface) has, with the exception of a few recent instances, received only passing mention. The purpose of the present work was, in general, to shed some light on the mechanism of stress corrosion cracking through the specific study of the chemical reactions at the surface of alpha brass during stress corrosion cracking.

Historically, the 'season cracking' of various forms of brass and bronze has always been a problem in the brass industry, but the first literature specifically devoted to this type of failure appeared in the early part of this century,<sup>(1)(2)(3)</sup> especially following a series of failures of brass bolts, cartridge cases, and condenser tubes.<sup>(4-9)</sup> These failures prompted a "Topical Discussion on Season and Corrosion Cracking of Brass" sponsored by the A.S.T.M.<sup>(10)</sup> In 1944, the A.S.T.M. and A.I.M.E. co-sponsored a symposium on stress corrosion cracking, and for the first time a considerable amount of time was devoted to the failures of other than copper-base alloys.<sup>(11)</sup> The widespread interest in the newer alloys, many of which were developed as war materials, gave further impetus to stress corrosion research, with more and more emphasis being given to the mechanisms of the process. These studies culminated in two other symposia, the first arranged by the Electrochemical Society in 1954,<sup>(12)</sup> and the second by the A.I.M.E. in 1959.<sup>(13)</sup> More recently, stress corrosion cracking has been given special consideration at several international corrosion conferences.<sup>(14)(15)(16)</sup>



Apart from the proceedings of the various symposia, several other publications serve as valuable references: Waber and McDonald's "Stress Corrosion Cracking of Mild Steel";<sup>(17)</sup> the A.S.T.M. special report on stress corrosion cracking of austenitic chromium-nickel stainless steels,<sup>(18)</sup> four recent Russian texts,<sup>(19-22)</sup> one of which<sup>(22)</sup> gives a good survey of the whole field of stress corrosion cracking; Bailey's excellent review on the stress cracking of brass;<sup>(23)</sup> and Rask's bibliography of stress corrosion in copper and copper alloys,<sup>(166)</sup> which alone contains over six hundred references.

Before considering some of the known facts about stress corrosion cracking, it is necessary to define the scope of the problem. We are considering here the unexpected or sudden failure of a metal or alloy that is subjected to a static tensile stress, and is in the presence of a unique chemical environment. This definition excludes such problems as corrosion fatigue, fire cracking, and creep at elevated temperatures. It also does not include embrittlement by liquid metals, although certain similarities between liquid metal embrittlement and stress corrosion cracking will be pointed out later. The type of failure which is generally known as hydrogen embrittlement will also be excluded arbitrarily from the discussions, although some reference will be made to the failure of steels in aqueous sulfide media, since this appears to be a borderline example of stress corrosion cracking.



It should also be noted that although this review of stress corrosion cracking will emphasize failures of brass, an attempt will be made to include significant work in the many other alloy systems in which stress corrosion cracking has been observed. Table I, part of which first appeared in the classic paper of Mears, Brown and Dix<sup>(24)</sup> shows the ubiquity of the problem, although many of the failures listed can be prevented by slightly altering the composition ranges or thermal treatment of the alloy. Thus, the appearance of a particular combination of alloy and environment in Table I does not necessarily mean that the combination is contraindicated in practice; rather, the list should be regarded as a survey of the attempts of investigators to more clearly delineate the worst possible conditions that can cause stress corrosion cracking.

The fact that stress corrosion cracking has always had a deleterious effect on materials seems to have led most people to overlook the possibility that this phenomenon may eventually be put to constructive use. Rostoker et al.<sup>(163)</sup> have made some imaginative suggestions for uses of liquid metal embrittlement which could also be applied to aqueous stress cracking systems; it is also conceivable that if the reduction of surface energy by specific adsorption plays an important role in stress cracking systems, one could devise more effective methods for estimating the surface energy of solids. Wherever industrial applications require the fracture of a solid (e.g., in the impact drilling of hard geological formation) any chemical environment that would promote cracking would be extremely useful.





Table I

## A List of Observed Stress Corrosion Cracking Systems

| <u>Alloy</u>                           | <u>Environment</u>  | <u>Reference</u> |
|--|---|------------------|
| <u>Aluminum Base</u>                   |   |                  |
| Al-Zn                                  | Air   | 25               |
| Al-Mg                                  | NaCl + H <sub>2</sub> O <sub>2</sub> , NaCl solutions; air  | 26               |
| Al-Mg                                  | } Sea water   | 27               |
| Al-Cu-Mg                               |   |                  |
| Al-Mg-Zn                               |   |                  |
| Al-Zn-Cu                               | NaCl, NaCl + H <sub>2</sub> O <sub>2</sub> solutions  | 26               |
| Al-Zn-Mg-Mn                            | } Sea water   | 28               |
| Al-Zn-Mg-Cu-Mn                         |   |                  |
| Al-Cu-Mg-Mn                            | NaCl + H <sub>2</sub> O <sub>2</sub> solution   | 24               |
| Al-Cu                                  | NaCl + H <sub>2</sub> O <sub>2</sub> solution   | 29               |
| Al-Cu                                  | } NaCl, NaCl + NaHCO <sub>3</sub> , KCl, MgCl <sub>2</sub> ,<br>CaCl <sub>2</sub> , NH <sub>4</sub> Cl, CoCl <sub>2</sub> solutions | 66               |
| Al-Mg                                  |   |                  |
| <u>Magnesium Base</u>                  |   |                  |
| Mg-Al                                  | a) HNO <sub>3</sub> , NaOH, HF solutions  | 31               |
|  | b) Distilled water  | 65               |
| Mg-Al-Zn-Mn                            | a) NaCl + H <sub>2</sub> O <sub>2</sub> solution  | 24               |
|  | b) Coastal atmos.; NaCl + K <sub>2</sub> CrO <sub>4</sub> solution  | 30               |
|  | c) Moist air + SO <sub>2</sub> + CO <sub>2</sub>  | 31               |
| Mg                                     | KHF <sub>2</sub> solution   | 65               |
| <u>Copper Base</u>                     |   |                  |
| Cu-Zn                                  | } NH <sub>3</sub> vapors and solutions  | 32               |
| Cu-Zn-Sn                               |   |                  |
| Cu-Zn-Pb                               |   |                  |
| Cu-Sn-P                                | Conc. NH <sub>4</sub> OH  | 33               |
| Cu-Zn                                  | Amines  | 34               |
| Cu-Zn-Ni                               | } NH <sub>3</sub> vapors and solutions  | 35               |
| Cu-Sn                                  |   |                  |
| Cu-Sn-P                                | } Air   | 36, 37           |
| Cu-As                                  |   |                  |
| Cu-P, -As, -Sb,<br>-Ni, -Al, -Si, -Zn, | } Moist NH <sub>3</sub> atmos.  | 38               |
| Cu-Si-Mn                               |   |                  |
| Cu-Zn-Si                               | Water Vapor   | 39               |
| Cu-Zn-Sn-Mn                            | Water   | 40               |



Table I (Cont'd)

| <u>Alloy</u>   | <u>Environment</u>  | <u>Reference</u> |
|--|---|------------------|
| <u>Copper Base (Cont'd)</u>  |   |                  |
| Cu-Au  | NH <sub>4</sub> OH, FeCl <sub>3</sub> , HNO <sub>3</sub> solutions  | 41               |
| Cu-Zn  | Moist SO <sub>2</sub> ; Cu(NO <sub>2</sub> ) <sub>2</sub> solutions   | 42               |
| Cu-Zn-Mn   |   |                  |
| Cu-Mn  | Moist SO <sub>2</sub> ; Cu(NO <sub>2</sub> ) <sub>2</sub> , H <sub>2</sub> SO <sub>4</sub> , HCl, HNO <sub>3</sub> solutions  | 42               |
| Cu-Zn plus minor amounts of Al, As, Be, B, Cd, Co, Au, Pb, Mn, Ni, Pd, Ag, Sr, Tl, Sn, Sb, Ba, Bi, Ca, Ce, Cr, Fe, Mg, P, Si, Te, Ti, Zr, Li, Nb, Mo, K, Se, Na, S, Ta |   |                  |
|  | Moist NH <sub>3</sub> atmos   | 42               |
| Cu-Ni-Si   | Moist NH <sub>3</sub> atmos   | 56               |
| Cu-Al-Fe   | Steam   | 64               |
| Cu-Be  | Moist NH <sub>3</sub>   | 179              |
| <u>Iron Base</u>   |   |                  |
| Mild Steel   | a) NaOH + Na <sub>2</sub> SiO <sub>3</sub>  | 43               |
|  | b) Ca(NO <sub>3</sub> ) <sub>2</sub> , NH <sub>4</sub> NO <sub>3</sub> , NaNO <sub>3</sub> solutions  | 44               |
|  | c) HCN + SnCl <sub>2</sub> + AsCl <sub>2</sub> + CHCl <sub>3</sub>  | 45               |
|  | d) Na <sub>3</sub> PO <sub>4</sub> solution   | 46               |
|  | e) Pure NaOH solution   | 47               |
|  | f) NH <sub>3</sub> + CO <sub>2</sub> + H <sub>2</sub> S + HCN   | 102              |
|  | g) NaOH, KOH solutions; Monoethanolamine solution + H <sub>2</sub> S + CO <sub>2</sub> , Fe(AlO <sub>2</sub> ) <sub>3</sub> + Al <sub>2</sub> O <sub>3</sub> + CaO solution | 48               |
|  | h) HNO <sub>3</sub> + H <sub>2</sub> SO <sub>4</sub>  | 49               |
|  | i) MgCl <sub>2</sub> + NaF solution   | 50               |
|  | j) Anhydrous liquid NH <sub>3</sub>   | 51               |
|  | k) H <sub>2</sub> S media   | 52, 53, 54       |
|  | l) FeCl <sub>3</sub> solution   | 221              |
|  | a) NH <sub>4</sub> Cl, MgCl <sub>2</sub> , (NH <sub>4</sub> )H <sub>2</sub> PO <sub>4</sub> , Na <sub>2</sub> HPO <sub>4</sub> solutions                                    | 55               |
|  | b) H <sub>2</sub> SO <sub>4</sub> + NaCl solution   | 57               |
|  | c) NaCl + H <sub>2</sub> O <sub>2</sub> solution, sea water   | 24               |
|  | d) H <sub>2</sub> S solutions   | 71, 72           |
| Fe-Cr-C  |   |                  |



Table 1 (Cont'd)

| <u>Alloy</u>                | <u>Environment</u>  | <u>Reference</u> |
|-----------------------------|---|------------------|
| <u>Iron Base (Cont'd)</u>   |   |                  |
| Fe-Ni-C                     | a) HCl + H <sub>2</sub> SO <sub>4</sub> , steam   | 58               |
|                             | b) H <sub>2</sub> S solutions   | 71, 72           |
| Fe-Cr-Ni-C                  | a) NaCl + H <sub>2</sub> O <sub>2</sub> solution, sea water   | 24               |
|                             | b) H <sub>2</sub> SO <sub>4</sub> + CuSO <sub>4</sub> solution  | 59               |
|                             | c) MgCl <sub>2</sub> , CoCl <sub>2</sub> , NaCl, BaCl <sub>2</sub> solutions  | 60               |
|                             | d) CH <sub>3</sub> CH <sub>2</sub> Cl + water   | 61               |
|                             | e) LiCl, ZnCl <sub>2</sub> , CaCl <sub>2</sub> , NH <sub>4</sub> Cl solutions   | 62               |
|                             | f) (NH <sub>4</sub> ) <sub>2</sub> CO <sub>3</sub> solutions  | 63               |
|                             | g) NaCl, NaF, NaBr, NaI, NaH <sub>2</sub> PO <sub>4</sub> ,<br>Na <sub>3</sub> PO <sub>4</sub> , Na <sub>2</sub> SO <sub>4</sub> , NaNO <sub>3</sub> , Na <sub>2</sub> SO <sub>3</sub> ,<br>NaClO <sub>3</sub> , NaC <sub>2</sub> H <sub>3</sub> O <sub>2</sub> solutions | 67               |
|                             | h) Steam + chlorides  | 69               |
|                             | i) H <sub>2</sub> S solutions   | 71, 72           |
|                             | j) NaCl + NH <sub>4</sub> NO <sub>2</sub> solution  | 70               |
|                             | NaCl + NaNO <sub>2</sub> solution   |                  |
| <u>Nickel Base</u>          |   |                  |
| Ni                          | NaOH, KOH solutions; Fused NaOH   | 73               |
| Ni-Cr-Fe                    | NaOH + sulfide solution, steam  | 73               |
| Ni-Cu                       | Fused NaOH, H <sub>2</sub> SiF <sub>6</sub> solution, chromic<br>acid, sulfonated oil, steam  | 73               |
| Ni-Cu-Al                    | HF acid vapor   | 74               |
| Ni-Cu                       |   |                  |
| Ni-Al                       |   |                  |
| Ni-Cr-Fe                    |   |                  |
| Ni-Cr-Fe-Ti                 |   |                  |
| <u>Miscellaneous Alloys</u> |   |                  |
| Au-Cu-Ag                    | FeCl <sub>2</sub> solutions   | 75               |
| Cu-Au                       | HNO <sub>3</sub> + HCl, HNO <sub>3</sub> , FeCl <sub>3</sub> , NH <sub>4</sub> OH<br>solutions  | 76               |
| Ag-Au                       | HNO <sub>3</sub> + HCl, HNO <sub>3</sub> , FeCl <sub>3</sub> solutions  | 76               |
| Ag-Pt                       | FeCl <sub>3</sub> solutions   | 77               |
| Pb                          | a) Pb (OAc) <sub>2</sub> + HNO <sub>3</sub> solutions   | 78               |
|                             | b) Air  | 79               |
| Zr                          | FeCl <sub>3</sub> solutions   | 80               |





## REVIEW OF STRESS CORROSION CRACKING

### 1. STRESS

It has already been mentioned that we are considering static stresses only, in order to exclude cyclic fatigue problems. It was also mentioned that the stresses are tensile in nature; this was not meant to limit the problem artificially, but arose from the fact that stress corrosion cracking does not occur under conditions of compression,<sup>(81)</sup> and, in fact, compressive stresses introduced by shot peening or shot blasting are used as a preventive measure.<sup>(82)</sup> Sobolev<sup>(83)</sup> has explored the nature of the stress more thoroughly; his experiments were carried out on a low carbon steel(exposed to a boiling 50%  $\text{NH}_4\text{NO}_3$  solution) under the influence of uni-axial tension, uni-axial compression, or torsion. No cracking was observed in the compression tests. The plane of failure in the torsion specimens was inclined at  $45^\circ$  to the axis of the specimen, in agreement with earlier conclusions<sup>(81)</sup> that the failure occurs normal to the plane of maximum tensile stress. Similar torsion results have been reported by Zhukov<sup>(84)</sup> for the cracking of brass in ammonia vapor.

It has long been recognized that the tensile stress need not be externally applied; as early as 1914, Heyn<sup>(3)</sup> showed that cold-worked brass retained a considerable amount of internal stress which could cause cracking if the metal were exposed to the proper environment. Besides mechanical working, internal or 'locked-up' stresses can result from



thermal processes such as welding, quenching and shrink fits, and it is not surprising that a great deal of attention was given to the nature and measurement of these internal stresses,<sup>(85)(86)</sup> since it is of great practical importance to anticipate these stresses and either over-design the material, or perform some thermal stress relieving treatment, if stress corrosion cracking is likely to be a problem.

Although an increase in the magnitude of the stress (applied or residual) leads to a more rapid failure, there is still a great deal of contention as to whether or not there exists a 'threshold' stress below which an alloy will not fail within a long period of time. Evidence pointing to the existence of a threshold stress has been obtained for magnesium alloys exposed to NaCl-K<sub>2</sub>CrO<sub>4</sub> solution,<sup>(30)</sup> brass in ammonia,<sup>(32)(87)</sup> magnesium-aluminum alloys in sea water,<sup>(88)</sup> aluminum alloys in sea water,<sup>(89)</sup> mild steel in boiling NH<sub>4</sub>NO<sub>3</sub>,<sup>(83)</sup> and iron-chromium alloys in fresh water.<sup>(98)</sup> On the other hand, for 18Cr-8Ni stainless steels exposed to boiling MgCl<sub>2</sub>, no well defined threshold stress has been established,<sup>(91)(92)(108)</sup> but it has been fairly well established that the relation between log failure time and applied stress can be represented by two straight lines which intersect at about 0.1% of the proof stress of the material.<sup>(204)(234)</sup> In general, it has been found that even when a threshold value could be determined it was very sensitive to the metallurgical history of the specimen, and thus was only of limited value in predicting an operating stress below which a material could be safely used.



Of more fundamental interest is the general influence of stress on the corrosion process at the surface of a metal or alloy. It is generally recognized that a strained metal corrodes more rapidly than an unstrained one (a few apparent exceptions to this rule are explained by Evans<sup>(98)</sup>). Where no film is present on the metal this accelerated corrosion may be caused by the fact that an atom in a disarrayed structure (after straining) will require less energy for dissolution than one occupying a stable position; or, a preferred orientation may result from the straining (such as occurs in rolling operations) to expose more susceptible crystal faces; or, impurities which are more soluble may segregate to the surface of the metal as a result of the stress. It appears, however, that the most important function of stress (in the absence of surface films) is to induce compositional heterogeneities on the surface of the alloy. The initiation of transgranular cracking in many alloy systems has been shown to be related to planar groups of dislocations,<sup>(247)(249)(251)</sup> and the increased activity of slip planes associated with these planar arrays has been variously attributed to the concentration of strain energy at Cottrell-Lomer barriers;<sup>(249)</sup> segregation of solute atoms to stacking faults,<sup>(248)</sup> destruction of short range order,<sup>(250)</sup> or segregation and precipitation on the slip planes,<sup>(247)</sup> depending on the metal or alloy under consideration. The important point is that, under the influence of stress, the dislocations may cross slip (in metals or alloys having high stacking fault energies)





to form cellular tangles of dislocations, or (in metals or alloys having low stacking fault energies) the dislocations may remain on their original slip planes to form planar distributions; as a rule, transgranular crack initiation can be associated with these planar distributions.

When surface films exist, the rupture of these films will expose fresh metal which may be anodic to the surrounding film and thus accelerate dissolution. As will be seen in the discussion of the various stress corrosion cracking mechanisms, film rupture may play an important part in the initiation of cracking.

Stress applied to a metal may also affect the electrochemical potential, but here the result is not easily predicted, since the potential will not only be affected by breakdown of the surface film, but also by the distribution of the strain energy. Yang et al.<sup>(93)</sup> have summarized the studies of the effect of elastic strain on electrode potentials, pointing out that most experimental results show cathodic shifts for metals stressed in tension, whereas theoretical considerations<sup>(94)</sup> of the elastic strain energy stored in a metal predict an anodic shift. More recent work<sup>(95)(96)</sup> has shown that elastically stressed silver and steel wires (in solutions of  $\text{AgNO}_3$  and  $\text{FeSO}_4$ , respectively) give a reproducible, reversible cathodic shift; brass wires (stressed in  $\text{CuSO}_4$  solution) give an anodic shift; while all three metals show an anodic shift when stressed in  $\text{NaCl}$  solutions. These results have been tentatively explained by considering the dynamics of the electrical double layer, but the original conflict between theory and experiment still remains.



## 2. COMPOSITION OF MATERIAL

The effect of the addition of alloying elements to, or the elimination of impurities from, susceptible materials has been well studied, and for copper alloys, at least, is well defined. At the onset it should be noted that some workers have flatly stated that pure metals are immune to stress corrosion cracking,<sup>(99)(100)</sup> and have suggested that stress cracking failure in a presumably "pure" material is simply evidence of trace impurities. This is a difficult statement to disprove, but there does not appear to be any sound theoretical reason why pure metals should be immune.

In homogeneous alloys, the situation is different. For example, elimination of impurities (down to the parts-per-billion range) in 70Cu-30Zn alloys does not confer immunity.<sup>(42)</sup> In complex alloys such as the stainless steels, impurities may have either beneficial or detrimental effects, and each system must be considered independently.

### A. FERROUS ALLOYS

#### a) Iron and Low Carbon Steel

The effect of carbon and nitrogen content on cracking of low carbon steels in  $\text{NH}_4\text{NO}_3$  or caustic solutions has been studied by Waber and McDonald,<sup>(17)</sup> and by Parkins,<sup>(101)(103)</sup> but, whereas Waber and



McDonald came to the conclusion that "free" nitrogen formed a corrosion-susceptible iron nitride precipitate at the grain boundaries, Parkins showed that carbon, not nitrogen, is the important agent, and proposed that grain boundary cementite is responsible for the susceptibility to stress cracking. In summary, his work showed the effect of carbon and nitrogen additions as follows: at carbon contents greater than 0.2%, steels did not fail even under high stresses, unless prolonged annealing at 700°C was carried out prior to testing (this presumably caused the migration of carbide to the grain boundaries). As the carbon content was lowered from 0.2% to 0.035% the cracking time was fairly short and constant. A further decrease in the carbon content increased the resistance to cracking, and at values below 0.02% (at which concentration little or no grain boundary cementite is expected) the steel was immune. However, some doubt has been cast on the importance of grain boundary carbides by Logan<sup>(106)</sup> who has produced cracking in very large-grained decarburized steels in which the carbon content was approximately 0.01%.

Steel containing small amounts of Mn, Cr, Mo and Si cracks readily in nitrate solutions,<sup>(104)</sup> but steel containing Ti or Ni has been found to be resistant.<sup>(105)</sup> Parkins and Brown<sup>(107)</sup> have clarified the effects of additions of copper, chromium, and aluminum: Copper steels containing 0.29-1.02%Cu cracked more readily than unalloyed steel; chromium and aluminum steels in the same composition range were immune.





## b) Iron-Chromium-Nickel Alloys

Although Table I lists many environments in which the alloy steels have been known to fail by stress cracking, by far the greatest amount of work in recent years has been devoted to the transgranular cracking of the austenitic stainless steels in chloride solutions (the most common testing medium being a boiling 42%  $\text{MgCl}_2$  solution). The effect of composition on the cracking of polycrystalline austenitic stainless steels is best summarized in recent papers by Uhlig and White,<sup>(108)</sup> Van Rooyen,<sup>(109)</sup> Phelps and Mears<sup>(67)</sup> and Lang.<sup>(111)</sup> Special attention has been given to the nickel content of ferrous alloys by Copson.<sup>(112)(113)</sup> A comprehensive survey (with special attention paid to the Russian literature) of the corrosion resistance of Fe-Cr, Fe-Cr-Ni and Ni alloys is included in the book by Shvartz and Kristal.<sup>(19)</sup>

The general effect of the main alloying elements, chromium and nickel, although influenced considerably by trace elements, can be summarized as follows: the ferritic stainless steels (Fe-Cr alloys) are resistant to transgranular cracking in chloride solutions. Martensitic stainless steels exposed to chloride environments have been found resistant according to Scheil,<sup>(60)</sup> but Shvartz<sup>(55)</sup> has obtained opposite results. Martensitic steels that have been heat-treated to very high strength levels have been found susceptible to relatively mild coastal atmospheres,<sup>(115)</sup> but in general the martensitic steels are quite



susceptible to cracking in acid media, especially if traces of arsenic, selenium or hydrogen sulfide are present; this has been a serious problem in the oil industry, as is reflected by the literature.<sup>(116)(117)(118)</sup>

In the austenitic stainless steels, both intercrystalline and transcrystalline modes of cracking have been found, but since intercrystalline cracking is associated with carbide precipitates at grain boundaries and thus can be prevented by control of carbon content or by heat treatment, more attention has been given to the unsolved problem of transgranular cracking in chloride solutions.

The beneficial influence of increasing nickel content in alloys of the 18% Cr type was first reported by Rocha<sup>(119)</sup> and has been confirmed by others<sup>(62)(109)(112)(121)(122)</sup> although the amount assumed necessary to confer immunity has varied from 16% to 45%. This spread is probably caused by the variation in the amounts of carbon, nitrogen or silicon, all of which have appreciable effects on the amount of ferrite formed (which is not susceptible).<sup>(108)</sup>

Uhlig and White<sup>(108)</sup> have found that 18Cr-8Ni alloys containing 0.015% carbon or 0.01% nitrogen (or less) were immune, whereas commercial 18Cr-8Ni alloys failed in less than two hours. Additions of columbium to 18Cr-8Ni (with low carbon and nitrogen contents) were detrimental, while titanium had no effect. Silicon, contrary to the results reported by Leu and Helle,<sup>(123)</sup> was beneficial. Hines



and Jones<sup>(232)</sup> carried out a statistical analysis of the effect of a number of alloying elements, and concluded that the important compositional variables were carbon and molybdenum.

In the completely austenitic 20Cr-20Ni steels, Uhlig and White<sup>(108)</sup> found nitrogen to be detrimental, while carbon, silicon, cobalt and boron were beneficial. Lang's studies<sup>(111)</sup> on the stable austenitic steels showed that additions of nitrogen, phosphorus, arsenic, antimony, bismuth, ruthenium, and aluminum were detrimental; additions of carbon and silicon were beneficial; no significant effect was produced by additions of sulfur, lead, tin, boron, titanium, niobium, zirconium, and cerium. Copson<sup>(112)</sup> reported variable effects in alloys containing manganese. Van Rooyen<sup>(109)</sup> showed that molybdenum increased the susceptibility. High nickel alloys (65-100%Ni) were completely immune.

## B. COPPER BASE ALLOYS

Unlike the stainless steels, the susceptibility of copper base binary alloys (in ammonia environments) cannot be reduced by the elimination of impurities. It is true that high purity copper itself has never been known to fail,<sup>(33) (35)(38)(128)</sup> but, as was mentioned earlier, a 70Cu-30Zn alloy prepared from spectroscopically pure starting materials is just as susceptible as commercial brass,<sup>(42)</sup> a fact that has been confirmed by several workers.<sup>(38)(124)(125)(126)</sup>





Thompson and Tracy<sup>(38)</sup> have compared a number of alloying elements added to pure copper to produce susceptibility to cracking in ammonia environments as follows (in order of decreasing cracking tendency): phosphorus, arsenic, antimony, silicon, zinc, aluminum, and nickel. Note that although the copper-zinc alloys crack more rapidly than the other copper alloys, zinc is rated low because so much of it must be added before the cracking rate increases. Figs. 1 and 2 comprise a summary of the effect of these elements. In each case the cracking time is plotted versus the per cent of alloying element for various stress levels; each graph also contains a curve showing the corrosion rate of the same alloy in the absence of stress.

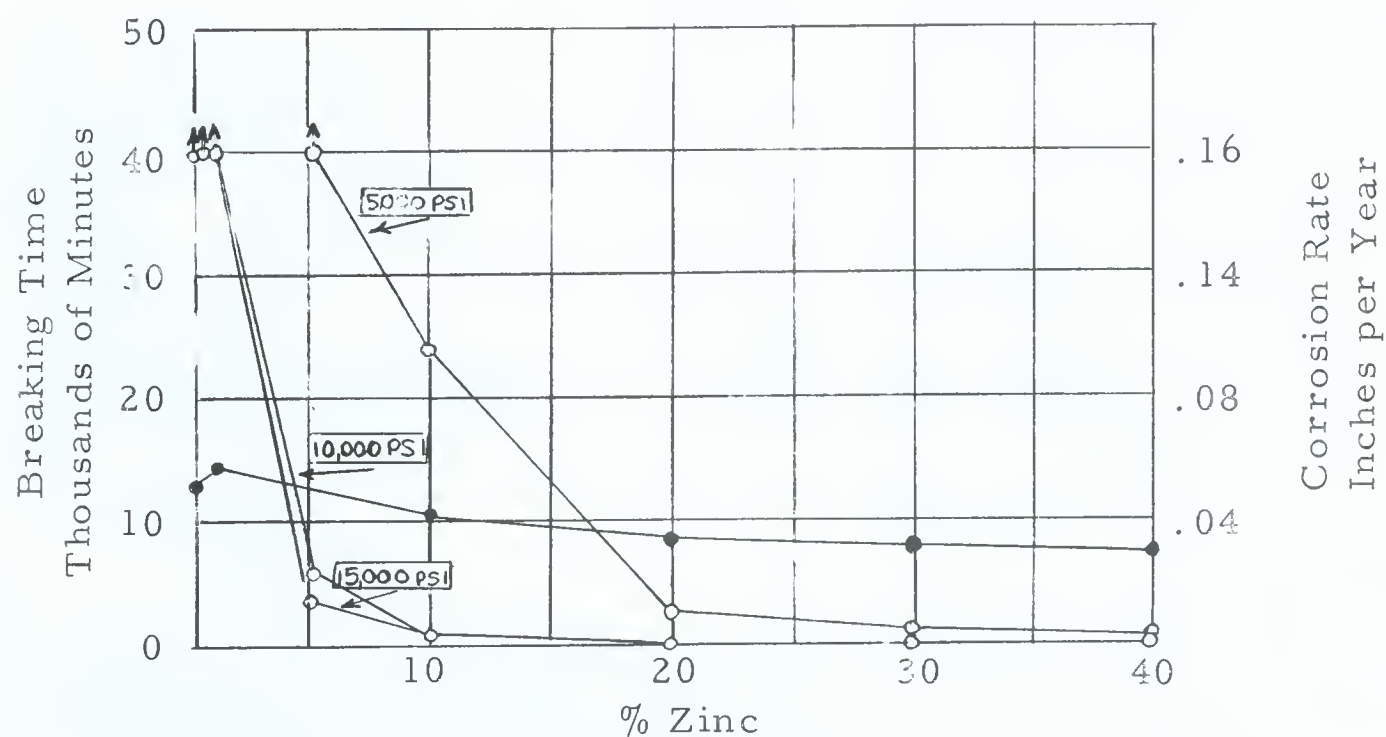


Fig. 1 Cu-Zn alloys in moist  $\text{NH}_3$  atmosphere;<sup>(38)</sup>  
 %Zn vs. cracking time under various stresses  
 (open circles); %Zn vs. corrosion rate, no  
 stress (solid circles)



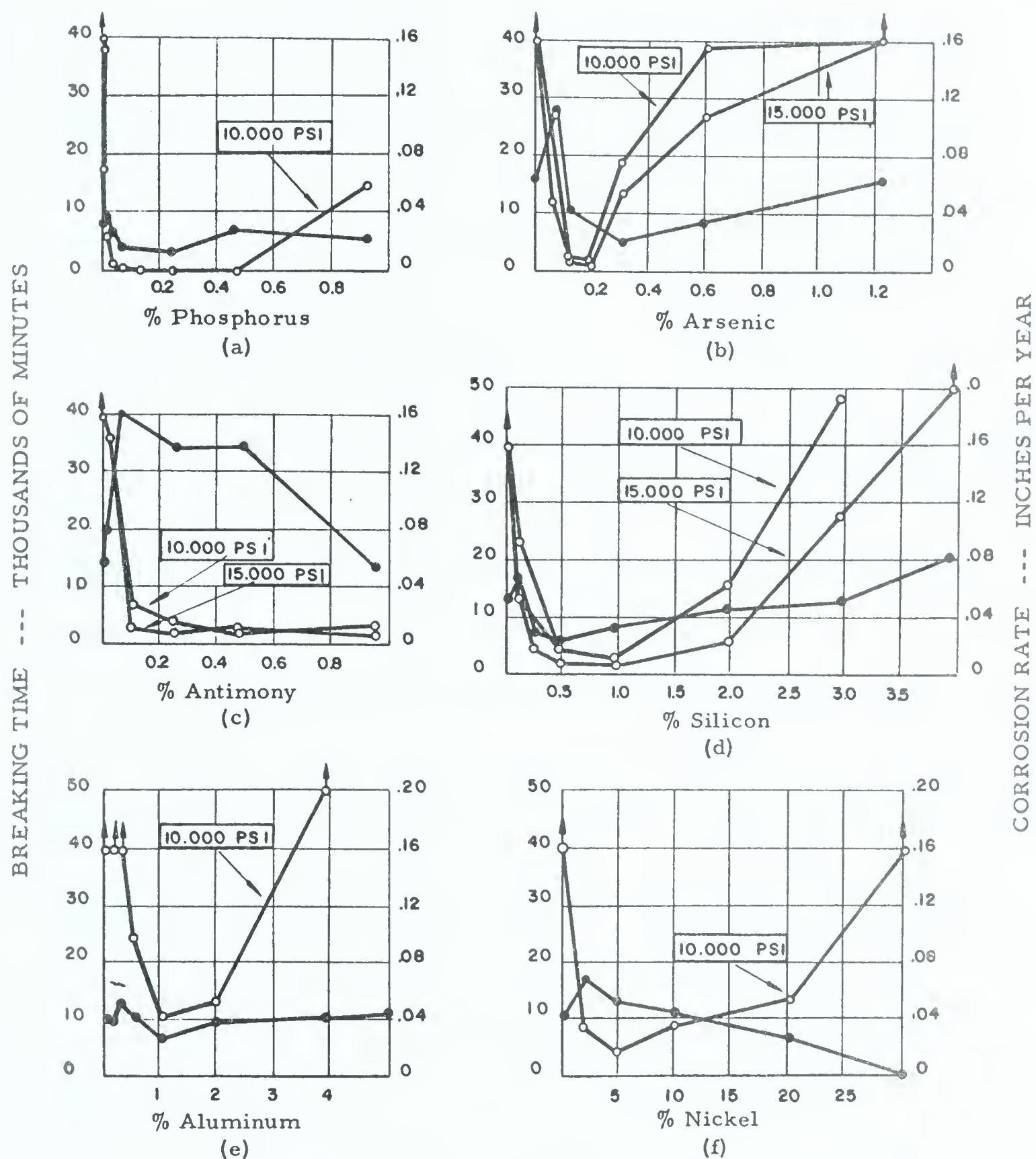


Fig. 2

Copper alloys in moist ammoniacal atmosphere, after Thompson and Tracy.<sup>(38)</sup> Solid circles, corrosion rate (no stress) vs. % alloying element; open circles, breaking time under various stress levels vs. % alloying element. a) Cu-P, b) Cu-As, c) Cu-Sb, d) Cu-Si, e) Cu-Al, f) Cu-Ni



### a) Copper-Zinc Alloys

It is well known that increasing the zinc content of brass increases the cracking tendency. Fig. 1 shows this, but does not clearly define the lower limit of zinc at which cracking first occurs. Other workers have variously reported the "safe" limit as 6%,<sup>(33)</sup> 15%<sup>(127)</sup> and 20% Zn,<sup>(35)</sup> but since cracking has definitely been observed in alloys containing as little as 3% Zn,<sup>(128)</sup> Fig. 1 is assumed to be reasonably accurate. It should be noted that high zinc alloys of the  $\alpha$  or  $\alpha+\beta$  type are inherently brittle and fail rapidly (although in  $\beta$  alloys the cracking is often transcrystalline rather than the intercrystalline type observed in  $\alpha$  and  $\alpha+\beta$  alloys).

### b) Copper-Phosphorus Alloys

Fig. 2a shows the extremely poor resistance of Cu-P alloys, which fail rapidly in ammonia environments with as little as 0.004% P present. This is below the limit of solid solubility of phosphorus in copper; increasing the phosphorus increases the resistance.

The addition of phosphorus to brass is reported to have a beneficial effect,<sup>(42)(127)</sup> although it does not confer immunity.

### c) Copper-Arsenic Alloys

Cu-As alloys are susceptible over a very limited range (Fig. 2b). Lynes<sup>(129)</sup> found that additions of arsenic had little effect on the cracking of brass, but Wilson et al.<sup>(42)</sup> noted slightly beneficial effects in some cases.





#### d) Copper-Antimony Alloys

The susceptibility of Cu-Sb alloys is shown in Fig. 2c. Added to brass in amounts from 0.03-0.53%, antimony has no effect, (42)(129) although one case of improved resistance in a 70Cu-30Zn brass containing 0.09% Sb has been reported. (127)

#### e) Copper-Silicon Alloys

A distinct minimum appears in the Cu-Si curve (Fig. 2d), with complete immunity appearing at about 4% Si. Silicon is one of the few elements that improves the cracking resistance of brass; (42) leaded silicon brasses are even more resistant. (130)

#### f) Copper-Aluminum Alloys

Fig. 2e shows the results obtained by Thompson and Tracy for the Cu-Al alloys. The immunity shown for Cu-5Al is debatable; Bobylev<sup>(131)</sup> has produced rapid cracking in alloys containing 7% Al.

#### g) Copper-Nickel Alloys

Copper-nickel alloys are generally classified as only slightly susceptible to cracking. Fig. 2f shows that they do fail over a wide range of nickel contents, but after a relatively long time. Bobylev<sup>(131)</sup> states that Cu-20Ni is immune to stress corrosion cracking in ammonia, but does not report the length of time of exposure.



In summary, small amounts of phosphorus, arsenic, antimony, silicon, aluminum and nickel, when added to pure copper, produce alloys which are susceptible to cracking in ammonia environments; further additions of the same alloying elements usually reduce the susceptibility, and may confer immunity. Copper-zinc alloys are very susceptible if the zinc content is greater than about 3%. There are no elements that have been observed to have an accelerating effect on the cracking of  $\alpha$  brass. Under some circumstances barium, cerium, manganese, tellurium, tin, beryllium and magnesium may have beneficial effects if added to brass.<sup>(42)</sup> Elements which do not have any effect include the following: cadmium, lead, iron, bismuth, silver, gold, strontium, boron, thallium, cobalt, palladium, calcium, titanium, zirconium, chromium, lithium, sodium, potassium, niobium, tantalum, molybdenum, sulfur and selenium. (31)(33)(42)(127)(132)

### C. MAGNESIUM ALLOYS

One instance of cracking of relatively pure magnesium has been reported,<sup>(65)</sup> but Romanov<sup>(133)</sup> gives four references to Russian literature in which pure and commercially pure magnesium have been shown to be immune to stress cracking. Additions of up to 2.5% manganese, and manganese plus 0.35% cerium do not make magnesium susceptible in accelerated tests ( $K_2CrO_4 + NaCl$  solutions), or to



industrial atmospheres, but alloys of the Mg-Al-Zn-Mn type are susceptible under these conditions.<sup>(31)(133)</sup>

Mg-Al alloys, which are commercially important because of their improved mechanical properties, become more susceptible to cracking as the aluminum content is increased.<sup>(31)(133)(135)</sup> The resistance of a Mg-5%Al alloy has been shown to be dependent on iron content by Perryman<sup>(65)</sup> and Pardue et al<sup>(136)</sup> but according to Timonova<sup>(31)</sup> iron has no effect. This point needs further clarification, since cracking mechanisms based on the formation of an iron-aluminum precipitate have been proposed.<sup>(135-138)</sup>

Mg-8%Al alloys, which are very susceptible to stress corrosion cracking, have benefited from additions of either manganese or zinc,<sup>(31)</sup> but not from simultaneous inclusion of both. Small amounts of cerium or tin have a slightly beneficial effect.

Matthaes<sup>(139)</sup> has shown that small additions of copper (up to 0.94%) drastically increase the susceptibility of a magnesium base alloy containing 5.5%Al, 0.3%Mn, 1.0%Zn, 0.1%Fe and 0.5%Ni.

#### D. ALUMINUM ALLOYS

No stress corrosion cracking failures of commercial or high purity aluminum have been observed, although intercrystalline corrosion in the absence of stress is possible.<sup>(143)</sup> Because of their





industrial importance, the stress corrosion properties of aluminum alloys containing zinc,<sup>(140)(141)(142)</sup> magnesium,<sup>(22)(144)</sup> and combinations of zinc and magnesium<sup>(145)(146)</sup> have been well evaluated.

In aluminum alloys containing more than 5% magnesium, stress corrosion susceptibility is evident and increases with increasing magnesium content, presumably because of the formation of a susceptible  $\beta$ -phase ( $\text{Mg}_2\text{Al}_3$ ) at the grain boundaries<sup>(148)(149)</sup> (although it has been suggested<sup>(147)</sup> that magnesium, and not  $\text{Mg}_2\text{Al}_3$ , is the segregating constituent).

The additions of iron or silicon to aluminum-magnesium alloys have little effect; small amounts of manganese and chromium are beneficial; copper is detrimental.

Additions of zinc to aluminum increase the susceptibility to stress corrosion cracking; the maximum "safe" zinc content appears to be in the range of 3 - 7% Zn. Both Perryman<sup>(144)</sup> and Herenguel<sup>(151)</sup> have observed intercrystalline cracking in "non-corrosive" atmospheres of "dry" air, as well as in salt solutions, and suggested that the phenomenon is due to a creep process in a ductile precipitate formed at the grain boundaries.

Al-Mg-Zn alloys have outstanding mechanical properties but are exceedingly susceptible to intercrystalline cracking, even in moist



air. Commercially pure alloys are more resistant than rigidly pure alloys. A number of wrought Al-Mg-Zn ternary alloys were tested by Chadwick et al;<sup>(146)</sup> their results showed that the susceptibility to cracking increased with total Zn + Mg content. Additions of iron and silicon were beneficial, presumably because of grain refinement. Copper, though reducing the stress cracking tendency, increased the general corrosion susceptibility. Chromium produced an elongated grain structure and reduced the cracking tendency. Other workers have reported beneficial effects through additions of zirconium, vanadium, or titanium.<sup>(151)(152)</sup>

Al-Cu alloys are also susceptible to stress corrosion cracking,<sup>(29)(66)</sup> the effect of copper being much the same as magnesium in that an intergranular precipitate is formed. The important difference is that whereas the magnesium-aluminum precipitate has been shown to be anodic to the grain bodies,  $\text{CuAl}_2$  is cathodic to the solid solution; however, it is possible that a narrow zone adjacent to the  $\text{CuAl}_2$  precipitate is depleted of copper and becomes subject to anodic dissolution. Al-Cu alloys containing magnesium and nickel are resistant to cracking when hardened, but lose their resistance upon slow cooling, again presumably due to the appearance of the  $\text{CuAl}_2$  phase.<sup>(152)</sup>



## E. MISCELLANEOUS ALLOYS

Very few systematic investigations have been carried out on the influence of cracking of nickel base alloys, although several instances of stress corrosion cracking in hydrofluoric acid vapors have been reported.<sup>(74)</sup>

Homogeneous alloys of the type Cu-Au, Ag-Au, Ag-Pt, and Mg-Al have been studied extensively by Graf.<sup>(76)</sup> He observed that small additions of soluble alloying elements had no effect on the stress cracking susceptibility, and formulated a set of general rules governing the cracking susceptibility of homogeneous alloys; these will be discussed in the section on stress corrosion cracking mechanisms.

Instances of cracking of zirconium and lead have been reported (see Table I), but no work has been done relating composition to susceptibility.





### 3. CHEMICAL ENVIRONMENT

As was mentioned earlier, one of the unique features of stress corrosion cracking is the fact that specific chemical environments are responsible for the failure of any particular alloy. There is no chemical that will cause cracking of all alloys, and there are no alloys that are susceptible to all of the chemicals known to cause cracking. It is therefore necessary to speak of stress cracking 'systems', e.g., the stainless steel-chloride system, the brass-ammonia system, and the carbon steel - nitrate system. But even if the general nature of the environment is specified, it seems intuitive that other chemical parameters (such as pH, concentration, presence of redox agents) will have an effect, and this is borne out by experiment.

It is important to point out that there is no general correlation between the corrosivity of the solution towards an unstressed metal and the stress corrosion cracking susceptibility (for example, see Figs. 1 and 2). It may be true, however, that a particular component of the alloy is subject to severe corrosion by the corrodent, even in the absence of stress. Such a possibility has many ramifications: If, for example, the corroding component is segregated at the grain boundaries, its dissolution will lead to a general weakening of the metal structure; the presence of a stress will mechanically aggravate



the situation, resulting in failure when the unattacked metal is unable to sustain the applied load. Such cases are examples of intercrystalline corrosion, and must be distinguished from stress corrosion cracking, in which there is little evidence of general corrosion in the absence of stress.

On the other hand, one component of the alloy may be susceptible to corrosion, but is distributed homogeneously throughout the alloy. Then, if the effect of stress is to induce segregation (on a microscopic scale) to specific sites (grain boundaries, stacking faults), these sites will be selectively attacked. For example, Pickering and Swann,<sup>(247)</sup> in their electron metallographic studies of deformed thin films, showed that a tubular type of attack occurred in films exposed to cracking solutions; this attack was initiated at grain boundaries and anti-phase boundary junctions in ordered Cu-Au alloys, but at precipitates and the substructure of twins in Mg-Al alloys.

#### A. Ferrous Alloys

Mild steel is subject to stress corrosion cracking in three general types of environments: nitrate solutions, caustic solutions ('caustic embrittlement') and solutions where the cathodic discharge of hydrogen is possible, leading to hydrogen embrittlement (e.g. 'sulfide stress cracking'). The effectiveness of various nitrate



solutions in producing cracking has been reviewed and re-examined by Parkins and Usher<sup>(218)</sup>. They rated the nitrates in order of decreasing aggressiveness as follows:  $\text{NH}_4\text{NO}_3$ ,  $\text{Ca}(\text{NO}_3)_2$ ,  $\text{LiNO}_3$ ,  $\text{KNO}_3$ ,  $\text{NaNO}_3$ , and also found that boiling solutions of Pb, Ni, Cd and Zn nitrates caused intercrystalline cracking, although the latter group forms insoluble hydroxides which normally inhibit the cathodic reaction in the corrosion of steel. Additions of oxidizing salts, or substances which formed soluble complexes with iron shortened the cracking times in nitrate solutions. The cracking was also pH-dependent, with rapid cracking at pH values below 6, and no cracking at high pH values. McGlasson et al.<sup>(220)</sup> found that additions of  $\text{CaCl}_2$  to  $\text{NaNO}_3$  solutions decreased the cracking time as the weight ratio  $\text{CaCl}_2:\text{NaNO}_3$  was increased; complete immunity was reached at a ratio of 4:1.

In the absence of nitrate ions, cracking of steel does occur at high pH values; Berk and Waldek<sup>(219)</sup> have shown that U-bend specimens were most susceptible to cracking in caustic solutions having a composition of 15 - 30% caustic, at temperatures above 200°C; but a survey by Schmidt et al.<sup>(48)</sup> shows that actual service failures have occurred over a much wider range of NaOH concentrations (5 - 75%), and at lower temperatures (125°C). Radeker and Grafen<sup>(222)</sup> found no correlation between cracking time and pH in caustic solutions;





additions of  $\text{MnSO}_4$  and  $\text{MnCl}_2$  inhibited the cracking.

The cracking of mild steel in the complex chemical mixtures found in coal gas liquors has been discussed by Parkins and Usher<sup>(102)</sup>; the relative effects of  $\text{H}_2\text{S}$  and  $\text{CO}_2$  (which have been investigated for the stress cracking of steels used for oil field tubular goods<sup>(223)</sup>) are complicated by the presence of cyanide ions which are capable of forming soluble complexes with iron.

The cracking of carbon steels in liquid ammonia<sup>(51)</sup> has been shown to be related to contamination by air;<sup>(224)</sup> cracking can be prevented by exclusion of air or by addition of more than 0.1% water.<sup>(224)</sup>

The Fe-Cr-Ni alloys are susceptible in a number of environments, but chloride solutions are the most commonly encountered in service, and are the most widely used in testing. Cracking of 18Cr-8Ni stainless steel has been found to occur in hot concentrated solutions of the chlorides of magnesium, calcium, barium, cobalt, zinc, lithium, ammonium and sodium;<sup>(60)(62)(231)</sup> but not in chlorides of tin, iron, strontium, nickel, chromium, or mercury; or in solutions of KBr, NaBr, KF, or NaF<sup>(62)</sup>. The data published by Logan and Sherman<sup>(70)</sup> seem to contradict some of these findings, but the results are not strictly comparable because of differences in test methods, concentration and pH of solutions.



Berg and Henrikson<sup>(225)</sup> attempted to correlate the effect of sodium, calcium, magnesium and lithium chloride solutions with cracking times by plotting only the chloride concentration versus cracking time, and found that for tests carried out at 100°C and pH 6, the cracking time was relatively constant above a chloride ion concentration of 14 wt.%; below this concentration the failure time was greatly extended.

Because the amount of chloride necessary to produce cracking is related to pH, stress level, oxygen concentration and temperature, it is difficult to compare the reported 'threshold' values of chloride concentration necessary to cause cracking within a reasonable time, although from a practical point of view, any cracking at all is undesirable. Thus, for instance, service failures have been reported for 18Cr-8Ni stainless steel exposed to heavy water containing only 0.01 - 0.03 ppm chloride (at 100°C), although no cracking could be produced in laboratory tests in heavy water containing 0.1 ppm chloride.<sup>(68)</sup> The results of Berg and Henrikson<sup>(225)</sup> give the erroneous impression that very high concentrations of chloride ( $\simeq$  14 wt. %) are required; a threshold value of 5 ppm is more realistic, based on a number of investigations carried out at temperatures from 85 - 300°C in solutions having pH values from 4 - 8.<sup>(68)(226)(227)(228)</sup> Increasing the pH of test solutions to 8.8 prevented cracking in hot water (85°C) containing 10 ppm chloride,<sup>(227)</sup>



The cracking which occurred in solutions of low chloride concentration required the presence of oxygen;<sup>(216)(226)(228)(229)</sup> on the other hand, if the concentration of oxygen is low, more chloride is required.<sup>(121)(229)</sup>

Aqueous media containing other compounds in combination with the halide salts have also caused cracking; Logan and Sherman<sup>(70)</sup> found that a 3.5% NaCl-1%  $\text{NH}_4\text{NO}_2$  solution was especially aggressive and therefore suited to accelerated testing of stainless steels. Sidorov and Ryabchenkov<sup>(200)</sup> studied the cracking of austenitic steel in aqueous solutions (330°C) of NaOH alone and in combination with NaCl, and found that both inter- and transgranular failures occurred rapidly in solutions of high NaOH concentration (up to 30%), while the addition of NaCl had an inhibiting effect.

The comparative behavior of stressed austenitic and martensitic stainless steels in a number of different test solutions (at room temperature) was reported by Phelps and Mears.<sup>(67)</sup> Whereas annealed types 302 and 304 stainless alloys were resistant to all the solutions except boiling 42%  $\text{MgCl}_2$ , type 410 was also susceptible to solutions containing 3% NaCl +  $\text{H}_2\text{S}$ , and 3% NaCl + 0.5% acetic acid +  $\text{H}_2\text{S}$ , but was still more resistant than a special 12MoV martensitic alloy (containing 12% Ni, 0.7% Cr, 1% Mo, 0.3% V) which failed in the above solutions and in solutions containing 3% NaCl, 10% NaCl +  $\text{H}_2\text{O}_2$ , or





10%  $\text{FeCl}_3$ , and was also susceptible to cracking in molar solutions of  $\text{NaF}$ ,  $\text{NaBr}$ ,  $\text{NaCl}$ ,  $\text{NaI}$ ,  $\text{NaH}_2\text{PO}_4$ ,  $\text{Na}_2\text{SO}_4$ ,  $\text{NaNO}_3$ ,  $\text{Na}_2\text{SO}_3$ ,  $\text{NaClO}_3$  and  $\text{NaC}_2\text{H}_3\text{O}_2$ . It has also been shown<sup>(230)</sup> that the cracking of the 12MoV alloy in oxygen-saturated 3%  $\text{NaCl}$  solutions is dependent on pH, with rapid cracking below pH 3 (associated with hydrogen evolution), no cracking above pH 11, and an intermediate range where the cracking mechanism is presumably controlled by oxygen.

### B. Copper Base Alloys

It is strange that although the brass-ammonia system has been studied for nearly sixty years, relatively little work has been done on the chemical factors that affect cracking. It has long been recognized that ammonia will cause failure in alpha brass, and as a result, most service failures of stressed brass parts exposed to industrial atmospheres have been ascribed to traces of ammonia. That this may not necessarily be true is shown by the fact that moist  $\text{SO}_2$  may also cause cracking,<sup>(3)(131)(155)</sup> although Thompson<sup>(156)</sup> exposed stressed brass samples to moist  $\text{SO}_2$  for two years with no effect. He also reported one instance of cracking in moist  $\text{H}_2\text{S}$  after a period of nine months, which is contrary to Johnston's findings<sup>(155)</sup>, and has not been substantiated by further work.



Nitrogen compounds other than ammonia have been studied by Rosenthal and Jamieson<sup>(34)</sup>, who found that cracking occurred in the presence of water vapor, air, and the vapor of the following amines: methylamine, dimethylamine, trimethylamine, aniline, ethylamine, diphenylamine and triethanolamine. The specimens did not crack in the presence of diethylamine, triethylamine and pyridine. However, both Jevons<sup>(157)</sup> and Morris<sup>(158)</sup> found pyridine effective in stress cracking, while Moore et al.<sup>(33)</sup> did not observe cracking in diphenylamine.

Moore et al.<sup>(33)</sup> also tried unsuccessfully to produce cracking in the vapors and solutions of a number of inorganic compounds, including  $\text{HNO}_3$ ,  $\text{H}_2\text{SO}_4$ ,  $\text{NaCl}$ ,  $\text{NaHSO}_4$ ,  $\text{Zn}(\text{NO}_3)_2$  and  $\text{Cu}(\text{NO}_3)_2$ . Cracking of brass cartridge cases stored in wooden boxes wetted with dilute  $\text{H}_2\text{SO}_4$  pickling solutions has been reported,<sup>(159)</sup> as has one instance of cracking in a cadmium plating solution containing  $\text{CdO}$ ,  $\text{NaCN}$  and  $\text{NiSO}_4$ .<sup>(160)</sup> Apart from these few instances, no cracking has been observed in non-ammoniacal environments until recently, when Bobylev<sup>(131)</sup> proposed that cracking of brass would occur in any solution which would react with the zinc in the brass. According to his most recent paper<sup>(131)</sup>, which unfortunately gives no experimental details, cracking has been observed in copper-complex solutions which do not contain ammonia, viz. nitrites, carbonates, pyrophosphates and



alkalies. He has also observed cracking of brass in air containing  $\text{SO}_2$  and nitrogen oxides. In all of these media pure zinc shows a high general corrosion rate.

Since most of the published work has dealt with ammoniacal environments, it is important to review other pertinent details. The first of these is the presence of moisture. It is generally agreed that dry ammonia gas will not cause cracking. Johnston<sup>(155)</sup> exposed stressed brass specimens to dry ammonia gas for over 14 months without the appearance of a tarnish or any cracks.

The effect of oxygen or air is not as clearly defined, although it appears that the substitution of gases other than air ( $\text{N}_2$ ,  $\text{H}_2$ ,  $\text{CH}_4$ ) greatly increases the time to cracking in a moist ammoniacal atmosphere.<sup>(162)</sup> Skorchelletti and Titova<sup>(165)</sup>, investigating the effect of oxygen concentration on samples partially immersed in ammonia solutions, found that the failure time was not significantly changed if the atmosphere above the solution was pure oxygen, air, or hydrogen containing 0.5%  $\text{O}_2$ . More significantly, they found that the addition of small quantities of a surfactant (propionic acid) sharply decreased the time to failure; further additions (above 0.005M) increased the failure time.

Carbon dioxide has been variously reported as accelerating the cracking process<sup>(164)</sup> or preventing it altogether<sup>(155)</sup>.





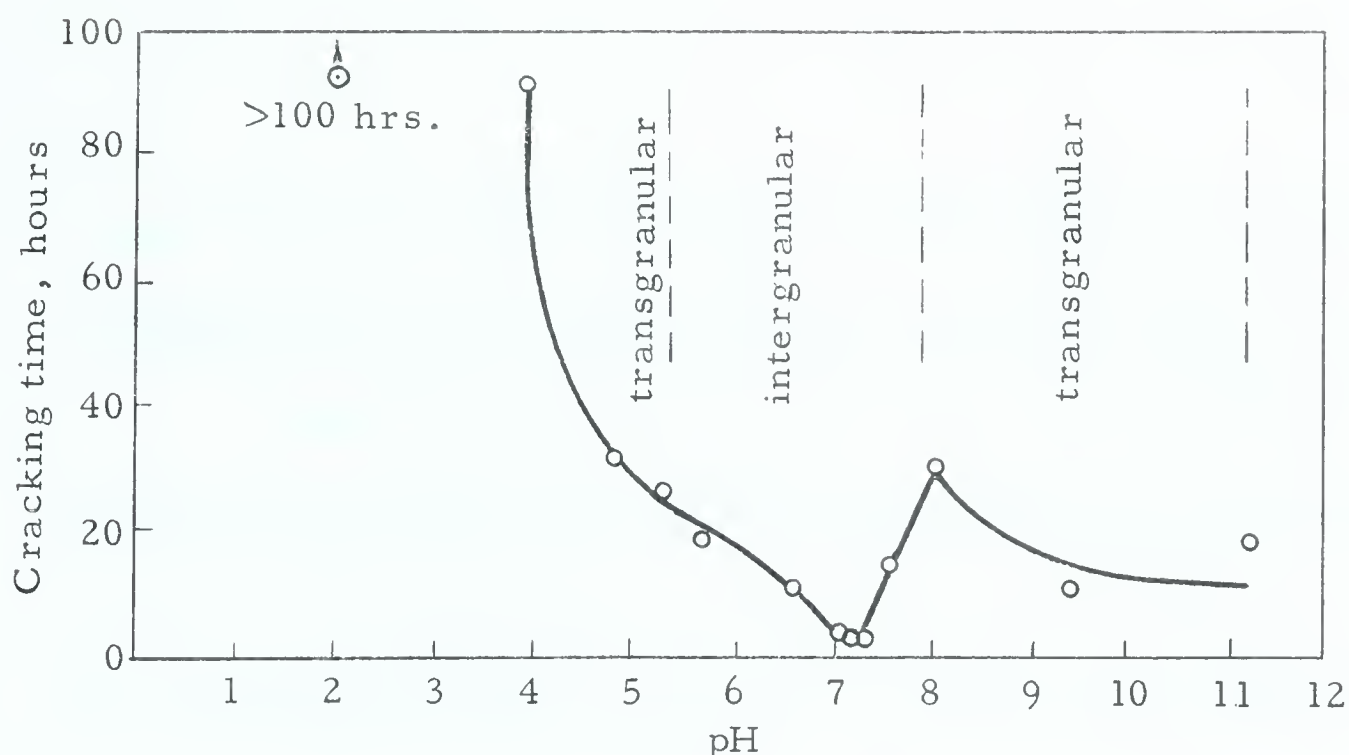


Fig. 3 Effect of pH on cracking of brass in copper-ammonia solutions ( $\text{Cu} = 0.05\text{M}$ , total  $\text{NH}_3 = 1.0\text{M}$ ), after Mattsson<sup>(168)</sup>

The most significant work on the chemistry of the brass-ammonia system was reported by Mattsson<sup>(167)(168)</sup> who found that the cracking time and type of cracking were related to the pH of the test solutions, which initially contained dissolved copper as well as ammonia. Fig. 3, which summarizes the main points of his work, shows that the cracking times in brass-ammonia solutions were most rapid in the pH range 7.0 - 7.3; the cracking was predominantly transgranular in the pH ranges 3.9 - 5.7 and 7.8 - 11.2, and mainly intergranular in the pH range 6.3 - 7.7. Unfortunately, the solutions used in obtaining the cracking times shown in Fig. 3 did not all have the same initial copper concentration, and were especially varied over the critical pH range 5.0 - 7.5. Since it will be shown later that the cracking time is also dependent on the initial concentration of dissolved



copper, Fig. 3 is not a true picture of the pH dependence of cracking, although the overall features are substantially correct.

Partly because of the errors in Fig. 3, and partly because of the improper construction of the pH/potential diagrams (see Appendix C) for the Cu-NH<sub>3</sub>-H<sub>2</sub>O and Zn-NH<sub>3</sub>-H<sub>2</sub>O systems, Mattsson correlated the cracking time with the appearance of a black tarnish on those specimens that failed most rapidly, and concluded that the intergranular cracking occurred as the result of intensified attack at pores in the tarnish, whereas at other pH values, precipitation of protective sulfates modified the attack and allowed transgranular failure.

In spite of these criticisms, Mattsson's work represents a major step towards the understanding of the chemistry of the brass-NH<sub>3</sub> system; the present work includes a more detailed study of the pH range 5.0 - 8.0, and a re-interpretation of his observations in the light of a proposed surface energy mechanism.

### C. ALUMINUM AND MAGNESIUM ALLOYS

Studies on the stress corrosion cracking of aluminum alloys have been mainly confined to aqueous chloride media, since service failures have often been associated with marine atmospheres. Perryman and Hadden (149) found that the cracking time of an Al-7% Mg alloy decreased with increasing NaCl concentration up to a chloride con-



centration of 9%, after which the cracking time was relatively unchanged. Under salt-spray conditions, the same authors found that a relative humidity of about 80% produced the most rapid cracking.  
(66)

Farmery and Evans showed that bicarbonate additions to 0.1N NaCl solutions decreased the cracking time of Al-7% Mg; this is evidently not related to the increased pH of the solution, because Gilbert and Hadden (153) have shown that the cracking time is most rapid in solutions of high acidity. Cracking occurred more readily in solutions made up from calcium, magnesium or ammonium chlorides, as compared with potassium chloride or sodium chloride; cobalt chloride was even more effective (66), presumably because of the plating out of metallic cobalt to provide locally intense galvanic action.

Pretreatment of the Al-7% Mg alloy by immersion in 20% AlCl<sub>3</sub> solution greatly reduced the time to failure (66) because of the removal of the natural oxide film from the alloy surface.

Oxygen was definitely necessary for the stress corrosion cracking of Al-7% Mg in chloride solutions (149)(153), since the cracking could be halted or re-started by the exclusion or admission of oxygen to the test solutions.

The use of hydrogen peroxide to provide an acceleration of the cracking of Al-4% Cu (for testing purposes) was advocated by Colner and Francis (154), who found that H<sub>2</sub>O<sub>2</sub> concentrations above





3.0 gms/liter markedly reduced the cracking times in NaCl solutions.

Magnesium alloys are also susceptible to cracking in salt solutions; the most popular testing solution is one containing a mixture of NaCl and  $K_2CrO_4$ , both of which have an accelerating effect on the cracking rate (199).

Other salt solutions causing cracking of Mg-Al alloys have been rated by Romanov (183) as follows (in decreasing order of effectiveness):  $Na_2SO_4 = NaNO_3 > Na_2CO_3 > NaCl > CH_3COONa$ . However, when  $K_2CrO_4$  was added to these solutions, no cracking occurred (in 260 hours) in the solutions containing  $NaNO_3$ ,  $Na_2CO_3$  and  $CH_3COONa$ , and these also were the solutions in which no pitting occurred in the absence of chromate ions. Romanov concluded that the additions of chromate seemed to intensify the pitting, which led to the formation of stress-raisers, and thus to cracking. (24)

Mears, Brown and Dix reported a change from intergranular to transgranular cracking (in Mg-6.5% Al-1% Zn) upon changing the pH of the test solution from 5.0 to 8.1, but later investigations have shown that the type of failure is independent of pH. The failure time is dependent on pH; according to Sager et al. (136)(137), cracking is most rapid (in NaCl- $K_2CrO_4$  solutions) at low pH values, with complete immunity being reached at pH values above 13. (199)



Vapor phase testing of magnesium alloys has shown that the relative humidity must be greater than 90% to produce cracking; at 100% humidity, increasing the  $\text{SO}_2$  or  $\text{CO}_2$  content of the gas phase decreases the cracking time, as compared with tests in pure oxygen or air (31). On the other hand oxygen has been shown to have an accelerating effect on the cracking time in distilled water (22), while  $\text{CO}_2$  (65) had an inhibiting effect.

Cracking of magnesium alloys has also been reported in solutions containing  $\text{HNO}_3$ ,  $\text{NaOH}$ ,  $\text{Hf}$  or  $\text{NaF}$  (31)(65); there is no correlation between general corrosion and stress corrosion cracking.

#### 4. METALLURGICAL FACTORS

##### A. HEAT TREATMENT AND PLASTIC DEFORMATION

A rigorous discussion of these two factors is beyond the scope of this review, but the following few examples give an idea of the complex effects which can be produced by variations of heat treatment, and by application of plastic deformation prior to, or during stress corrosion cracking tests:

It is well known that 18Cr-8Ni stainless steels are susceptible to intergranular corrosion if they are 'sensitized' by heating to a temperature at which chromium carbide is precipitated at the grain boundaries, producing a chromium-depleted region which is susceptible



to attack, even in the absence of stress. In the presence of stress, this attack is accelerated, and in some instances may lead to intergranular cracking. The problem is easily circumvented by

- a) using 'stabilized' stainless steels (which contain elements that form carbides more readily than chromium does)
- b) using steels of extremely low carbon contents
- c) heat-treating the 'sensitized' steel at a temperature high enough to allow the carbides to go into solid solution.

In chloride solutions the 18Cr-8Ni steels are vulnerable to transgranular stress corrosion cracking, unless the austenite phase is transformed to the ferrite phase, either by cooling from 1050°C (if the carbon and nitrogen contents are low enough to prevent stabilization of the gamma phase), or by plastic deformation at or below room temperature (108) (204). In the fully austenitic 18Cr-8Ni alloys, Hines found that cold working (prior to testing) decreased the time to failure if the applied stress was low, and if the plastic deformation did not exceed about 8%. At applied stresses greater than the 0.1% proof stress, cold working up to about 8% had no effect; and finally, heavily cold worked specimens showed improved resistance over a wide range of applied stress. The beneficial effect of severe cold working has also





been reported by Scheil <sup>(233)</sup>, but Hawkes et al. <sup>(234)</sup> did not observe an increase in cracking time (as compared with annealed specimens) for material that had been cold worked about 30%.

In testing austenitic stainless steels that do not transform at all (20Cr-20Ni, 25Cr-20Ni), Uhlig and White <sup>(108)</sup> found that bending the specimens at liquid nitrogen temperatures (before immersion in the testing solution) improved their resistance by 65% (as compared with specimens deformed at room temperature); on the basis of this observation and the knowledge that trace amounts of nitrogen were detrimental to these alloys, the authors <sup>(108)</sup> proposed that crack sensitive paths in these alloys may be created by strain-induced nitride precipitates.

The sensitized austenitic stainless steels are not the only alloys in which grain boundary precipitation is associated with intergranular attack. Mention has already been made of the susceptibility conferred on mild steels after prolonged annealing to induce cementite precipitation at grain boundaries <sup>(103)</sup>, (although the recent work of Uhlig and Sava <sup>(246)</sup> shows that susceptibility may not be entirely due to carbide or nitride precipitates). Another example is Al-7% Mg, which was not susceptible to stress corrosion cracking unless heat treatments were carried out which caused grain boundary precipitation of  $\text{Al}_3\text{Mg}_2$  <sup>(153)</sup>.



The ageing of Al-Zn alloys at room temperature produced zinc-rich grain boundary precipitates which made the alloy susceptible, but slow furnace cooling from 450°C (prior to ageing) reduced or eliminated the precipitation, and produced a corresponding reduction in susceptibility to cracking (142).

The type of cracking in a Mg-6% Al-1% Zn-0.2% Mn alloy was influenced by heat treatment and grain size: at small grain sizes, water quenching made the alloy susceptible to transgranular attack (in NaCl-K<sub>2</sub>CrO<sub>4</sub>) solutions, while furnace cooled specimens failed intergranularly; at large grain sizes the failures were transgranular regardless of the heat treatments (137).

## B. CRYSTALLOGRAPHIC ORIENTATION

The relation of crystallographic orientation to the cracking mechanism has only been studied for a few systems, using either single crystals or very large-grained samples. In Fe-20Cr-20Ni alloys the crack plane followed the (100) plane that had the highest normal stress (236), but in other austenitic stainless steels the crack planes were randomly oriented with respect to the crystallographic planes (70)(123)(236).

Random fracture plane orientations have also been observed in large-grained low carbon steel exposed to NH<sub>4</sub>NO<sub>3</sub> (106); in Cu<sub>3</sub>Au single crystals exposed to FeCl<sub>3</sub> solution (239); and in alpha brass (128)(237)(240).



(240)  
 and beta brass exposed to ammonia, although the cracks in single  
 (238)  
 crystals of alpha brass sometimes followed slip line traces .

The basal (0001) plane was the favored fracture plane observed  
 (137)  
 in the transgranular cracking of a Mg-6% Al-1% Zn-0.2% Mn alloy .

The relative orientation of adjacent crystals appears to be  
 important in intergranular stress corrosion cracking. In studies of  
 the ammonia cracking of 70Cu-30Zn, and 90Cu-10Zn large grained  
 (240)  
 alloys, Logan observed that for over 70% of the cracks the angles  
 between bounding planes (of adjacent crystals) at the crack origins were  
 in the range of  $13^{\circ}$  -  $23^{\circ}$ , which corresponds to the range where grain  
 boundary energies are highest. In a similar study of the intergranular  
 (106)  
 cracking of low carbon steel in  $\text{NH}_4\text{NO}_3$ , Logan found that the  
 majority of the cracks occurred at grain boundaries where the relative  
 orientation of the bounding planes was in the range of  $10^{\circ}$  -  $30^{\circ}$ , which  
 again suggests that grain boundaries having high energies are most  
 susceptible.

## 5. ELECTROCHEMICAL ASPECTS

Electrochemical studies of stress corrosion cracking fall into  
 three general categories:

- a) Measurement of the relative electrochemical potentials  
 of the constituents involved in the cracking mechanism





(e.g. grain boundaries, grains, intermetallic compounds) with and without the application of stress to the specimens;

- b) Measurement of the overall electrochemical potential (vs. a suitable reference electrode) of a specimen during the time preceding failure;
- c) Control of the electrochemical potential (by means of an externally applied potential) of the corroding specimen to study the effect of anodic and cathodic polarization.

It has long been suspected that many instances of intergranular stress corrosion cracking could be attributed to the anodic dissolution of material from grain boundaries, but the first direct evidence that the grain boundaries of alloys might be anodic to the grains was reported (26) by Dix in 1940. In the experiments performed by his colleagues, the potential differences between the grains and the grain boundaries of a coarse-grained, aged Al-4% Cu alloy (in NaCl - H<sub>2</sub>O<sub>2</sub> solution) were measured after carefully masking the grains of one specimen and the grain boundaries of another specimen with Bakelite varnish. The technique was further refined so that the potentials of individual areas on the specimens could be measured with a capillary-tipped electrode. Both methods showed that the grain boundaries were substantially anodic



to the grain centers, and in some cases the difference was as high as 0.20 volts. The cause of the potential difference was attributed to the fact that grain boundary precipitation produced a solid solution (adjacent to the precipitate) depleted in copper, and this depleted solid solution was the anodic constituent.

Another technique used to determine the relative potentials of possible constituents has been described by Timonova<sup>(31)</sup> for a Mg-8% Al alloy exposed to solutions of NaOH, NaCl, HF and HNO<sub>3</sub>. He compressed concentric rings of Mg<sub>4</sub>Al<sub>3</sub> (representing the inter-metallic compound), Mg-1.65% Al (impoverished solid solution) and Mg-8% Al (homogeneous solid solution), and measured the potentials across the surface of this 'model' alloy. In all of the test solutions mentioned above, the impoverished solid solution was anodic to the other two phases.

Although grain boundary precipitation may account for the anodic regions in some alloys, there is ample evidence of grain boundary activity in materials in which no precipitate is evident. Thus, for example, Dix<sup>(26)</sup> reported that 99.986% Al showed grain boundary activity if the specimens were water-quenched from 620°C, whereas if the specimens were slowly cooled, the grain boundaries were cathodic.<sup>(181)</sup>

For brass exposed to ammonia, Dix found that the grain



(201)  
 boundaries were anodic to the grains, while Bakish and Robertson  
 said that this was true only if oxygen was present. In the absence of  
 oxygen the grain boundaries were cathodic, which apparently agreed  
 (202)  
 with the findings of other workers .

(207)  
 Engell and Baumel have shown that the grain boundaries  
 of mild steel are anodic to the grains when immersed in hot  $\text{Ca}(\text{NO}_3)_2$   
 (26)  
 solutions (using the measurement technique described by Dix ).

The measurement of the overall potential of a specimen under-  
 going stress corrosion cracking has been used with a great deal of  
 success in the studies of the susceptible austenitic stainless steels.  
 (91)(92)(203)  
 In a series of papers, Hoar and Hines have shown that  
 potential-time curves for 18Cr-8Ni steel wires stressed in boiling  
 $\text{MgCl}_2$  solutions exhibit an initial increase in potential which corres-  
 ponds to the repair of the surface film which was initially formed in  
 air, followed by an abrupt decrease in potential when the anodic acidity  
 leads to breakdown of the film at some points, leading to a period of  
 localized corrosion during which the potential does not change; sub-  
 sequently, the potential shows a smooth continuous fall before fracture,  
 during which period the development of open cracks is apparent. This  
 general form of the potential-time curve has been confirmed for the  
 (205)(235)  
 18Cr-8Ni steels ; similar curves have been obtained for





16Cr-20Ni stainless alloys (206) and other Fe-Cr-Ni alloys (217).

Among the other stress corrosion cracking systems, potential-time curves have been recorded for mild steel stressed in boiling  $\text{Ca}(\text{NO}_3)_2$  solutions (107)(207)(235), for mild steel with minor alloying additions of either Cu, Cr or Al (107), for Mg-8% Al alloys stressed in  $\text{HNO}_3$  or  $\text{NaCl} + \text{K}_2\text{Cr}_2\text{O}_7$  solutions (31), for brass stressed in copper-ammonia solutions (191), (235) (153)(235), and for Al-4% Cu and Al-7% Mg alloys stressed in 3%  $\text{NaCl}$  solutions.

The studies of cathodic and anodic polarization of various alloys undergoing stress corrosion cracking have vividly demonstrated the importance of electrochemical stages in the cracking mechanism; if we exclude hydrogen embrittlement (where cathodic polarization increases the probability of failure), it is a well-established fact that application of a potential sufficiently cathodic can prevent stress corrosion cracking, and that anodic potentials stimulate the cracking process. (137) Priest et al. have even shown that the cracking can be stopped or started at will by interrupted application of a sufficient cathodic potential to the stressed specimen.

Investigations to determine the effect of the application of an external potential to alloys undergoing stress corrosion cracking include the following: mild steel (in nitrate solutions) (17)(103)(207)(208)(210)



magnesium alloys (in NaCl -  $K_2CrO_4$  solutions) <sup>(24)(31)(137)(211)</sup>,  
 aluminum alloys (in NaCl solutions) <sup>(29)(31)(66)(147)(153)</sup>, copper alloys  
 (in ammonia solutions) <sup>(31)(165)(173)</sup>, and stainless steels (in chloride  
 solutions) <sup>(91)(92)(206)(212-216)</sup>.

## 6. MISCELLANEOUS FACTORS

### A. TEMPERATURE

The general effect of temperature is, of course, to reduce the time to failure by stress corrosion cracking. One exception to this rule was reported by Romanov <sup>(22)</sup>, who found that for Mg-7% Al alloy exposed to NaCl +  $K_2CrO_4$  solutions the cracking time decreased as the temperature was raised from 5 - 30°C, but increased at higher temperatures, and above 40°C the alloy developed a fairly high resistance to cracking.

Very little systematic work has been done on the effect of temperature. Hoar and Hines <sup>(91)</sup> estimated activation energies of 40 and 10 kcal/mole for the induction period and crack propagation period, respectively, for the cracking of austenitic stainless steel in  $MgCl_2$  solutions over the temperature range 125 - 155°C, but the points on their curves show enough scatter to cast doubts on the linearity of the plots of log rate vs.  $1/T$ .



(134)

Wasserman found that over the temperature range 23 - 100°C, the relation of temperature to cracking time for Al-4% Zn-2% Mg alloys exposed to 3% NaCl solution was a linear plot on log-log co-ordinates (log cracking time vs. log T), but offered no explanation for his choice of log T rather than 1/T.

(200)

Sidorov and Ryabchenkov showed a linear plot of log failure time vs. 1/T for austenitic steels exposed to steam containing NaOH and NaCl over the temperature range 253 - 374°C, but did not calculate the activation energy for the process.

(154)

More recently, Gruhl has derived activation energies of 12.7 and 9.2 kcal/mole for the cracking of an unworked and worked (5% elongation) Al-5% Zn-3% Mg alloy stressed in 3% NaCl solution at 25 - 70°C, and has proposed that the mechanism is therefore related to the migration of single and double vacancies, respectively.

(179)

Nichols and Rostoker compared the temperature dependence of three alloys in which cracking can occur by exposure to either liquid metals or aqueous media. For an age-hardened aluminum alloy exposed to NaCl-Na<sub>2</sub>CrO<sub>4</sub>-HCl solutions, the cracking time was almost independent of temperature over the range 3 - 60°C, as was the embrittlement by liquid mercury over the range 10 - 80°C. For a 70Cu-30Zn alloy exposed to ammonia, the cracking time decreased





slightly with temperature (15 - 75°C) although there was considerable scatter in the points (this will be discussed later); the same alloy, exposed to mercury, also showed a slight decrease in fracture stress with temperature, although the choice of fracture stress as a suitable parameter makes the comparison less reliable. The only large temperature dependence was found for an age-hardened Cu-2% Be alloy exposed to ammonia or mercury (25 - 85°C). For both types of cracking, the temperature dependence did not conform to the Arrhenius relation.

(208)

An apparent activation energy of 10 kcal/mole has been found for the cracking of mild steel in  $\text{NH}_4\text{NO}_3$  solution over the range 40 - 96°C, which agrees with the values found by Winterstein et al. for the cracking of mild steel in  $\text{Ca}(\text{NO}_3)_2$ - $\text{NH}_4\text{NO}_3$  solutions.

(209)

## B. TOPOGRAPHY

(114)

Gulbransen and Copan have shown that the growth of oxides on the surfaces of iron, nickel chromium and stainless steel oxidized in oxygen or steam is affected by stress, in that thin oxide platelets (about 100 Å thick) are favored in the presence of stress, presumably because of an ordered pattern of nucleation sites. Since the formation of these platelets presumably depends on a very localized source of metal ions, the authors proposed that a 'trench' may be formed at the



base of the platelets. In aqueous media the corrosion product might dissolve, so that the trench could lead to the initiation of cracks under the influence of applied stress.

### C. WEDGING ACTION OF CORROSION PRODUCTS

(110)

Nielsen was the first to demonstrate that the cathodic deposition of corrosion products within cracks in an 18Cr-8Ni stainless steel might exert large hydrostatic pressures, and suggested that such pressures would contribute<sup>to</sup> the propagation of stress corrosion cracks.

(120)

Pickering et al. followed up Nielsen's work with a quantitative study of the wedging action produced by the solid corrosion products formed in notched specimens of 18Cr-8Ni stainless steel exposed to acidic NaCl solutions. It was found that pressures in excess of 7000 psi were developed in the cracks, and that these pressures were sufficient to propagate pre-existing cracks without the application of any external stress. It seems clear that in those systems where solid corrosion products (having a larger specific volume than the alloy from which they are formed) can be formed in cracks, the wedging action will undoubtedly contribute to the crack propagation, but according to Pickering (120) et al. this extended propagation is limited to only a few atomic distances ahead of the crack tip, and cannot be responsible for a freely 'running' crack.



## 7. STRESS CORROSION CRACKING MECHANISMS

A phenomenological description of stress corrosion cracking is simple: cracks which are initiated by electrochemical processes at the surface of the alloy propagate even under low applied tensile stresses to produce a failure which is very rapid compared with the usual rates of metal dissolution, but still is slower than would be expected for a brittle fracture. However, the information presented in the previous six sections shows that the mechanism of the process is not simple, because the following observations must be explained:

a) The crack initiation cannot be predicted merely on the basis of the general corrosive behavior of the electrolyte with respect to the alloy as a whole, or with respect to individual constituents of the alloy. In other words, the chemical medium must possess certain unique characteristics which make it effective as a cracking agent.

b) The crack initiation sites in polycrystalline material can be changed from grain boundaries to grain bodies by a change in metallurgical factors (e.g., alloy composition, heat treatment) or by a change in the chemical environment.

c) The path of the crack propagation can similarly be changed by a change in chemical or metallurgical factors.

d) The crack propagation can occur with little evidence of plastic deformation, in alloys that normally fail in a ductile manner.





e) Both crack propagation and initiation steps can be prevented by the application of cathodic protection.

Many theories have been proposed for the mechanism of stress corrosion cracking in specific systems, but in general they can be divided into two groups, depending on the relative emphasis placed on the electrochemical or mechanical factors. These two groups are (using Barnartt's<sup>(100)</sup> terminology):

a) Continuous Electrochemical (CE) mechanism, in which the crack propagation occurs solely by rapid anodic dissolution of metal along selective paths;

b) Periodic Electrochemical-Mechanical (PEM) mechanism, in which the anodic dissolution of the metal only creates a notch which then acts as a stress raiser; when the stress exceeds a critical value, the crack propagates mechanically for a short distance until halted by the relaxation of the stress, or by an encounter with obstacles.

A review of these mechanisms has been presented by Barnartt<sup>(100)</sup>.

In summary, the main points are:

a) The PEM mechanism is indicated in many systems by the discontinuous nature of crack propagation. Intermittent crack bursts have been observed for intergranular cracking of Al-7Mg<sup>(153)(235)</sup> and Al-4Cu<sup>(235)</sup> alloys in NaCl solutions, for mild steel in nitrate solutions<sup>(207)(210)(235)</sup> for the transgranular cracking of Mg-6Al-1Zn



in  $\text{NaCl-K}_2\text{CrO}_4$ ,<sup>(136)</sup> for austenitic steels subjected to intermittent wetting and drying in  $\text{NaCl}$  solutions,<sup>(241)</sup> and for intergranular and transgranular cracking of brass in ammonia.<sup>(238)</sup> On the other hand, no sudden fracture steps have been detected during the intergranular cracking of  $\text{Mg-6Al-1Zn}$  in  $\text{NaCl-K}_2\text{CrO}_4$ ,<sup>(136)</sup> or during the transgranular cracking of stainless steels in boiling 42%  $\text{MgCl}_2$ .<sup>(91)235)</sup> However, as Barnartt<sup>(100)</sup> points out, the mechanical fracture steps may be so short and frequent that they have escaped detection in these last two systems.

b) One of the chief arguments against the CE mechanism is that the estimated current densities that would be required at the crack tip must be extremely high in order to account for the rapid crack propagation. For the intergranular cracking of mild steel in  $\text{Ca}(\text{NO}_3)_2$  the required current density was calculated to be 400  $\text{amps/cm}^2$  by Engell and Baumel,<sup>(207)</sup> and 0.15  $\text{amps/cm}^2$  by Logan.<sup>(210)</sup> The large difference in these calculations is due to the difference in estimated crack propagation rates: the first calculation is based on the observation that discontinuous elongations of the specimens occurred in one second (or less) jumps (giving an average crack penetration rate of  $2 \times 10^{-2}$   $\text{cm/sec}$ ) whereas Logan assumed that the crack tip was continuously dissolved (giving an average penetration rate of  $5 \times 10^{-6}$   $\text{cm/sec}$ .)

The required current density (at the crack tip) for the transgranular cracking of 18Cr-8Ni stainless steels in  $\text{MgCl}_2$  was calculated to be in the range 0.4 - 2.0  $\text{amps/cm}^2$ ;<sup>(173)</sup> for the cracking of  $\text{Mg-3Al-1Zn}$



in NaCl-K<sub>2</sub>CrO<sub>4</sub> it was calculated to be 14 amps/cm<sup>2</sup>.<sup>(211)</sup> All of these values are high, but Hoar and West<sup>(242)</sup> showed that an 18Cr-8Ni stainless steel wire could sustain current densities of 0.5 amps/cm<sup>2</sup> if it was strained at a rate of about 300%/minute in a streaming solution. Van Rooyen<sup>(109)</sup> could not confirm these results, but according to Hoar,<sup>(173)</sup> additional recent work in his laboratory has shown that strain rates of 100%/minute (in streaming solutions) can produce a 10<sup>4</sup> increase in the dissolution rate (as compared with the anodic dissolution rate of static metal at the same potential). Concentration polarization in the crack is said to be avoided by the yawning of the crack, sucking in fresh supplies of electrolyte.<sup>(243)</sup> Thus the CEM mechanism is presumed to operate by the rapid anodic dissolution of the plastically yielding metal at the tip of the crack.

c) A PEM mechanism, based on observations made of the cracking of single crystals of brass in ammonia, has been proposed by Forty.<sup>(238)(245)</sup> According to his theory, cracks, once initiated, can propagate (microscopically) only in those alloys in which slip is highly restricted; this propagation is halted when the crack reaches a pre-existing slip band. Further chemical reaction leads to a re-initiation of the crack, and the process repeats itself.

Logan's film-rupture mechanism<sup>(245)</sup> makes use of both the CEM and PEM mechanisms. He has proposed that the rupture of





passivating films on an alloy surface produces fresh areas of metal that are anodic to the film; intense dissolution in these areas can proceed only if the local strain rate is great enough to prevent healing of the film. Crack propagation can then proceed by anodic dissolution of fresh metal at the tip of the crack where high yielding rates prevent film formation (CEM) unless the strains are readjusted to lower values, in which case the crack will stop. If, however, the stresses become more concentrated, a mechanical fracture step may result (PEM).

The correlation of dislocation substructure with stress corrosion susceptibility<sup>(247)(251)</sup> has provided the best explanation to date for the structural dependence of crack initiation and propagation; further electron metallographic studies will undoubtedly clarify the many metallurgical factors involved. However, none of the work so far has been able to adequately explain why stress corrosion cracking is limited to a few chemical environments, which are specific for each alloy, and yet apparently quite different, chemically, from one system to another.

In order to explain the chemical dependence of the cracking of homogeneous alloys, Graf<sup>(76)</sup> has formulated a set of general rules which state that

- a) Susceptibility is caused by addition of alloying components more noble than the principal alloy component;
- b) susceptibility increases with the increasing concentration



- of the more noble component, reaching a maximum at 20-30at%.
- c) The corrosive agent must react strongly with the least noble component.

His predictions are borne out for a number of homogeneous alloys, but one of the notable exceptions is the Cu-Zn system, which according to his rules should be immune to cracking.

## SURFACE ENERGY CONCEPTS IN STRESS CORROSION CRACKING

In order to account for the specific action of certain chemicals in stress corrosion cracking, it has been suggested<sup>(184-187)</sup> that specific adsorption of surface active species may either reduce the surface energy of the metal to facilitate the creation of surface slip steps, or penetrate into microcracks and provide lateral pressures by strong adsorption there. The most commendable features of this suggestion are that it is simple and that it augments rather than contradicts the PEM mechanism or the film-rupture mechanism.

There is ample proof that surfactants can have a marked effect (the Rehbinder effect) on the flow stress of metals and alloys<sup>(253)</sup> but to-date there have been very few papers dealing with surface energy



lowering in stress corrosion cracking systems. It is interesting to note, however, that there are at least two examples in the literature where the addition of a 'known' surfactant to a stress corrosion system has produced a significant reduction in cracking time. The first example was reported by Titova<sup>(31)</sup> and has been mentioned in the literature review. The second example is provided by Backensto and Yurick,<sup>(254)</sup> who found that commercially available amine-type inhibitors increased the susceptibility of several austenitic stainless steels exposed to  $\text{NH}_4\text{Cl}$  solutions.

Much of the development of the surface energy mechanism is due to Rostoker and his co-workers; their quantitative treatment of the surface energy lowering, which was developed during extensive studies of liquid metal embrittlement,<sup>(163)</sup> may be summarized as follows: The Griffith formula for brittle crack propagation is

$$\sigma \propto (E\gamma/C)^{1/2}$$

where  $\sigma$  is the applied stress needed to propagate an elastic crack of length  $C$  in a material of Young's modulus  $E$ .  $\gamma$  is the surface free energy. Clearly, if  $\gamma$  is reduced by adsorption of a surface active species, the crack may propagate under lower applied stresses.

The effective surface energy associated with brittle fracture can be estimated from the Stroh-Petch relationship

$$\sigma_F = \sigma_0 + K \cdot d^{-1/2}$$





where  $\sigma_F$  = fracture stress;  $d$  = average grain diameter;  $\sigma_0$  and  $K$  are functional constants of which

$$K = \left( \frac{6\pi G\gamma}{1-\nu} \right)$$

where  $G$  is the rigidity modulus, and  $\nu$  is Poisson's ratio. Thus a plot of  $\sigma_F$  vs.  $d^{-1/2}$  allows the estimation of the effective surface energy.

Coleman, Weinstein and Rostoker<sup>(184)</sup> have used the Stroh-Petch equation to calculate the effective surface energies of 157 ergs/cm<sup>2</sup> and 93 ergs/cm<sup>2</sup> associated with the transgranular cracking of 18Cr-8Ni stainless steel in MgCl<sub>2</sub> solution and the cracking of Mg-6Al in NaCl-K<sub>2</sub>CrO<sub>4</sub> solution, respectively. Both of these values are much lower than the estimated surface free energies of stainless steel (about 10<sup>3</sup> ergs/cm<sup>2</sup>) and of Mg-6Al (about 500 ergs/cm<sup>2</sup>), showing that the lowering of surface free energy did occur.

No similar calculations have yet been made for the cracking of brass in ammonia, but Robertson and Tetelman<sup>(249)</sup> have replotted the data of Edmunds<sup>(128)</sup> to show that a linear relation between cracking time and  $d^{-1/2}$  exists; for the embrittlement of brass by mercury, Nichols and Rostoker<sup>(254)</sup> have calculated an effective surface energy of 280 ergs/cm<sup>2</sup>, which is considerably lower than the estimated surface free energy of brass with respect to its own vapor (about 1500 ergs/cm<sup>2</sup><sup>(188)</sup>).

Nichols and Rostoker<sup>(179)</sup> have also found that temperature and prior cold working have similar influences on the cracking rates of



an Al-4.5%Cu -1.5%Mg-0.6%Mn alloy exposed to either mercury or NaCl-Na<sub>2</sub>CrO<sub>4</sub>-HCl solution and of a Cu-2%Be alloy exposed to either mercury or ammonia. The effect of temperature on the cracking of 70Cu-30Zn exposed to mercury or ammonia was not comparable, for reasons that will be discussed later.

The Griffith equation requires the prior existence of a micro-crack, which in the Stroh-Petch equation is assumed to be generated by a dislocation mechanism. In stress corrosion cracking, this micro-crack may be caused by the intensified corrosion at specific reaction sites; this would account for the influence of electrochemical factors. On the other hand, the surface active species responsible for the reduction of the surface free energy may be a transient species, generated by an electrochemical reaction; a third possibility is that the electrochemical potential of the solid/solution interface may affect the adsorption step in the same way that the potential affects the adsorption of solutes on mercury (the electrocapillary effect).

It is important to note that the Griffith criterion assumes that the surface free energy term represents only the energy needed to provide two new uncontaminated and 'undeformed' surfaces; if some plastic deformation precedes fracture, the brittle fracture criterion of the form

$$\sigma \approx \left( \frac{E_p}{C} \right)^{1/2}$$



has to be used, where  $p$  is the effective surface energy term which includes  $\gamma$  and the energy expended in plastic deformation. Since  $p$  may be orders of magnitude greater than  $\gamma$ ,<sup>(256)</sup> it is important to determine how much plastic deformation takes place. Observations of alpha brass embrittled by mercury<sup>(255)</sup> or cracked by ammonia<sup>(170)</sup> have not shown any plastic deformation which could contribute to large values of  $p$ .

In summary, it seems reasonable to conclude that the specific action of certain chemicals in stress corrosion cracking is governed not only by the corrosive action they have towards certain sites on the surface of a stressed metal, but also by the ability of some ionic species (even transient in nature) to adsorb and to modify the surface free energy at the tip of a microcrack, reducing the effective energy requirements to a point where the fracture criterion is satisfied.





## EXPERIMENTAL METHODS

## 1. MATERIALS

Brass wire (0.036" diameter) of commercial purity was obtained locally and used in the as-received condition (except for chemical cleaning). Spectroscopic analysis (Table II, below) showed an average composition of 65.3% Cu, 34.7% Zn, 0.003% Fe.

TABLE II  
SPECTROSCOPIC ANALYSIS OF BRASS

|            | % Average Composition |        |
|------------|-----------------------|--------|
|            | Wire                  | Strip  |
| Copper     | 65.27                 | 69.51  |
| Zinc       | 34.71                 | 30.46  |
| Lead       | <0.001                | <0.001 |
| Tin        | <0.001                | <0.001 |
| Iron       | 0.003                 | 0.01   |
| Arsenic    | <0.003                | <0.003 |
| Aluminum   | <0.001                | <0.001 |
| Magnesium  | <0.001                | <0.001 |
| Manganese  | <0.001                | <0.001 |
| Silicon    | <0.001                | <0.001 |
| Nickel     | <0.001                | 0.003  |
| Antimony   | <0.001                | <0.001 |
| Bismuth    | <0.001                | <0.001 |
| Phosphorus | <0.005                | <0.005 |
| Sulfur     |                       | <0.01  |



Brass strips (10 x 85 mm) were sheared from cold-rolled brass sheet (0.48 mm thickness) which had an average composition of 69.5% Cu, 30.5% Zn, 0.01% Fe and 0.003% Ni (Table II). The strips were sheared with their length normal to the rolling direction. After chemical cleaning, they were stressed by bending over a one-half inch mandrel, and the 'legs' of the specimens were inserted in a 5 ml glass cup (Beckman semi-micro pH beakers). This stressing procedure provided a satisfactory degree of reproducibility in the tests.

All chemicals were reagent grade unless otherwise specified. The distilled water used to make up solutions contained less than 3 ppm dissolved salts.

"Linde" high purity argon (containing < 1 ppm oxygen) was passed through a bed of anhydrous  $\text{CaSO}_4$  (Drierite) before use. Bottled hydrogen (Linde), oxygen (Linde) and carbon dioxide (Matheson Co.) were used without further purification. Ammonia gas containing < 50 ppm  $\text{H}_2\text{O}$  was supplied by the Matheson Co.

## 2. EXPERIMENTS WITH WIRE SPECIMENS

### A. Vacuum System 'A'

Preliminary experiments with wire specimens were designed to allow the corrosion reactions to be carried out in gaseous environments containing gaseous ammonia alone, or in combination with oxygen, carbon dioxide, or air; it was hoped that the change in pressure of the

# THE HISTORY OF THE CITY OF LONDON

OF THE CITY OF LONDON, FROM THE FIRST BEGINNING OF THE CITY, TO THE PRESENT TIME. BY JOHN STOW, AN INHABITANT OF THE SAME. LONDON, PRINTED BY I. B. AT THE SIGN OF THE TUN, IN ST. MARTIN'S PARISH, IN THE CITY OF LONDON. 1618.

THE HISTORY OF THE CITY OF LONDON, FROM THE FIRST BEGINNING OF THE CITY, TO THE PRESENT TIME. BY JOHN STOW, AN INHABITANT OF THE SAME. LONDON, PRINTED BY I. B. AT THE SIGN OF THE TUN, IN ST. MARTIN'S PARISH, IN THE CITY OF LONDON. 1618.

THE HISTORY OF THE CITY OF LONDON

OF THE CITY OF LONDON, FROM THE FIRST BEGINNING OF THE CITY, TO THE PRESENT TIME.

BY JOHN STOW, AN INHABITANT OF THE SAME.

LONDON, PRINTED BY I. B. AT THE SIGN OF THE TUN, IN ST. MARTIN'S PARISH, IN THE CITY OF LONDON.

1618.

THE HISTORY OF THE CITY OF LONDON

OF THE CITY OF LONDON, FROM THE FIRST BEGINNING OF THE CITY, TO THE PRESENT TIME.

BY JOHN STOW, AN INHABITANT OF THE SAME.

LONDON, PRINTED BY I. B. AT THE SIGN OF THE TUN, IN ST. MARTIN'S PARISH, IN THE CITY OF LONDON.

1618.

THE HISTORY OF THE CITY OF LONDON

OF THE CITY OF LONDON, FROM THE FIRST BEGINNING OF THE CITY, TO THE PRESENT TIME.

reacting gas or gases would be a suitable reaction parameter. For this purpose a vacuum system was constructed that would allow evacuation of the reaction chamber containing the stressed wire sample, with subsequent dosage of the various gases from previously calibrated bulbs. Although the reaction of stressed brass in ammonia environments did not prove to be amenable to study in the gas phase, the design and operation of the system is included since they may prove applicable to other metal-gas systems.

A schematic diagram of the apparatus is shown in Fig. 4 ; details of the major components are given in Appendix A. The pumping system consists of a mechanical fore-pump  $P_1$  connected in series with a three-stage oil fractionation pump  $P_2$ . Cold traps (liquid nitrogen)  $C_1$  and  $C_2$  prevent backstreaming of vapor from the pumps. The reaction vessel A, which is connected by a ball joint  $I_3$  to the system, can be roughed out through the bypass line passing through taps  $T_2$ ,  $T_8$  and  $T_{11}$ ; the vessel can then be evacuated to high vacuum (about  $10^{-7}$  torr) through the oil fractionation pump.

Reaction gases are admitted at  $I_2$  to the various-sized calibrated bulbs  $B_1$ - $B_4$ . The gases are then admitted to the reaction vessel through the capillary line (hatched line in Fig. 4) passing through  $T_9$ .

Pressure during evacuation is measured by means of a thermocouple gauge  $G_1$  or a Bayard-Alpert ionization gauge  $G_2$ . Pressure of



(1) The first part of the paper is devoted to the study of the properties of the function  $f(x)$  defined by the equation  $f(x) = \sum_{n=0}^{\infty} a_n x^n$ , where  $a_n$  are the coefficients of the power series. It is shown that  $f(x)$  is a continuous function of  $x$  and that it satisfies the functional equation  $f(x) = x f(x^2) + 1$ . This equation is solved by the method of successive approximations, and it is shown that the function  $f(x)$  is unique.

(2) In the second part of the paper, the function  $f(x)$  is studied in more detail. It is shown that  $f(x)$  is a monotonic increasing function of  $x$  and that it is concave down. It is also shown that  $f(x)$  is a solution of the differential equation  $f'(x) = 2x f(x)$ . This equation is solved by the method of separation of variables, and it is shown that the function  $f(x)$  is unique.

(3) In the third part of the paper, the function  $f(x)$  is studied in still more detail. It is shown that  $f(x)$  is a function of bounded variation and that it is differentiable almost everywhere. It is also shown that  $f(x)$  is a function of bounded variation and that it is differentiable almost everywhere.

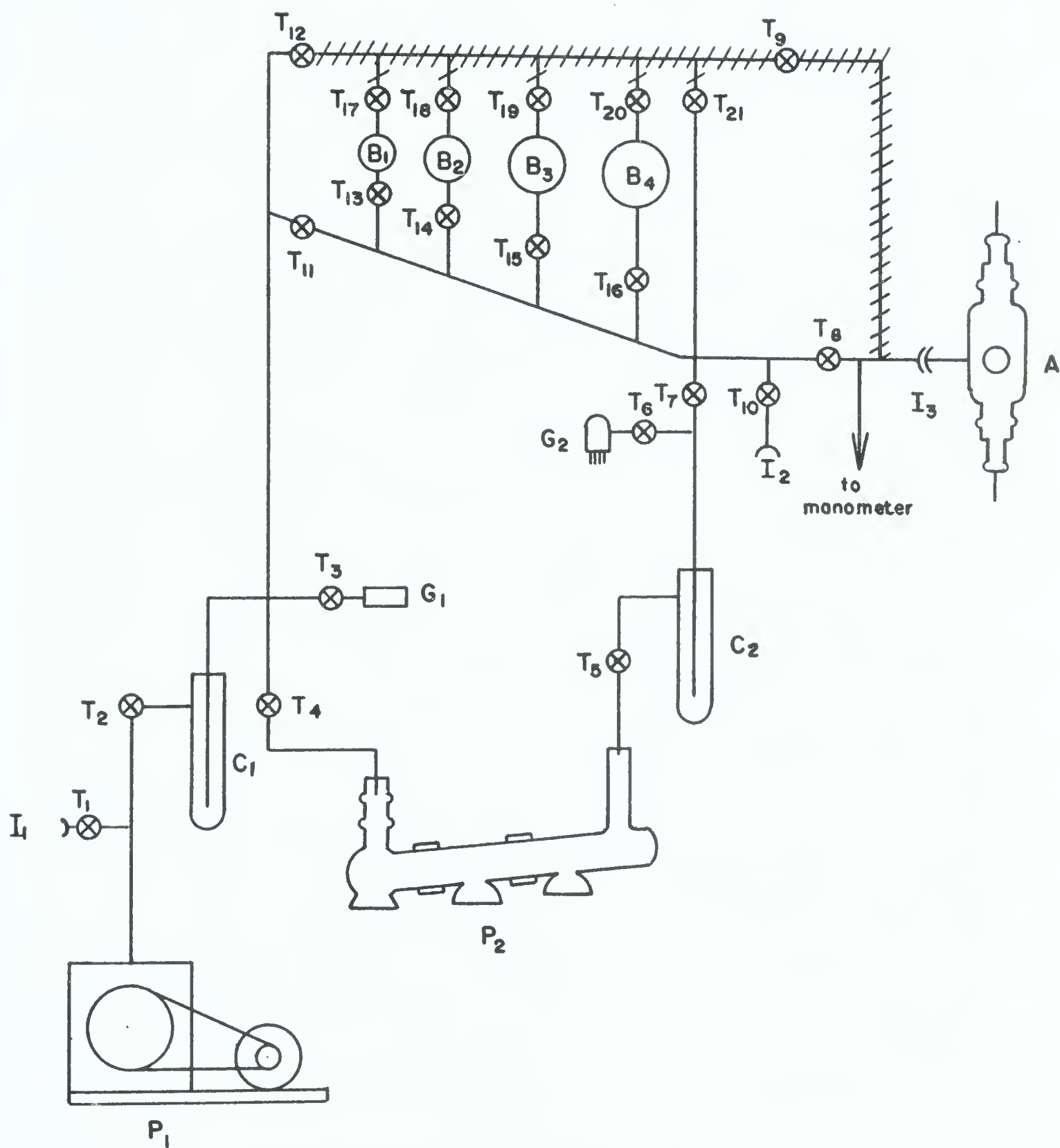


Fig. 4 Schematic diagram of vacuum system "A"



the reacting gases can be monitored by the manometer connected between  $T_8$  and  $I_3$ .

#### B. Reaction Vessel Design

Several reaction vessels were built to study the corrosion of stressed wire specimens in controlled atmospheres. Three of the modifications will be described here, since each has certain advantages, although none satisfies all the critical testing requirements, which are:

- a) the vessel components must be non-reactive with the  
chosen environment
- b) the stress on the specimen, which is applied from outside  
the reaction chamber, must be uniform, measurable and  
reproducible
- c) the seal through which the stress is transmitted must be  
vacuum-tight
- d) the volume should be as small as possible in relation to  
the surface area of the specimen
- e) some means of visual and/or microscopic viewing of the  
specimen surface should be provided.

In the designs sketched in Figs. 5 and 6, the basic reaction vessel is a cylindrical glass tube (70 mm O.D. x 150 mm long) fitted with a ball joint side tube for connection to the vacuum system, and 45/50 tapered glass outer joints at each end to accomodate the seals

1. The first part of the paper is devoted to the study of the

properties of the

operator  $T$  defined by

$Tf(x) = \int_0^x f(t) dt$  for  $f \in L^p(\mathbb{R})$ .

It is shown that  $T$  is a bounded operator from  $L^p(\mathbb{R})$  to  $L^p(\mathbb{R})$ .

2. The second part of the paper is devoted to the study of the

operator  $T$  defined by  $Tf(x) = \int_0^x f(t) dt$  for  $f \in L^p(\mathbb{R})$ .

It is shown that  $T$  is a bounded operator from  $L^p(\mathbb{R})$  to  $L^p(\mathbb{R})$ .

3. The third part of the paper is devoted to the study of the

operator  $T$  defined by  $Tf(x) = \int_0^x f(t) dt$  for  $f \in L^p(\mathbb{R})$ .

It is shown that  $T$  is a bounded operator from  $L^p(\mathbb{R})$  to  $L^p(\mathbb{R})$ .

4. The fourth part of the paper is devoted to the study of the

operator  $T$  defined by  $Tf(x) = \int_0^x f(t) dt$  for  $f \in L^p(\mathbb{R})$ .

It is shown that  $T$  is a bounded operator from  $L^p(\mathbb{R})$  to  $L^p(\mathbb{R})$ .

5. The fifth part of the paper is devoted to the study of the

operator  $T$  defined by  $Tf(x) = \int_0^x f(t) dt$  for  $f \in L^p(\mathbb{R})$ .

It is shown that  $T$  is a bounded operator from  $L^p(\mathbb{R})$  to  $L^p(\mathbb{R})$ .

6. The sixth part of the paper is devoted to the study of the

operator  $T$  defined by  $Tf(x) = \int_0^x f(t) dt$  for  $f \in L^p(\mathbb{R})$ .

It is shown that  $T$  is a bounded operator from  $L^p(\mathbb{R})$  to  $L^p(\mathbb{R})$ .

7. The seventh part of the paper is devoted to the study of the

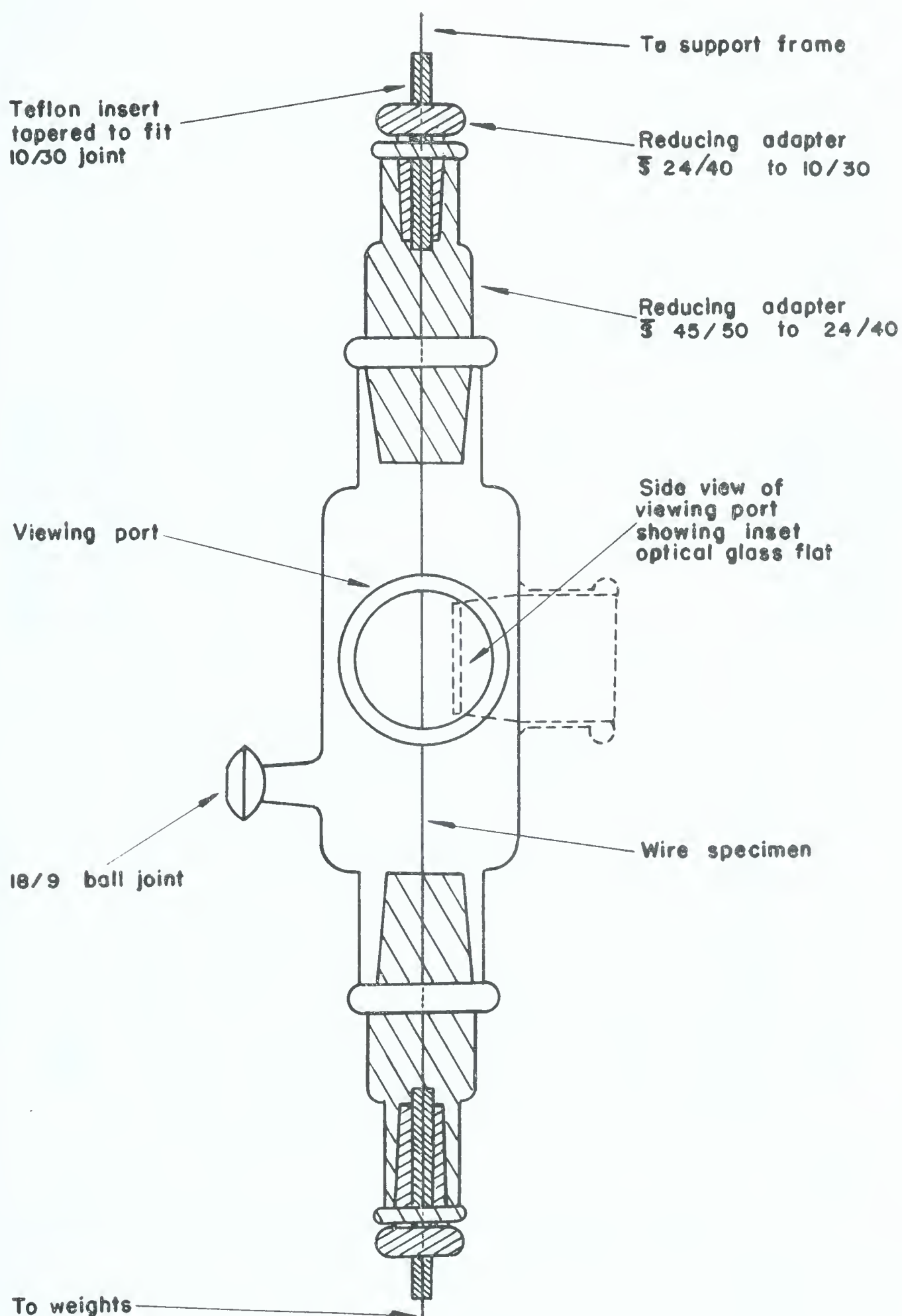


Fig. 5 Reaction vessel with seal modification I





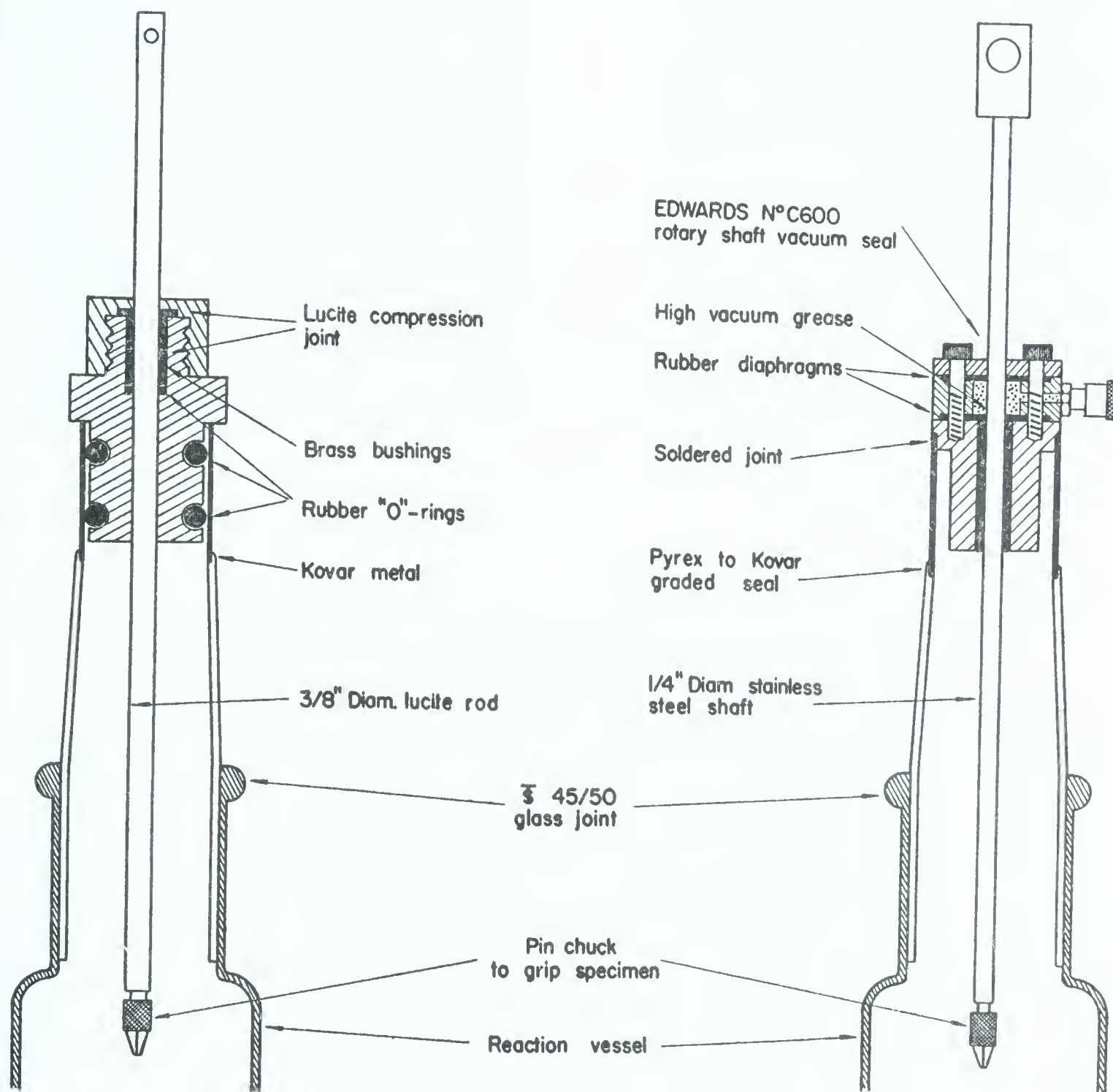


Fig. 6 Details of seal modifications II and III



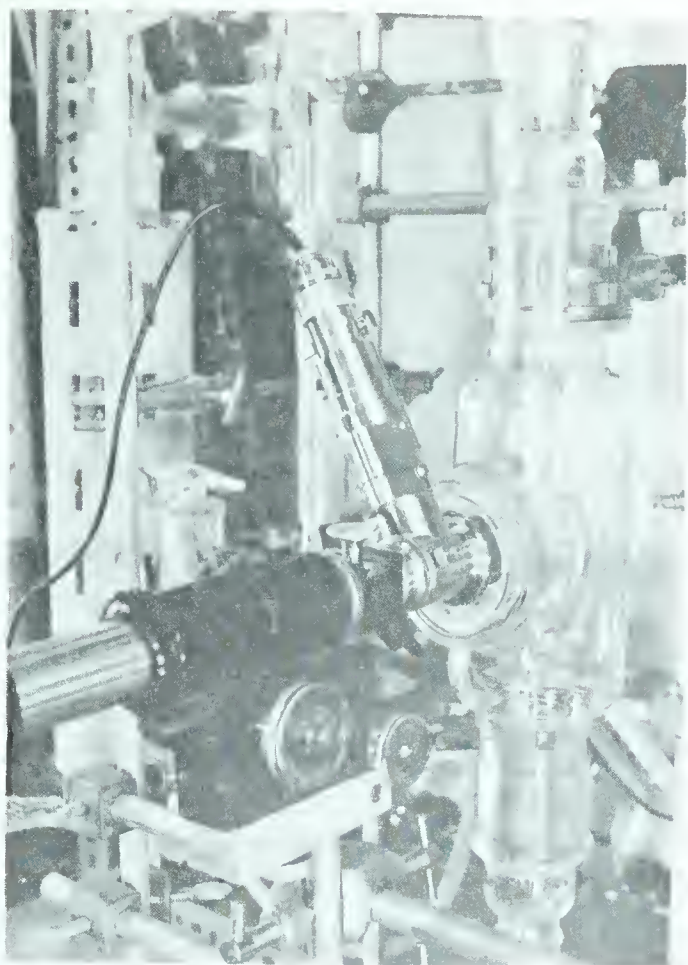
through which the linear motion of the stress is transmitted. An optical glass flat (50 mm diameter) is recessed into the center of the vessel to allow microscopic viewing of the specimen. The microscope is fitted with a Leitz Ultropak incident light illuminator and Achromat objectives which have a working distance of either 26.3 or 33 mm, and in combination with a 25X eyepiece, allow examination at magnifications up to 125X.

Fig. 7a is a photograph of the reaction vessel (with the microscope in position) using the seal modification(I) sketched in Fig. 5 . Seal (I) consists of a cylindrical Teflon insert, tapered on the outside to fit a 10/30 tapered glass reducing adapter. The specimen passes through a hole drilled in the Teflon insert; the size of the hole is critical, and should be as near to the diameter of the wire as possible, in order to prevent leakage of air into the vessel. Seal (I) is simple and non-reactive; however, the attainment of a high vacuum means a sacrifice in the reproducibility of the applied stress, since there will be some frictional drag in the seal if the hole size is too small (even though Teflon, lubricated with high vacuum grease, offers very little resistance).

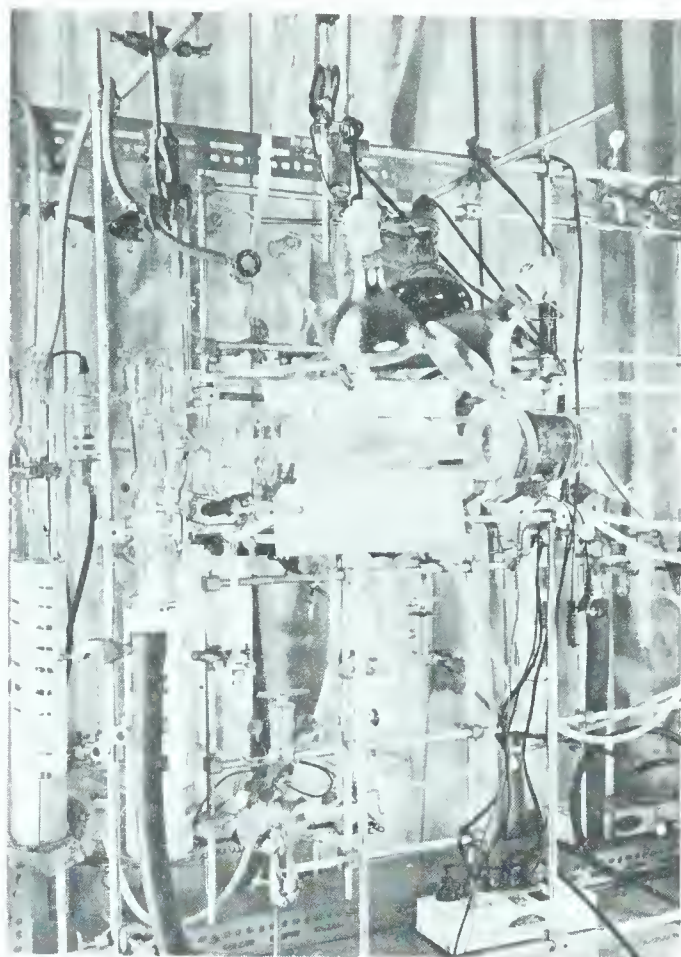
In Fig. 6 , only the details of modified seals (II) and (III) are sketched, the reaction vessel being the same as in Fig. 5. Seal (II) is constructed from non-reactive Lucite plastic, and relies upon two double sets of rubber 'O-rings' for its vacuum tightness. The wire



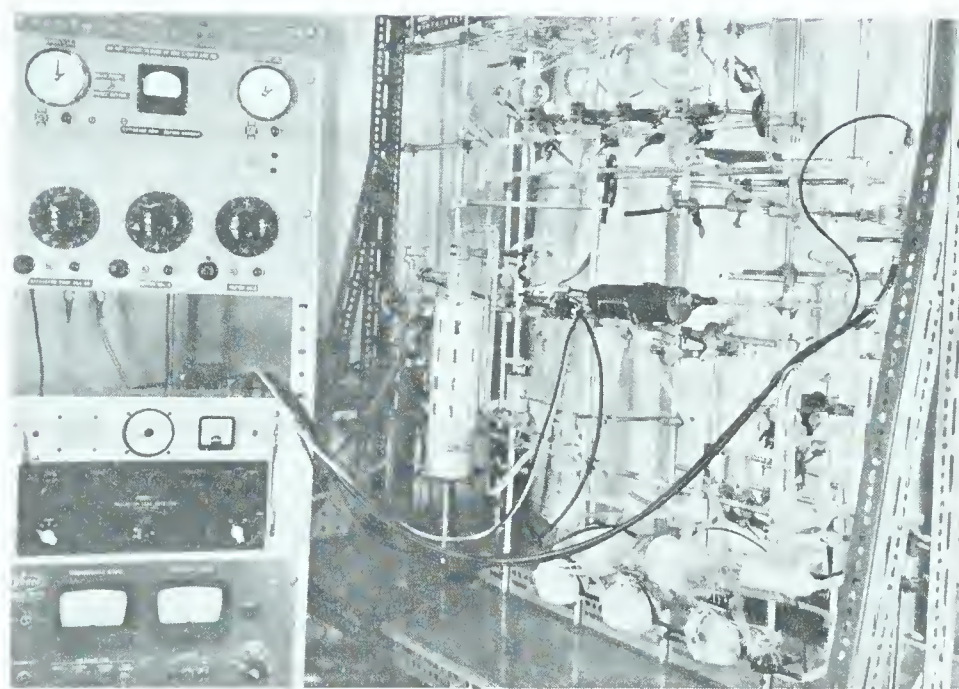




(a)



(b)



(c)

Fig. 7 a) Reaction vessel (for wire specimens) in operation using seal modification I  
 b) Vacuum system "B"; stressed strip specimen is visible in reaction vessel in center of photograph  
 c) General view of basic pumping system and controls used for vacuum systems "A" and "B"





specimen is gripped by a pin chuck which is threaded into the end of a 3/8" diameter Lucite rod. The frictional drag exerted on this rod by the smaller set of 'O-rings' can be adjusted by means of the Lucite compression joint. As in Seal (I), the tightness of this joint necessitates a compromise between the desired vacuum and the reproducibility of the applied stress.

Both Seals (II) and (III) are mounted in 45/50 glass joints which are fitted with Kovar metal cylinders at the ends opposite the glass taper. Seal (III), which is joined to the Kovar by a soldered joint, is an Edwards No. C600 rotary shaft vacuum seal. As in Seal (II), the wire specimen is gripped in a pin chuck fastened to the end of a 1/4" diameter stainless steel shaft which passes through the body of the seal. Vacuum tightness is maintained by two rubber diaphragms enclosing an annular space filled with high vacuum grease. Although this seal is primarily designed for rotary movement, it shows very little frictional drag for the small linear movements required in this application. Its chief disadvantage lies in its metal construction, which makes large metallic areas available for reaction with the corrosive environment. To a lesser extent, this disadvantage also applies to Seal (II), since the pin chuck and part of the Kovar cylinder are exposed.



### C. Loading Device

In all three of the seal modifications described above, the rod or wire protruding through the upper seal was securely fastened to a rigid frame which could be adjusted in the horizontal plane in order to position the reaction vessel with respect to the vacuum connection  $I_3$ .

The specimen was then put in tension by a direct load of weights fastened to the rod or wire which extended through the bottom seal. For un-notched specimens, the load was 20 lbs (about 18,000 psi). The weight was reduced to 5 lbs for notched specimens; no attempt was made to calculate the stress.

### D. Procedure

A suitable length of wire was cut, etched in dilute nitric acid, washed in distilled water, rinsed in acetone, dried in air and mounted in the test chamber. (A few specimens were notched before chemical cleaning to reduce the cross-sectional area to about two-thirds of the original area. This notch was positioned so that it could be viewed through the microscope). The load was applied before the seals were tightened. The system was then evacuated to about  $10^{-7}$  torr, and the reaction gas or gases admitted from a storage bulb. In all tests the original pressure of the gas or gas mixture was one atmosphere; expansion into the test chamber resulted in an estimated pressure of about 50 cm Hg.



### 3. EXPERIMENTS WITH STRIP SPECIMENS

#### A. Vacuum System 'B'

Because of the problems encountered in transmitting a reproducible stress to the wire specimens in vacuum system 'A', and because of the failure to produce cracking in purely gaseous atmospheres, modifications were made to the apparatus to allow a stressed strip specimen to be totally enclosed in a reaction vessel, thus obviating the need for a seal. Under these conditions the system could be evacuated, the surface of the specimen treated with a stream of hot hydrogen; and a corrosive solution could be admitted in a controlled atmosphere.

A schematic diagram of the modified system is shown in Fig. 8. The basic pumping system is the same as in Fig. 4, with pumps  $P_1$  and  $P_2$  providing the means for evacuating the reaction vessel B, which is connected directly to the system by tap  $T_{23}$ ; this eliminates the ball joint  $I_3$  which was a source of many air leaks. Pump  $P_3$  is used for roughing out the reaction vessel when flushing with argon, which is admitted at  $I_4$ ; an additional thermocouple gauge  $G_3$  is used for pressure measurement during the flushing procedure. Hydrogen is admitted at  $I_5$  through a three-way tap  $T_{26}$  and a tapered joint  $I_6$ ; unreacted hydrogen and water vapor are vented to atmosphere (where the hydrogen is burned) through  $I_4$ .





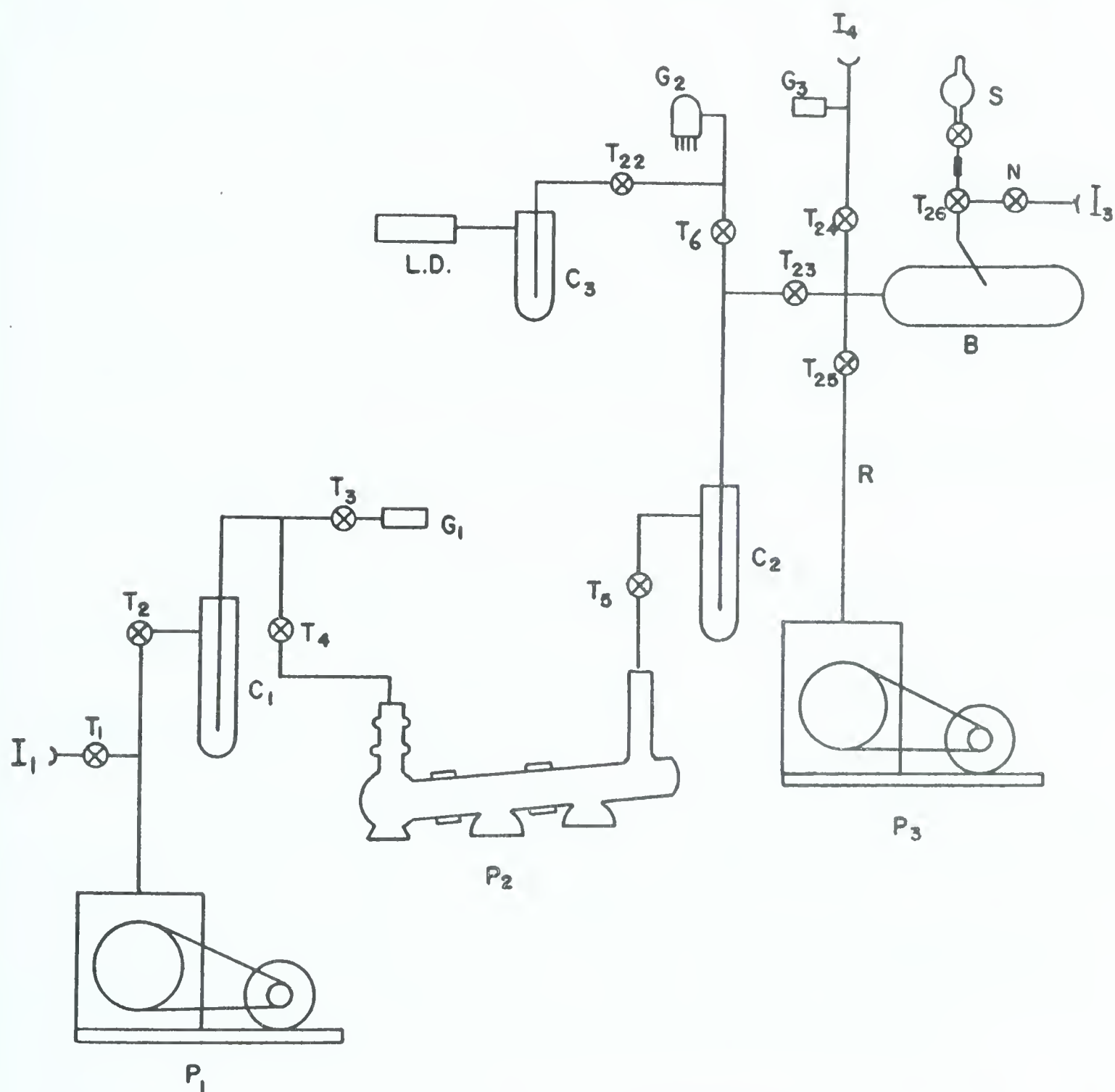


Fig. 8 Schematic diagram of vacuum system "B"



For ease in leak testing, a palladium barrier leak detector L.D. and accompanying cold trap  $C_3$  are connected to the system via  $T_{22}$ .

General views of the system and accompanying controls are shown in Figs. 7b and 7c.

### B. Reaction Chamber

The reaction chamber (Fig. 9) is a Pyrex cylinder (70 mm diameter x 300 mm long) fitted at both ends with 71/60 tapered glass joints for dismantling, and an inlet  $I_6$  through which a tapered tube with a 10/30 joint can be inserted to admit either hydrogen gas (via needle valve N) or a corrosive solution from the separatory funnel S by means of a three-way tap  $T_{26}$ .

Tygon tubing encircling both ends of the reaction chamber permit water cooling of the greased joints to prevent vaporization of the vacuum grease (Apiezon T) during heating of the tube.

The stressed specimen, which is mounted in a glass cup, slides on a flat glass 'platform' and can be manipulated from outside the vessel by means of a magnetic pushing device sealed in glass which easily responds to the influence of another magnet placed against the exterior wall of the vessel.

The specimens are heated by radiation from three 250-watt infrared heat lamps. During heating, aluminum foil is wrapped around the vessel and lamps in order to increase the heating efficiency; the temperature in the vessel reaches 250 - 300°C.



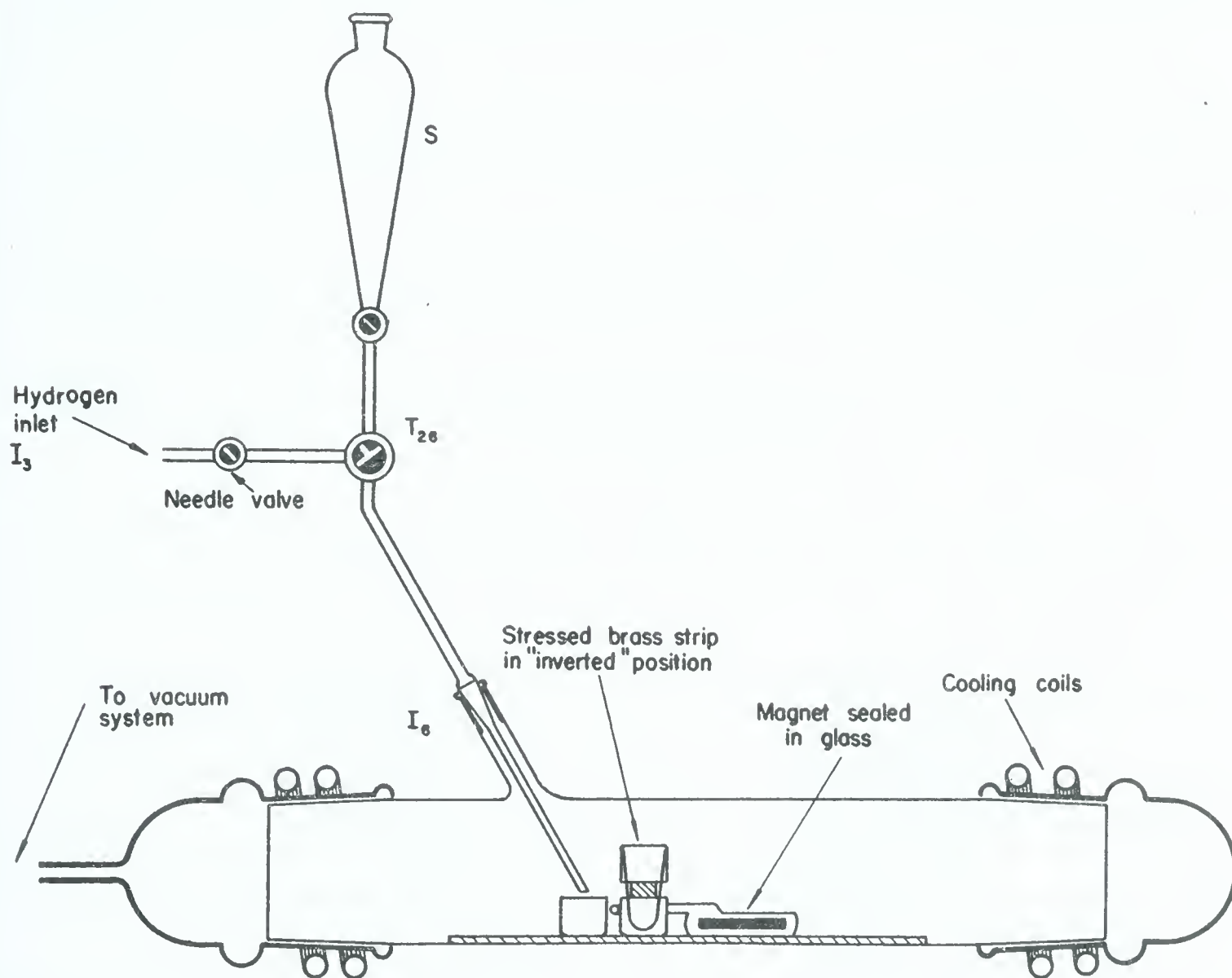


Fig. 9 Details of reaction chamber (for strip specimens)





### C. Procedure for Experiments in Vacuum System 'B'

Brass strips were cleaned by immersion in 45% nitric acid solution for 25 - 30 seconds; they were then washed in distilled water, rinsed in acetone, dried in air, bent and mounted in the 5 ml glass cups. Specimens and cups were handled with rubber gloves or absorbent tissue to avoid contamination of the samples. Fig. 10a shows the stressed specimen in what will be referred to as the 'normal' position; in Fig. 10b the specimen has been inverted in a second glass cup and supported by a rectangular glass block so that the curved surface of the brass is about 4 mm above the bottom of the glass cup.

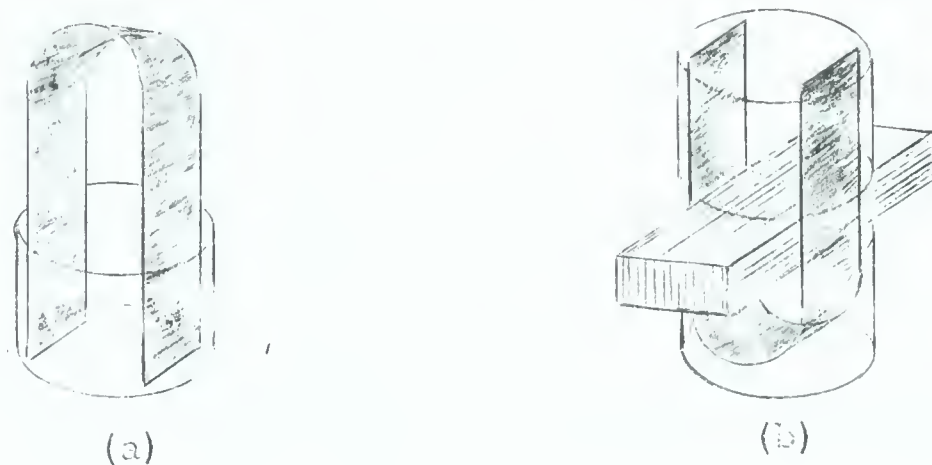


Fig. 10 Stressed brass strip; a) 'normal' position  
b) 'inverted' position



After cleaning and mounting the specimen in the 'inverted' position, it was placed in the reaction vessel and pushed to a position under the heat lamps with the magnetic manipulator. The vessel was then pumped down to about 30 microns Hg through the roughing line R (Fig. 8 ); tap  $T_{25}$  was then closed and argon admitted through  $I_4$  to bring the pressure up to atmospheric. This flushing procedure was repeated three times. Taps  $T_{24}$  and  $T_{25}$  were then closed,  $T_{23}$  opened, and the vessel evacuated to about  $10^{-7}$  torr.  $T_{23}$  was then closed and hydrogen slowly admitted through needle valve N and  $T_{26}$ . When the pressure in the vessel reached atmospheric, the unreacted hydrogen was exhausted to the atmosphere at  $I_4$  and burned. As soon as a steady flow of hydrogen was obtained, water was circulated through the cooling coils and the heat lamps turned on. Additional cooling of the ends of the vessel was provided when needed by means of two cold-air 'guns' mounted above the apparatus. During the hydrogen reduction procedure a wire mesh safety shield was suspended in front of the equipment.

While the surface of the specimen was being treated with the hot hydrogen, the cracking solution was prepared and transferred to the separatory funnel S which was connected to tap  $T_{26}$  with a short piece of Tygon tubing. At the conclusion of the hydrogen reduction, the heat lamps were turned off, but the flow of hydrogen was continued until the vessel cooled to room temperature. The hydrogen flow was then stopped,



and the cracking solution admitted through inlet tube  $I_6$  into the glass cup containing the stressed specimen. In some of the tests, the first few ml of solution were caught in an empty glass cup and used as blanks to follow pH changes.

The time at which the solution contacted the specimen was recorded as zero time; visual observations were made at frequent time intervals until the specimen showed visible cracking, at which time it was removed from the apparatus, washed in water, dried and stored for examination.

Variations in the above procedure included the substitution of argon for hydrogen during the heating period; and the replacement of hydrogen by oxygen, argon, air and carbon dioxide before the solution was admitted.

#### D. Procedure for Reactions in Aqueous Solutions

Strip specimens were prepared in the same manner as described above, and placed in the 'normal' position in a test tube (29 mm O.D.) containing 25 ml of the cracking solution; the specimen was completely covered by the solution. Inverting the specimen did not change the cracking time, nor did stirring (at room temperature); consequently, all reactions were carried out in the 'normal' position, in unstirred solutions. Unstressed brass strips were also completely immersed in 25 ml of cracking solution in a 20 mm diameter test tube.





The majority of the tests were carried out in solutions containing  $\text{CuSO}_4 \cdot 5\text{H}_2\text{O}$  and  $(\text{NH}_4)_2\text{SO}_4$  adjusted to the desired pH with approximately 1N  $\text{NH}_4\text{OH}$ . Because ageing phenomena have been reported in basic solutions of this type,<sup>(167)(170)</sup> separate stock solutions of 1.5M  $(\text{NH}_4)_2\text{SO}_4$  and 0.15M  $\text{CuSO}_4 \cdot 5\text{H}_2\text{O}$  were made up, and the actual mixing of these and pH adjustment were always carried out immediately before a test. In some of the runs, a visible spectrum and a polarogram of each solution were recorded before and after the tests. Cracking time ( $t_c$ ) was taken as the time interval between immersion of the specimen and the first appearance of cracking visible to the naked eye.

pH measurements were made with a Beckman Zeromatic pH Meter which gave results reproducible to  $\pm 0.03$  pH units, or with a Radiometer Model 4 pH Meter, which had a reproducibility of  $\pm 0.005$  pH units.

#### 4. ANALYTICAL TECHNIQUES

##### A. Polarography

A polarographic technique was selected as the most rapid and precise means of simultaneously determining the total copper and zinc concentrations in test solutions. Both copper and zinc ions give well-defined reduction waves in  $\text{NH}_4\text{Cl-NH}_4\text{OH}$  supporting electrolytes, and since no interfering ions are present, no preliminary treatment of the



unknown solution is necessary. The diffusion currents ( at the half-wave potentials) obtained for unknown solutions are compared with the currents obtained for standard solutions.

Details of the procedure, adapted from a method described by Tyler and Brown,<sup>(171)</sup> are as follows:

- a) Standard Brass Solution -- contained approximately 0.05M Cu (as  $\text{CuSO}_4 \cdot 5\text{H}_2\text{O}$ ) and 0.02M Zn (as  $\text{ZnSO}_4 \cdot 7\text{H}_2\text{O}$ ). The exact copper content was determined volumetrically by the iodine-thiosulfate method (using starch indicator), and the zinc content determined by titration of the same sample with 0.0500N EDTA (using xylenol orange indicator).
- b) Supporting Electrolyte -- was made 1M with respect to  $\text{NH}_4\text{Cl}$  and 1.5M in  $\text{NH}_4\text{OH}$ ; it also contained 76.7 gms/liter  $\text{Na}_2\text{SO}_3$  to eliminate dissolved oxygen, and 0.67 gms/liter of gelatin to suppress any polarographic maxima. Because this solution deteriorates in contact with air, it was renewed weekly and kept tightly corked when not in use.
- c) Tarnish 'solvent' -- The solution used to dissolve brass tarnish for analysis contained 80 gms/liter  $(\text{NH}_4)_2\text{S}_2\text{O}_8$  and was 1.5M in  $\text{NH}_4\text{OH}$ .
- d) Standard Persulfate Solution -- 43.8 gms  $(\text{NH}_4)_2\text{S}_2\text{O}_8$  and 66 ml conc.  $\text{NH}_4\text{OH}$  were diluted to 250 ml with distilled water.



The polarograph is a Radiometer Model PO3 Polariter equipped with an automatic voltage scanning device coupled to a recorder which allows automatic recording of the diffusion currents over a two-volt potential range. The polarographic cell consists of a conventional dropping-mercury cathode, with a saturated calomel reference electrode connected to the cell through a KCl salt bridge.

The analytical procedure is as follows: 3.0 ml of standard or unknown solution are placed in the polarographic cell, and 15.0 ml supporting electrolyte are added. The solution is allowed to stand for five to ten minutes to allow for elimination of dissolved oxygen. Provision is made for a blanket of nitrogen to be maintained on the surface of the solution in the polarographic cell. The instrument was set to measure diffusion currents while the voltage was varied from 0.0 to -2.0 volts (vs. SCE). A bank of resistors in the current measuring circuit permits a change in the sensitivity; in this way concentrations down to  $10^{-5}$ M may be detected. Fig. 11 shows a typical polarogram obtained for the standard brass solution. The diffusion current  $i_d$  was measured graphically as the wave height at the half-wave potential of each ion (-0.63V for Cu, -1.51V for Zn). The wave height is defined as the vertical distance between the straight lines approximating the residual and the diffusion current.





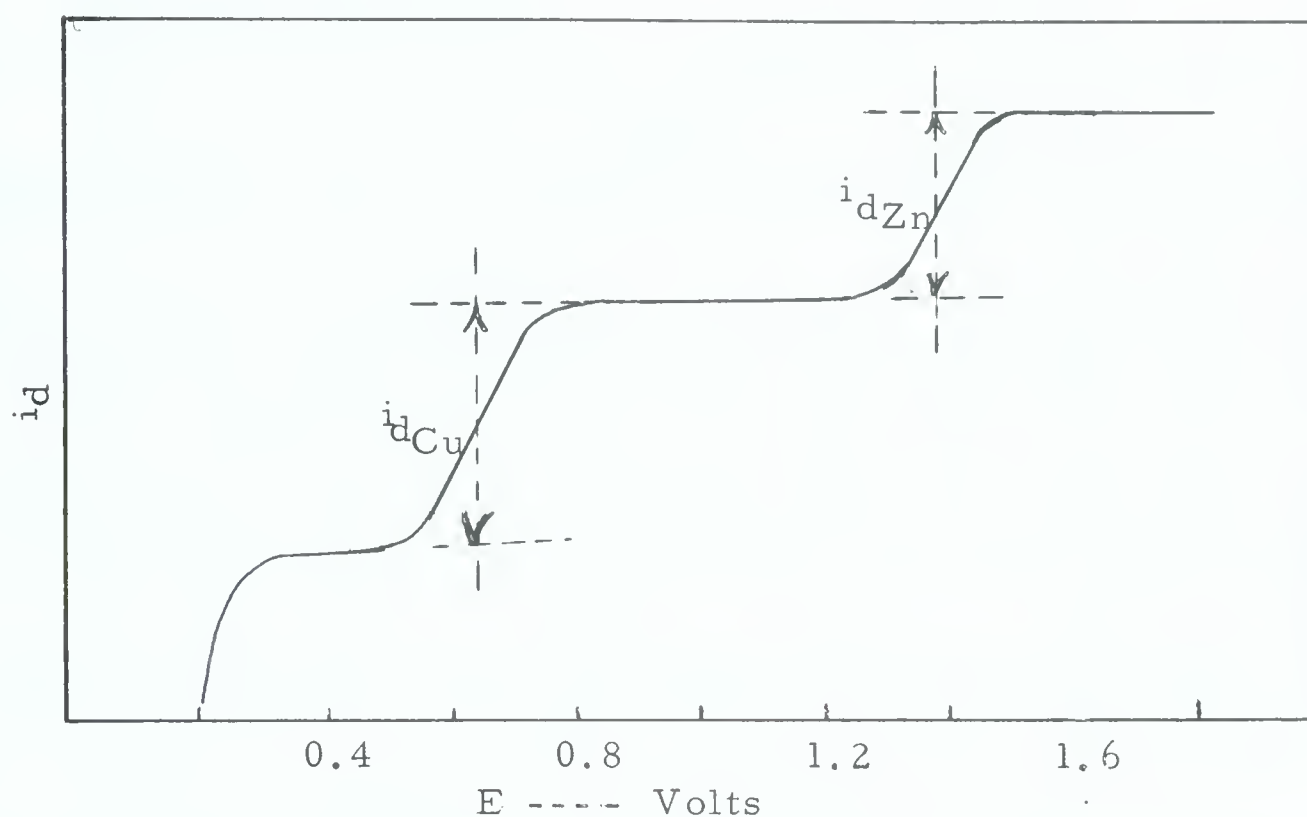


Fig. 11 Typical polarogram of standard brass solution

Because the diffusion current is temperature-sensitive, measurements were carried out in a thermostatically controlled room, and at least one polarogram of a standard solution was made during each 'batch' of analyses.

In order to determine the composition of the black tarnish formed on brass in the copper-ammonia cracking solutions, a weighed amount was scraped from a specimen and dissolved in 5.0 ml of the tarnish 'solvent'; this solution was mixed with 15.0 ml supporting electrolyte and the resulting polarogram compared with a standard polarogram obtained from a solution containing 3.0 ml standard brass solution, 2.0 ml standard persulfate solution and 15.0 ml supporting electrolyte.



## B. Spectrophotometry

Spectrophotometric determinations of the copper-ammonia complexes present in the test solutions were carried out with a Perkin-Elmer Model 350 double-beam, recording spectrophotometer, using a tungsten incandescent light source. The sample cells had a path length of 1.0 cm; water was used as a reference. Absorption measurements were made in the visible wavelength range (350 - 750  $m\mu$ ). A plot of absorbance ( at  $\lambda = 630 m\mu$ ) vs. copper concentration in copper-ammonia solutions of pH 7.10 (Fig. 12) shows the expected negative deviation from Beer's Law, at copper concentrations greater than 0.02M. Because of this deviation, only semi-quantitative comparisons could be made between test solutions of similar pH values.

The wavelength of the absorption peak in the test solutions was correlated with the number of  $NH_3$  groups in the colored copper(II)-amine complexes by comparison with the absorption spectra published by Bjerrum et al.<sup>(172)</sup>(Fig. 13). Because the molar absorptivities of the different complexes vary widely, no quantitative comparisons could be made between solutions having differing absorption peaks.

## C. X-ray Diffraction

X-ray diffraction patterns of the surfaces of tarnished brass strips and of tarnish powder samples were obtained on a Philips X-Ray Diffractometer using copper  $K\alpha$  radiation and a Geiger tube goniometer.



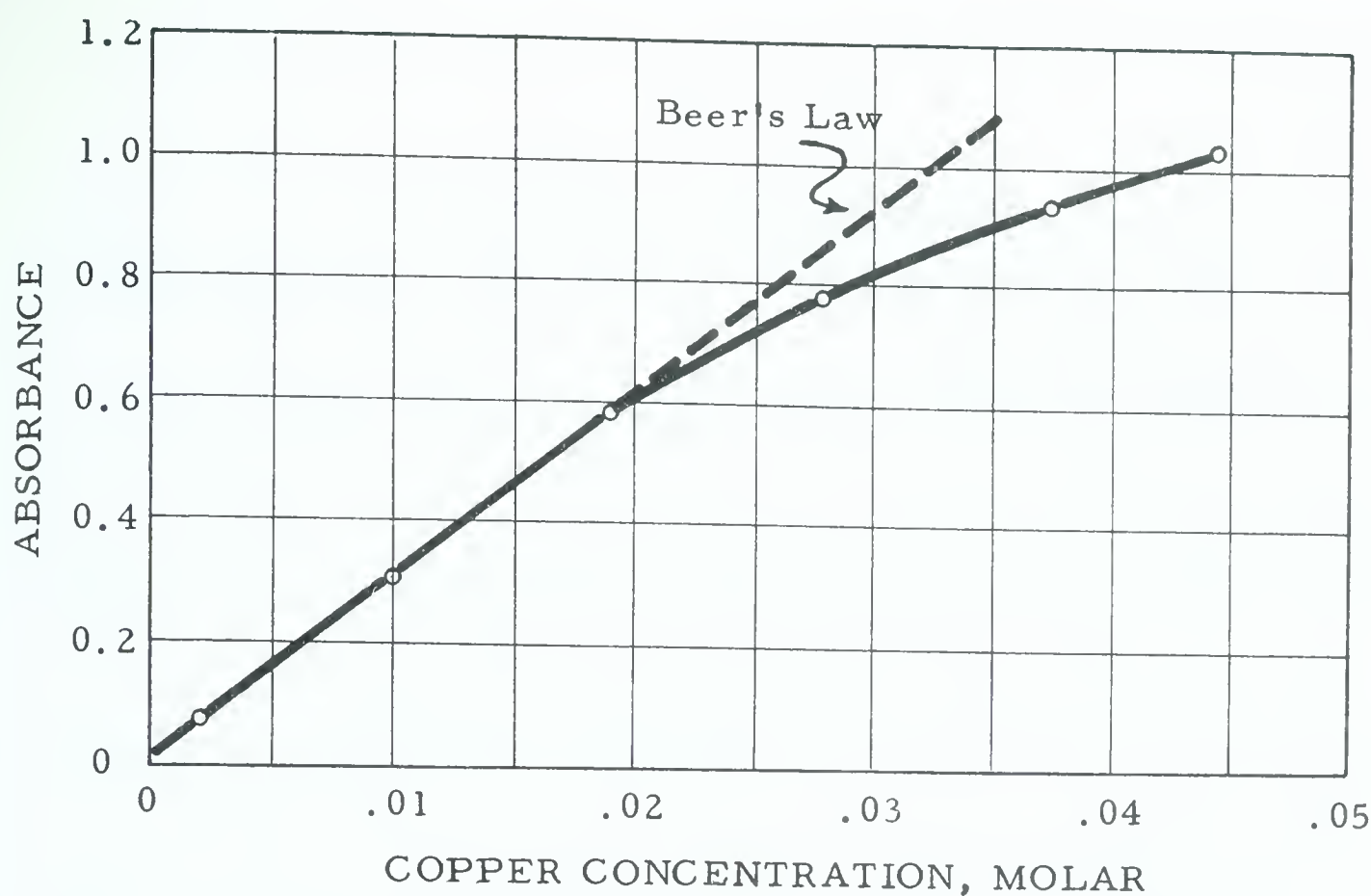


Fig. 12 Absorbance (at  $\lambda = 630 \text{ m}\mu$ ) vs. copper concentration in 0.75M  $(\text{NH}_4)_2\text{SO}_4$  solution at pH 7.1, showing negative deviation from Beer's Law

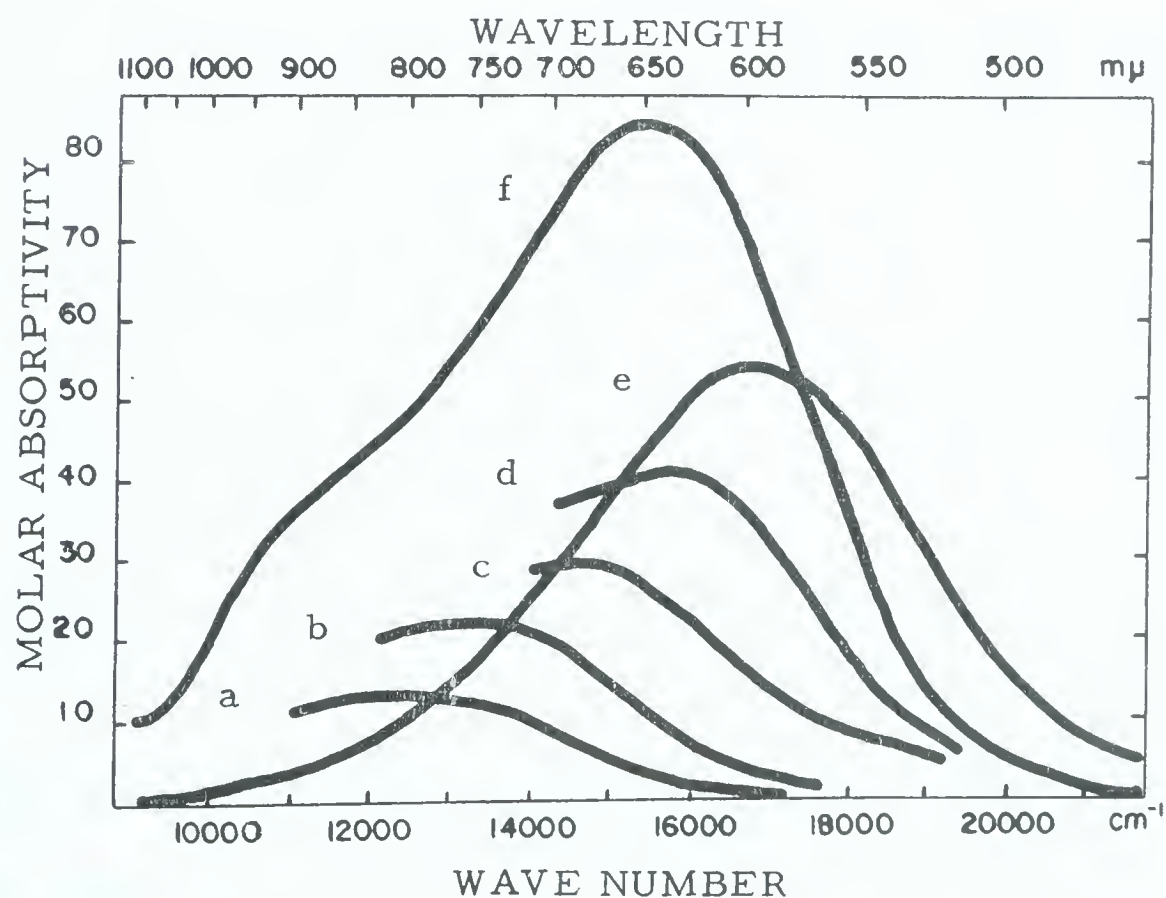


Fig. 13 Absorption spectra of copper(II)-ammonia complexes in 2M  $\text{NH}_4\text{NO}_3$ , after Bjerrum et al<sup>(172)</sup>; a)  $\text{Cu}^{++}$ , b)  $\text{Cu}(\text{NH}_3)^{++}$ , c)  $\text{Cu}(\text{NH}_3)_2^{++}$ , d)  $\text{Cu}(\text{NH}_3)_3^{++}$ , e)  $\text{Cu}(\text{NH}_3)_4^{++}$ , f)  $\text{Cu}(\text{NH}_3)_5^{++}$





## RESULTS AND DISCUSSION

### 1. PRELIMINARY EXPERIMENTS WITH WIRE SPECIMENS

Since many of the industrial failures of brass by stress corrosion have been ascribed to 'atmospheric' traces of ammonia, it was initially hoped that the reaction could be conveniently studied in the gas phase, with the expectation that the adsorption isotherms obtained for the various combinations of reactant gases would give an insight into the mechanism of stress corrosion failure. However, using the equipment described in Experimental Methods, Section 2, no cracking was observed for wire specimens stressed in the following gaseous environments (at room temperature) for 200 hours:

- a) dry ammonia (<50 ppm water) at pressures up to one atmos.
- b) ammonia saturated with water vapor ( $p_{\text{H}_2\text{O}} = 35 \text{ mm Hg}$ ) at pressures up to 50 cm Hg
- c) ammonia plus oxygen ( $p_{\text{NH}_3} = p_{\text{O}_2} = 25 \text{ cm Hg}$ ) plus water vapor ( $p_{\text{H}_2\text{O}} = 35 \text{ mm Hg}$ )
- d) ammonia plus air ( $p_{\text{NH}_3} = p_{\text{air}} = 25 \text{ cm Hg}$ ) plus water vapor ( $p_{\text{H}_2\text{O}} = 35 \text{ mm Hg}$ )
- e) ammonia plus carbon dioxide ( $p_{\text{NH}_3} = p_{\text{CO}_2} = 25 \text{ cm Hg}$ )

These results show that direct adsorption of ammonia molecules from the gas phase does not produce cracking within 200 hours even when small amounts of water are present. Since the subsequent



experiments showed that the cracking is related to the presence of ionic copper-ammine complexes, it can be assumed that cracking in gaseous atmospheres can occur only if enough water is present to provide a film of electrolyte in which the copper-ammine complexes can be formed and/or transported to suitable reaction sites on the metal surface. It is clear that the chemistry of brass-ammonia stress corrosion cracking is not suited to study in gaseous environments; metallurgical factors affecting the rate of cracking may be studied if the testing conditions are such that a reproducible amount of electrolyte is present on the surface of the test specimens, although such reproducibility may be difficult to achieve.

It should be noted that much of the earlier work on the brass-ammonia system was done in the vapor phase above solutions of ammonia. It is not surprising that under these conditions the influence of other gases, especially carbon dioxide, was not clearly defined, because in addition to the necessary presence of an aqueous film, one must add a co-requisite, viz. the proper solution pH (as shown by Mattsson<sup>(168)</sup>). Thus Hoar<sup>(173)</sup> has suggested that the presence of carbon dioxide promotes cracking by buffering the solution to a pH of about 7.3, which would account for the observations of Edmunds et al.<sup>(164)</sup> On the other hand, if large amounts of CO<sub>2</sub> are present, as in the experiments of Johnston<sup>(155)</sup>, the formation of copper



carbonate is thermodynamically more favorable than the formation of the copper(II)-tetrammine complex ( $\Delta G^\circ_{\text{CuCO}_3} = -123.8$  kcal/mole,  $\Delta G^\circ_{\text{Cu}(\text{NH}_3)_4^{++}} = -27.4$  kcal/mole), and no cracking would be expected, as Johnston found,

## 2. EXPERIMENTS WITH STRIP SPECIMENS

### A. Effect of Gaseous Environments

After redesigning the testing system to accomodate stressed strip specimens as previously described (Experimental Methods, Section 3), several qualitative experiments were carried out using copper-ammonia solutions of the type described by Mattsson<sup>(168)</sup>. It will be shown later that the cracking time in these solutions is dependent not only on the pH but also on the initial concentration of copper-ammine complexes; for this reason the comparison of results in this section will be confined to solutions having approximately the same pH (7.1) and the same initial concentration of reactants ( $\text{Cu} = 0.05\text{M}$ ,  $\text{total NH}_3 = 1.3\text{M}$ ). A summary of the results is shown in Table III.

The first objective of this group of experiments was to produce as clean a metal surface as possible before introducing the cracking solution. This was accomplished by flushing the reaction chamber with argon, evacuating to  $10^{-7}$  torr, and subsequently reducing any surface oxide on the specimen by treatment with hydrogen at a





temperature of about 300°C. It became apparent in the initial tests that heating the specimen to this temperature for four hours resulted in a partial annealing of the specimen, which prolonged its life considerably; this can be seen by comparing tests (a) and (b) in Table III. In (a), the specimen was cleaned chemically, and mounted in the 'inverted' position in a glass cup containing 3.0 ml of the cracking solution, with no heating period or special treatment of the solution. The cracking time was about 42 minutes, compared with 342 minutes for test (b) in which the specimen was subjected to a four-hour heating period in argon before introduction of the cracking solution. The eight-fold increase in cracking time illustrates the pronounced beneficial effect of stress-relieving, even at relatively low temperatures.

The elimination of dissolved air from the cracking solution had no significant effect, as shown by comparison of tests (b) and (c).

Tests (d) and (e) show the effect of reducing the surface oxides of the specimen before introducing de-aerated (test (d)) or oxygenated (test (e)) cracking solution. It is surprising that the reduction in hydrogen had so great an effect (viz., a three-fold decrease in cracking time as compared with tests (b) and (c)), since the amount of oxide film on the specimens after chemical cleaning should not have exceeded about 50 - 75 Å in thickness, and was probably less. (This estimate is based on the following facts: the specimens were exposed



Table III

Effect of gaseous environments on stress corrosion cracking  
of stressed brass strip specimens in aqueous solutions  
(pH  $\simeq$  7.1, Cu  $\simeq$  0.05M, total NH<sub>3</sub>  $\simeq$  1.3M)

| Position of specimen | Heated @ 300°C for four hours | Atmosphere during heating period | Solution de-aerated | Atmosphere after solution admitted | Cracking time, min.      |
|----------------------|-------------------------------|----------------------------------|---------------------|------------------------------------|--------------------------|
| a) Inverted          | No                            | ----                             | No                  | Air                                | 42 $\pm$ 5               |
| b) Inverted          | Yes                           | Argon                            | No                  | Air                                | 342 $\pm$ 75             |
| c) Inverted          | Yes                           | Argon                            | Yes - Argon         | Argon                              | 348 $\pm$ 20             |
| d) Inverted          | Yes                           | Hydrogen                         | Yes - Hydrogen      | Hydrogen                           | 99 $\pm$ 3               |
| e) Inverted          | Yes                           | Hydrogen                         | No - Oxygenated     | Oxygen                             | 90 $\pm$ 20              |
| f) Inverted          | Yes                           | Hydrogen                         | No                  | Carbon Dioxide                     | 1440 $\pm$ 60            |
| g) Normal            | Yes                           | Hydrogen                         | No                  | Argon                              | Not cracked in four days |



to the laboratory atmosphere for less than 15 minutes between chemical cleaning and mounting in the apparatus; the oxidation resistance of 70Cu-30Zn is higher than that of copper;<sup>(174)</sup> the oxide thickness produced in the dry oxidation of copper at 25°C is less than 100 Å over a period of months;<sup>(175)</sup> and the oxide film produced on copper in oxygenated water is about 70 Å in one hour.<sup>(176)</sup> One possible explanation is that the heating period in argon may have slightly thickened the oxide film on the specimen (assuming some oxygen contamination in the argon), and/or the composition of the oxide film may have been changed from predominantly Cu<sub>2</sub>O to a mixture of Cu<sub>2</sub>O and ZnO (this type of change has been reported for alpha brass heated to 450°C<sup>(177)</sup>).

The most significant result of tests (d) and (e) was the fact that changing from a de-aerated solution to an oxygen-saturated solution made no difference in the cracking time. It was thus concluded that dissolved oxygen does not take part in the chemical reaction between the cracking solution and the stressed metal in solutions of the type used in these tests.

One example of the effect of carbon dioxide is shown in Table III as test (f); in this particular test, carbon dioxide was introduced into the test chamber after the hydrogen reduction period, and before the solution was admitted. The color of the cracking solution quickly





changed from dark blue to very light blue when admitted to the reaction vessel; this color change corresponds to a decrease in pH and a change in the copper-ammine complex, as will be shown later. The increased cracking time in the  $\text{CO}_2$  atmosphere is related to this pH change, as was mentioned in the previous section. It should be mentioned that the cracking times in  $\text{CO}_2$  atmospheres were difficult to reproduce because of the seemingly variable amounts of  $\text{CO}_2$  absorbed by the cracking solutions as they were introduced through the solution inlet tube.

One other experiment, test (g), is included in Table III because of its significance with respect to the proposed cracking mechanism involving adsorption of surface-active compounds. In test (g) the specimen was placed in the 'normal' position before reduction with hydrogen, so that when the solution was admitted to the glass cup, only the 'legs' of the specimen contacted the solution. No cracks were observed in the stressed portion of the specimen in four days, although the 'legs' showed the usual black tarnish that formed in solutions of this pH. This was taken to show that if a surface-active compound is responsible for the cracking, it is only produced where the metal is in contact with bulk solution; otherwise one would expect rapid surface diffusion of the surface-active substance over the whole surface of the specimen, with subsequent cracking at suitable reaction sites on the highly stressed portions of the specimen.



## B. Composition of Tarnish

The black, shiny tarnish formed on brass immersed in copper-ammonia cracking solutions (pH 7.1) was tentatively identified as  $\text{Cu}_2\text{O}$  by Mattsson<sup>(167)(168)</sup> only on the basis of microscopic examination. Forty and Humble,<sup>(170)</sup> in their study on the nature of the tarnish, also suggested that it was most probably composed of cuprous oxide, on the basis of ring patterns obtained during electron diffraction of tarnish flakes that had been damaged by mishandling or by heating and curling in the electron beam.

In the present work, the existence of  $\text{Cu}_2\text{O}$  as the major constituent in the tarnish has been definitely established by means of X-ray diffraction patterns obtained from tarnished brass strips and from tarnish powder scraped from brass specimens. This result was confirmed by a polarographic analysis of the tarnish powder: in a 5.93 mg sample, 0.074 mM Cu and 0.005 mM Zn were detected; expressed as  $\text{Cu}_2\text{O}$  and  $\text{ZnO}$ , this gives 5.29 mg and 0.41 mg, respectively, or a total of 5.70 mg, which agrees satisfactorily within the limits of experimental error.

The presence of  $\text{ZnO}$  in the tarnish could not be definitely established by X-ray diffraction, since the line of strongest intensity for  $\text{ZnO}$  is coincident with a line of strong intensity for  $\text{Cu}_2\text{O}$ ; no other lines corresponding to  $\text{ZnO}$  were detected, but this could simply be due to the relatively small amount present in the sample.



It should be noted that the X-ray diffraction patterns of untarnished brass strips showed a strong preferred orientation, with the (220) plane parallel to the rolling plane. The  $\text{Cu}_2\text{O}$  pattern obtained on tarnished strips also showed preferred orientation, indicating that the  $\text{Cu}_2\text{O}$  is formed from copper atoms in the metal lattice, and not as a buildup of a surface film. This confirms the work of Forty and Humble<sup>(170)</sup> who found that the tarnishing reaction penetrates inwards, with no gross changes in the volume or shape of the specimen, and suggested that the outwards diffusion of zinc provides the accommodation for the oxygen.

### C. Effect of pH

In Mattsson's<sup>(167)(168)</sup> studies on the effect of pH on cracking time in copper-ammonia solutions, the most rapid cracking was found to occur in the pH range 7.0 - 7.3, and for this reason solutions having a pH of about 7.1 were used in the experiments described in the preceding section. However, in attempting a more precise study of the effect of pH in the range 5.0 - 8.0 (using the procedure described in Experimental Methods, Section 3D), we found that the most rapid cracking occurred over the pH range 6.0 - 7.0, as shown in Fig. 14. Our solutions did not show the ageing effects (precipitation of basic copper sulfate) reported by Mattsson, and were used immediately after





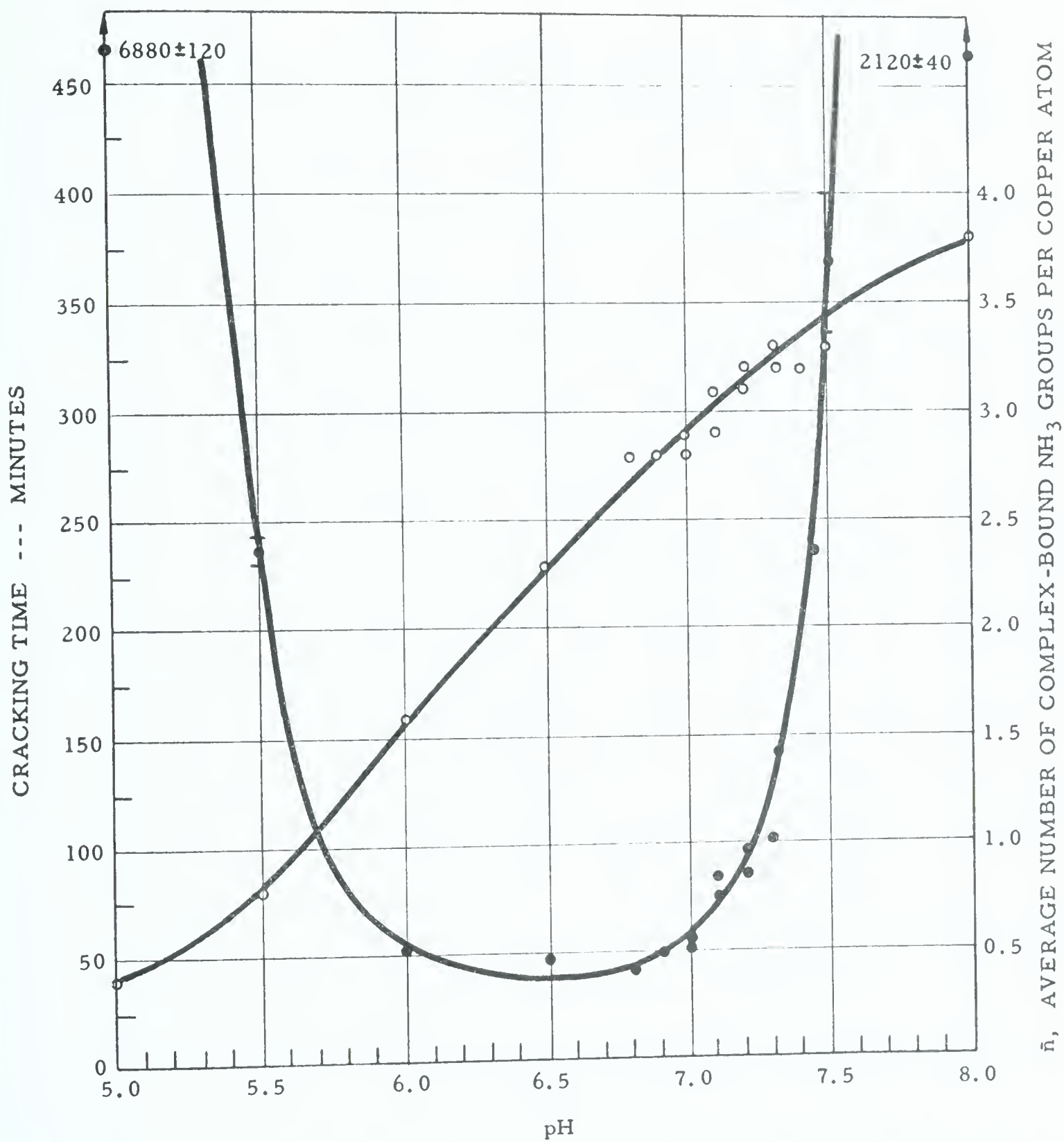


Fig. 14 Cracking time vs. pH (solid circles) for stressed brass strips in copper-ammonia solutions ( $\text{Cu} \approx 0.04\text{M}$ , total ammonia  $\approx 1.5\text{M}$ ) at  $22.5^\circ\text{C}$ ; pH vs.  $\bar{n}$  (open circles), the average number of complex-bound  $\text{NH}_3$  groups per Cu atom



being prepared, rather than after a storage period, so this may explain the difference in results, although it is not clear why the precipitation phenomena did occur at all in Mattsson's solutions. Fig. 14 is a composite of runs made using two different pH meters; the tests made with the more accurate meter, which had a reproducibility of  $\pm 0.005$  pH units, are also shown in tabular form in Table IV, along with the pH measurements made on a blank solution, and individual duplicate solutions containing unstressed and stressed samples. These pH measurements show that, in the pH range 6.0 - 7.3, where the cracking time is relatively short (from 50 - 100 min), there is a small but definite decrease in pH (over and above the pH decrease occurring in the blank solution) during the time in which the specimens were exposed to the solutions, and this decrease is greater in solutions containing unstressed specimens than in those containing stressed specimens. This will be discussed later.

Superimposed on the plot of pH vs. cracking time in Fig. 14 is a plot of pH vs.  $\bar{n}$ , the average number of complex-bound  $\text{NH}_3$  groups per copper atom. The formation of the familiar dark blue copper(II)-tetrammine complex  $\text{Cu}(\text{NH}_3)_4^{++}$  in solutions such as the ones used in these tests, can be regarded as the stepwise addition of  $\text{NH}_3$  ligands to the cupric cation as the pH is increased to give a higher concentration of available  $\text{NH}_3$  groups from the dissociation



Table IV

Effect of pH on cracking of stressed brass strips in copper-ammonia solutions (Cu = 0.04M, total NH<sub>3</sub> = 1.5M) at 22.5°C.

| Initial pH | $\bar{n}$ | $\lambda$<br>m $\mu$ | Final pH |          |             | Cracking time,<br>min. | Increase in concentration, moles/liter |         |            |         |
|------------|-----------|----------------------|----------|----------|-------------|------------------------|--|---------|------------|---------|
|            |           |                      | Blank    | Stressed | Un-stressed |                        | Stressed                               |         | Unstressed |         |
|            |           |                      |          |          |             |                        | Cu                                     | Zn      | Cu         | Zn      |
| 5.00       | 0.37      | >750                 | 5.00     | 5.38     | 5.17        | 6880 $\pm$ 120         | 0.004                                  | <0.001  | 0.002      | 0.002   |
| 5.50       | 0.84      | >750                 | 5.44     | 5.48     | 5.44        | 238 $\pm$ 5            | 0.001                                  | <0.0005 | 0.001      | <0.0005 |
| 6.00       | 1.56      | 715                  | 5.97     | 5.98     | 5.96        | 52 $\pm$ 2             | 0.003                                  | "       | 0.002      | "       |
| 6.50       | 2.26      | 680                  | 6.50     | 6.48     | 6.46        | 48 $\pm$ 2             | <0.001                                 | "       | <0.001     | "       |
| 6.80       | 2.77      | 660                  | 6.79     | 6.80     | 6.75        | 42 $\pm$ 3             | "                                      | "       | "          | 0.0006  |
| 6.90       | 2.82      | 655                  | 6.86     | 6.90     | 6.84        | 49 $\pm$ 1             | 0.004                                  | "       | 0.002      | <0.0005 |
| 7.00       | 2.94      | 650                  | 6.97     | 6.95     | 6.95        | 57 $\pm$ 2             | 0.003                                  | "       | 0.002      | "       |
| 7.10       | 3.08      | 640                  | 7.06     | 7.02     | 7.01        | 85 $\pm$ 3             | 0.004                                  | 0.002   | 0.004      | 0.002   |
| 7.20       | 3.24      | 635                  | 7.17     | 7.10     | 7.07        | 86 $\pm$ 4             | 0.005                                  | 0.002   | 0.006      | 0.002   |
| 7.30       | 3.28      | 630                  | 7.25     | 7.18     | 7.14        | 102 $\pm$ 5            | 0.005                                  | 0.004   | 0.007      | 0.003   |
| 8.00       | 3.83      | 600                  | 7.90     | 7.35     | 7.38        | 2120 $\pm$ 40          | 0.037                                  | 0.015   | 0.030      | 0.013   |





of  $\text{NH}_4^+$ . The method used for calculating  $\bar{n}$  has been given by Bjerrum,<sup>(178)</sup> and is outlined in Appendix B. From Fig. 14, it can be seen that the most rapid cracking occurs in solutions where  $\bar{n}$  is about 1.5 - 3, i.e., in solutions where the copper(II)-ammine complexes are present as  $\text{Cu}(\text{NH}_3)^{++}$ ,  $\text{Cu}(\text{NH}_3)_2^{++}$ ,  $\text{Cu}(\text{NH}_3)_3^{++}$ , or mixtures of these.

In order to check the values obtained for  $\bar{n}$  against those previously reported in the literature, the spectra of the various test solutions were recorded before each test, and the absorption peaks compared with those shown in Fig. 13. Table IV includes the  $\bar{n}$  values calculated for a number of runs, and the corresponding observed absorption peak wavelength. In Fig. 15, these wavelengths are plotted as solid circles, while the open circles represent the values of the peaks in Fig. 13 (after Bjerrum et al.<sup>(172)</sup>). It can be seen that the agreement is good, and that there is an almost linear decrease in  $\bar{n}$  with increasing wavelength of the absorption peak (about 0.1  $\bar{n}$  per 5  $\text{m}\mu$ ).

The results of the spectra obtained on solutions in the pH range 6.0 - 7.3 (corresponding to the solutions listed in Table IV) are shown in Table V. The insignificant differences between initial and final absorption peak wavelengths are due primarily to the short reaction time. For the solutions in which cracking occurred most quickly,



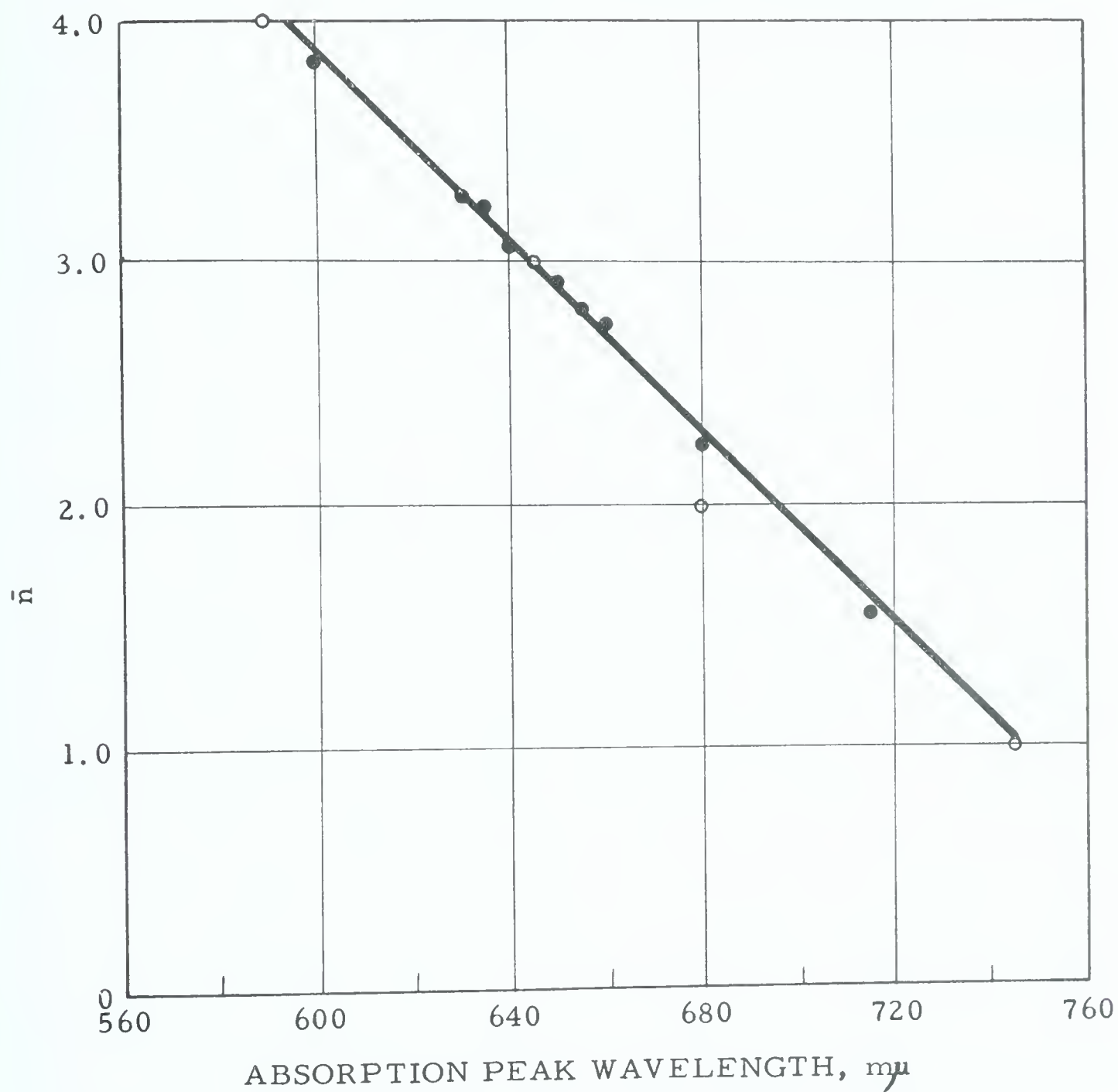


Fig. 15 Wavelengths of the absorption peaks of the copper(II) - ammonia complexes,  $\text{Cu}(\text{NH}_3)_n^{++}$ , vs.  $\bar{n}$ ; solid circles, present work; open circles, after Bjerrum et al.<sup>(172)</sup>



Table V

Absorption spectra of test solutions listed in Table IV

 $\lambda$  = wavelength of absorption peak,  $m\mu$ A = absorbance at  $\lambda$ 

| pH   | Initial   |      | Final     |      |            |      | Cracking<br>time/min. |
|------|-----------|------|-----------|------|------------|------|-----------------------|
|      |           |      | Stressed  |      | Unstressed |      |                       |
|      | $\lambda$ | A    | $\lambda$ | A    | $\lambda$  | A    |                       |
| 6.00 | 715       | .80  | 715       | .80  | 715        | .80  | 52 $\pm$ 2            |
| 6.50 | 680       | .91  | 685       | .90  | 685        | .89  | 48 $\pm$ 2            |
| 6.80 | 660       | .97  | 660       | .96  | 660        | .95  | 42 $\pm$ 3            |
| 6.90 | 655       | .99  | 660       | .97  | 660        | .95  | 49 $\pm$ 1            |
| 7.00 | 650       | 1.00 | 650       | .98  | 650        | .98  | 57 $\pm$ 2            |
| 7.10 | 640       | 1.01 | 645       | 1.01 | 645        | 1.01 | 85 $\pm$ 3            |
| 7.20 | 635       | 1.03 | 640       | 1.04 | 640        | 1.04 | 86 $\pm$ 4            |
| 7.30 | 630       | 1.03 | 635       | 1.05 | 635        | 1.05 | 102 $\pm$ 5           |





there appeared to be almost always a greater reduction (about 1%) in absorption in the solutions containing unstressed samples, as compared with solutions containing stressed samples. The last four columns of Table IV show the results of polarographic analyses on the test solutions. It should be borne in mind that the solutions initially contained about 0.04M dissolved copper, so that an increase of 0.001M represents the smallest change in copper concentration that could be detected within the limits of experimental error. The lower limit of sensitivity for zinc was about  $5 \times 10^{-4}$  M.

It is apparent that for all the solutions except the one at a pH of 8.00, there was only a slight increase in total dissolved copper (about 0.003M), and barely detectable traces of zinc. No significant differences in analyses of solutions containing stressed and unstressed samples are evident.

At a pH of 8.00 (and at higher pH values), some general corrosion occurs; the results in Table IV show that at pH 8.00, the increase in soluble copper and zinc in the test solutions is slightly greater for the stressed than the unstressed sample. The copper/zinc ratio for this increase is about the same as the copper/zinc ratio in the brass, suggesting that this is a fairly uniform general corrosion.



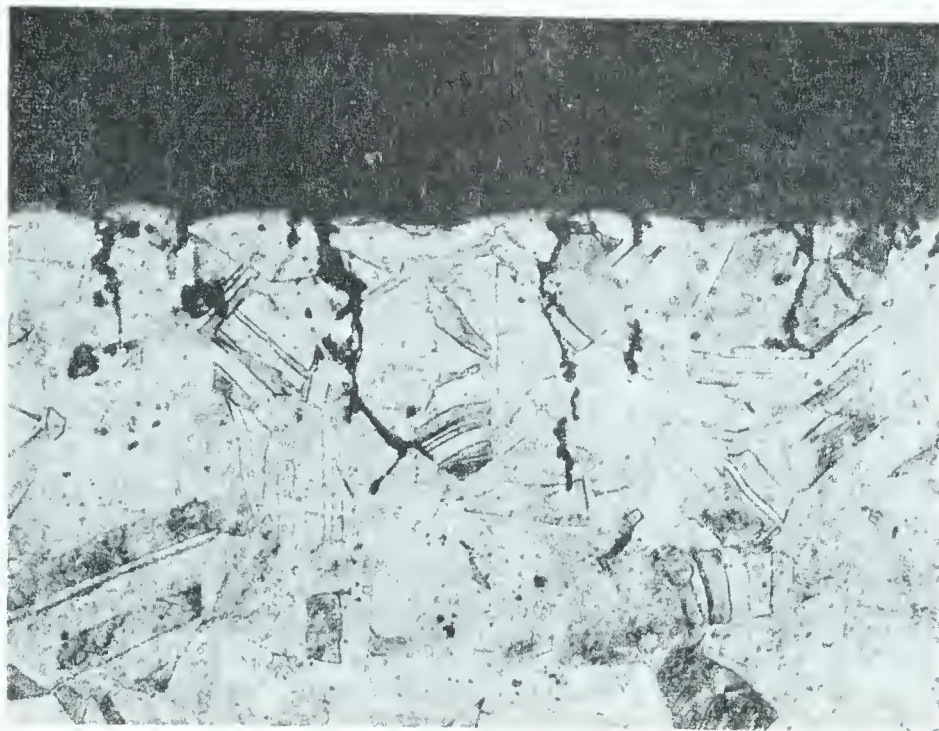
The photomicrographs in Fig. 16 show the three general types of cracking encountered over the pH range 5.0 - 8.0. At pH 5.0 (Fig. 16a) the cracks were blunt, relatively shallow (apart from the crack leading to failure) and showed no preference for inter- or transgranular paths. In contrast, the cracks which occurred in the pH range 6.0 - 7.5 were almost exclusively intergranular; they were narrow in section, well developed, and were accompanied by little or no general roughening of the specimen surface, as is illustrated by Fig. 16b. At pH 8.0 (Fig. 16c), there was severe intergranular penetration at almost every grain boundary in the stressed portion of the specimens, accompanied by some general corrosion of the surface. In fact, the mode of failure at pH 8.0 represents a 'borderline' example of stress corrosion cracking, and is more probably an example of intergranular corrosion accelerated by stress, although the distinction between the two is admittedly not clear-cut. The cracking which occurred in the pH range 6.0 - 7.5 is definitely stress corrosion cracking in the strictest sense of the term, since it is accompanied by little or no general corrosion.

Fig. 17, which is a general view of the region of failure in a specimen exposed to a solution of pH 7.1, shows the 'spidery' appearance of the crack systems, which always originate on the tension side of the specimen.

The blue-black  $\text{Cu}_2\text{O}$  tarnish was observed on all specimens







(a)

(b)



(c)

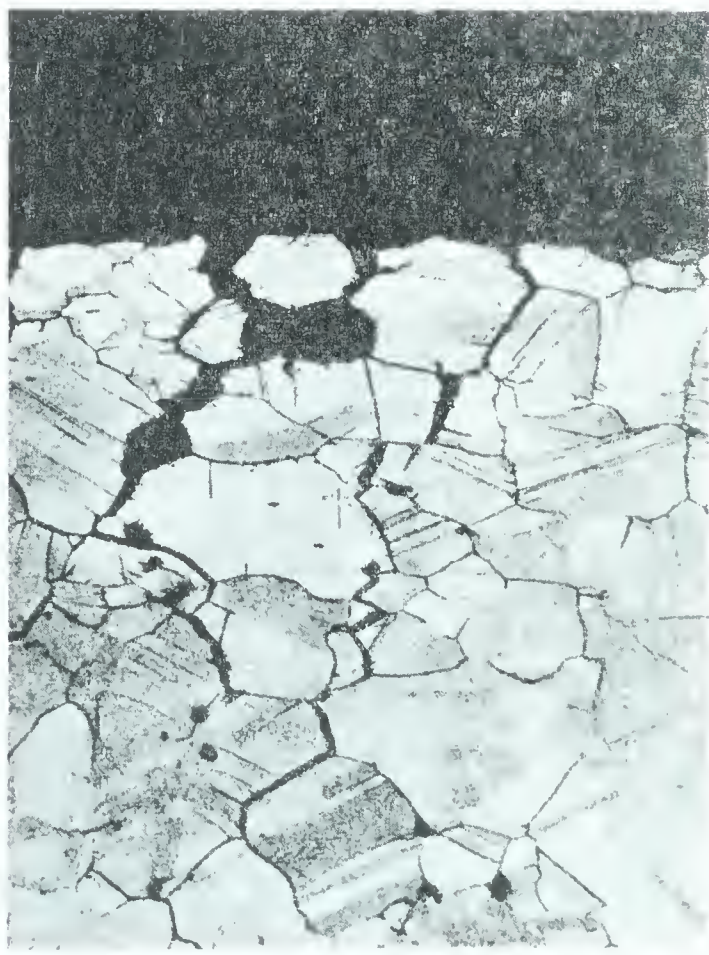


Fig. 16 Typical stress corrosion cracking of brass immersed in copper-ammonia solutions ( $\text{Cu} = 0.04\text{M}$ , total ammonia  $= 1.5\text{M}$ ) at  $22.5^\circ\text{C}$ ; a) pH 5.0; b) pH 6.0 - 7.5; c) pH 8.0. Etchant: 5% alc.  $\text{FeCl}_3$ ; X 175





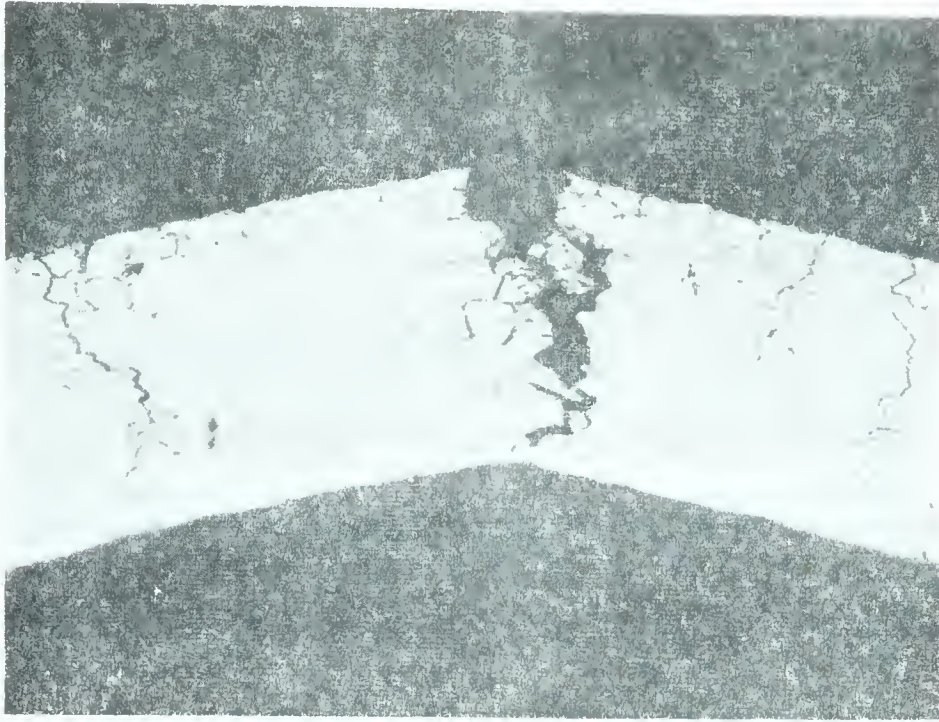


Fig. 17 Stress corrosion cracking of brass in copper-ammonia solution ( $\text{Cu} = 0.05\text{M}$ , total  $\text{NH}_3 = 1.5\text{M}$ ,  $\text{pH} = 7.1$ ) at  $24^\circ\text{C}$ , showing main crack 'system' and auxiliary crack 'systems', all originating from tension side of U-bend specimen. X 70



Fig. 18 Section through brass specimen partially immersed in copper-ammonia cracking solution ( $\text{pH} = 7.1$ ) for one hour, showing penetration of  $\text{Cu}_2\text{O}$  tarnish into brass. X 750



listed in Table IV except those in the solutions at pH 5.00 (where the specimens had a copper color at the conclusion of the test) and at pH 5.50 (where the surface was gold-colored).

In an experiment similar to the one performed by Forty and Humble,<sup>(170)</sup> a polished specimen (lightly etched in dilute  $\text{HNO}_3$ ) was partially immersed in a cracking solution of pH 7.1 for one hour. Fig. 18 is a photomicrograph of a section through the specimen at the solution-air interface; (a pencil line showing the demarcation line between the tarnish surface and the mounting plastic has been added because the contrast between the dark-colored tarnish and the plastic was lost in the reproduction process) the tarnish penetrates into the brass, as Forty and Humble demonstrated. Microscopic examination of this and other tarnished specimens showed that the maximum tarnish thickness varied from 1 - 5 microns.

#### D. Effect of Initial Complex Concentration

The cracking time increases exponentially with a decrease in concentration of initial copper(II)-ammine complex, as shown in Fig. 19, which is a plot of log cracking time vs. initial concentration of dissolved copper, at pH 7.1. Table VI lists the analytical results obtained from duplicate runs corresponding to the open circles in Fig. 19. These results follow a similar pattern for all runs in which some dissolved copper was initially present in the solution: there was a decrease in the



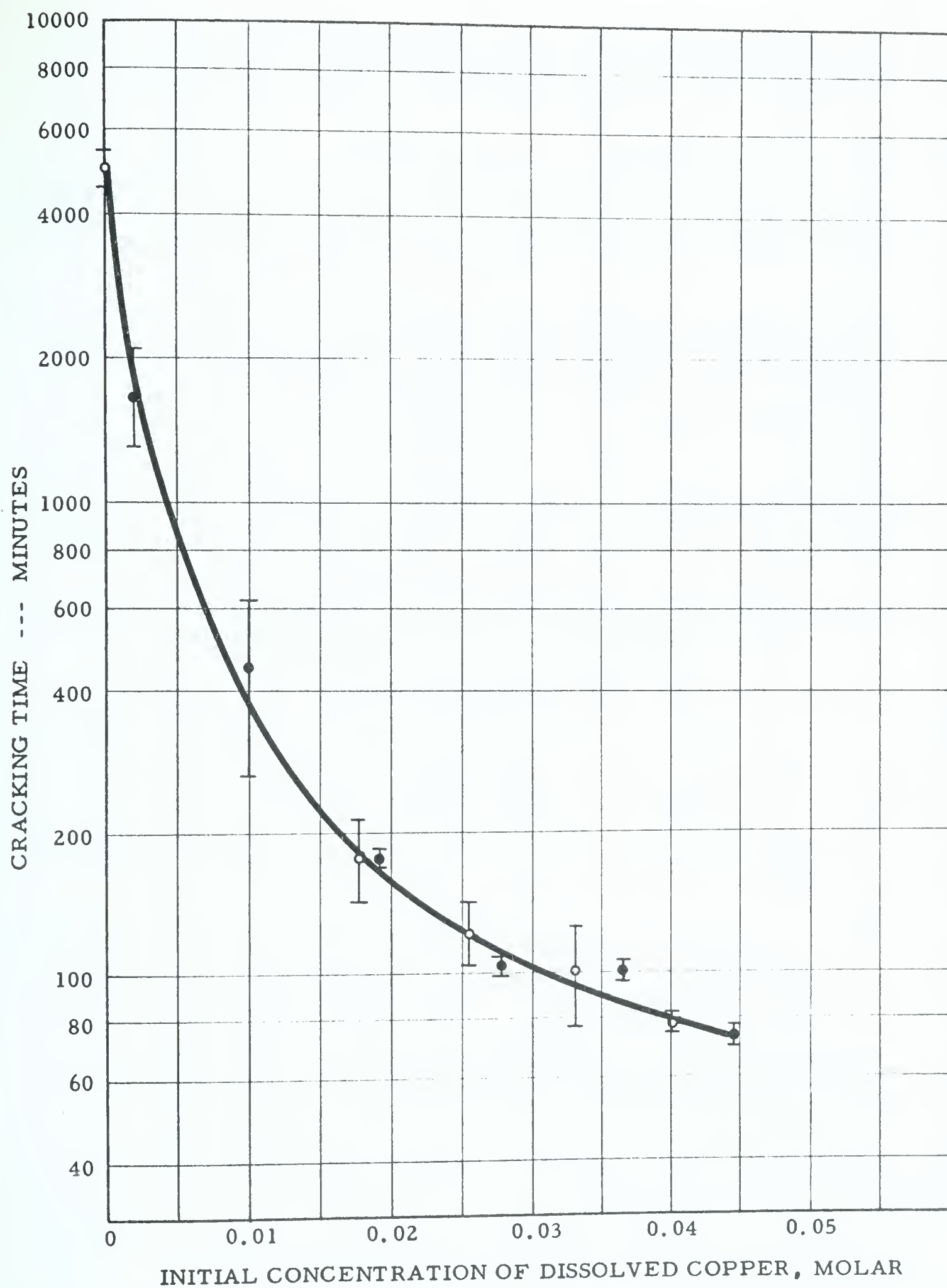


Fig. 19 Effect of initial concentration of dissolved copper on cracking of brass in 1.5M ammonia solutions, pH 7.1, at 22.5°C. Solid circles, single specimens; open circles, average of duplicate runs





Table VI

Cracking of stressed brass in solutions containing  
varying initial amounts of dissolved Cu, 1.5M total  $\text{NH}_3$ .  
Temp.  $22.5^\circ \pm .5^\circ\text{C}$ .

| Initial Cu<br>conc., M | pH      |       |          |            | Cracking time,<br>minutes |
|------------------------|---------|-------|----------|------------|---------------------------|
|                        | Initial | Final |          |            |                           |
|                        |         | Blank | Stressed | Unstressed |                           |
| 0.040                  | 7.10    | 7.07  | 6.98     | 6.98       | 78 $\pm$ 3                |
| 0.033                  | 7.10    | 7.06  | 6.99     | 6.98       | 100 $\pm$ 25              |
| 0.026                  | 7.10    | 7.05  | 6.97     | 6.95       | 122 $\pm$ 16              |
| 0.018                  | 7.10    | 7.03  | 6.93     | 6.90       | 176 $\pm$ 33              |
| 0.000                  | 7.10    | 6.90  | 6.70     | 6.76       | 5000 $\pm$ 440            |

|       | Increase in concentration, moles/liter |       |            |       |
|-------|--|-------|------------|-------|
|       | Stressed                               |       | Unstressed |       |
|       | Cu                                     | Zn    | Cu         | Zn    |
| 0.040 | 0.003                                  | 0.002 | 0.005      | 0.002 |
| 0.033 | 0.004                                  | 0.003 | 0.005      | 0.003 |
| 0.026 | 0.006                                  | 0.002 | 0.006      | 0.002 |
| 0.018 | 0.004                                  | 0.001 | 0.004      | 0.002 |
| 0.000 | 0.017                                  | 0.007 | 0.004      | 0.002 |

|       | Absorption Peak and Absorbance |      |           |      |            |      |
|-------|--------------------------------|------|-----------|------|------------|------|
|       | Initial                        |      | Final     |      |            |      |
|       |                                |      | Stressed  |      | Unstressed |      |
|       | $\lambda$                      | A    | $\lambda$ | A    | $\lambda$  | A    |
| 0.040 | 640                            | 1.04 | 645       | 0.95 | 645        | 0.92 |
| 0.033 | 640                            | 0.96 | 645       | 0.88 | 645        | 0.78 |
| 0.026 | 640                            | 0.81 | 645       | 0.75 | 645        | 0.65 |
| 0.018 | 640                            | 0.64 | 650       | 0.52 | 650        | 0.45 |
| 0.000 | -                              | -    | 665       | 0.49 | 665        | 0.12 |



pH of the solutions, slightly more pronounced in the solutions containing the unstressed samples; the increase of total dissolved copper and zinc was about 0.004M and 0.002M, respectively, for both stressed and unstressed samples; there was an approximately equal increase of the wavelength of the absorption peak in all solutions, but the absorbance was noticeably greater in the solutions containing stressed samples.

In the solutions that did not contain any dissolved copper at the start of the tests, the pH decreased more in the solution containing the stressed sample; the increase in total dissolved copper and zinc was four times greater for the stressed sample, as was the absorbance at the wavelength peak in the final solutions.

It should also be noted that there was no visible tarnish formation on the specimens exposed to the copper-free solutions; in the solutions that initially contained copper, the tarnish formation appeared to be roughly proportional to the copper content, with a continuous blue-black coloration at concentrations above 0.03M.

#### E. Effect of Temperature

The effect of temperature on cracking in solutions with the same initial pH and copper concentration is shown in Fig. 20. The scatter in the curve for solutions of pH 7.1 is probably due to poor precision in the pH measurements for this set of runs (because of a fault in the pH meter, detected later on). The curve for pH 6.80 is well-defined, although the



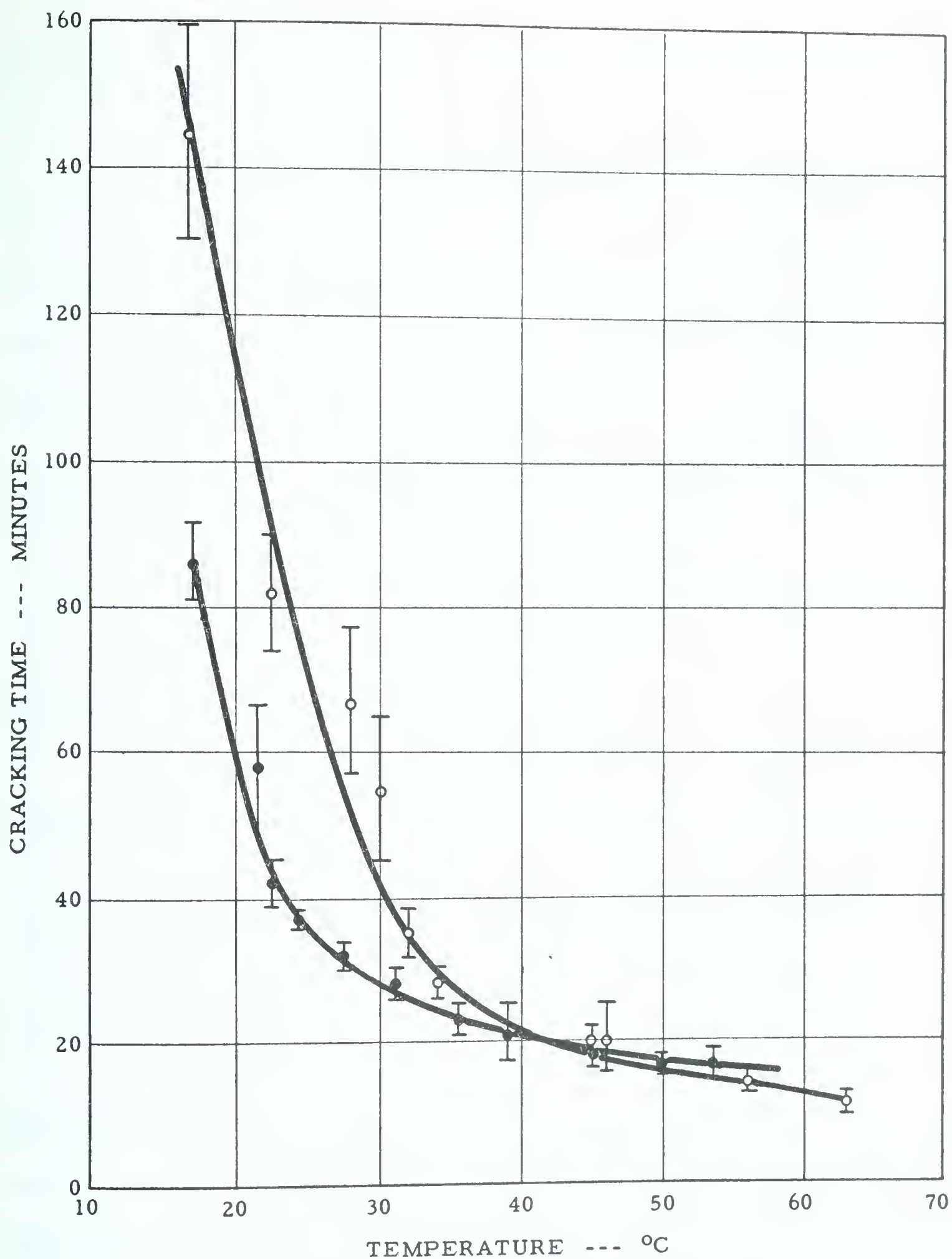


Fig. 20 Effect of temperature on cracking of brass in copper-ammonia solutions ( $\text{Cu} = 0.04\text{M}$ , total ammonia  $= 1.5\text{M}$ ). Open circles, pH 7.1; solid circles, pH 6.80





temperature range is a short one, since the volatilization of ammonia becomes apparent at temperatures above 65°C.

In Figs. 21 and 22, log rate (where rate is taken as the reciprocal of the cracking time) vs. the reciprocal of the absolute temperature is plotted as solid circles for the two curves from Fig. 20. The curvature of these plots shows that the temperature dependence is definitely not of the Arrhenius type. Nichols and Rostoker<sup>(179)</sup> were unable to obtain a definite temperature dependence over the range 17 - 75°C because of scatter in their results; however, their specimens were partially immersed in a concentrated ammonia solution which had ammonia gas and air bubbling through it, so it is likely that their scatter was caused by either pH and/or concentration fluctuations.

In Figs. 21 and 22, the open circles represent plots of rate (right-hand ordinate) vs.  $1/T$ , rather than log rate vs.  $1/T$ . This plot shows some linearity for the results at pH 6.80 (Fig. 22), but the 'fit' of points in Fig. 21 is very poor. The lines were included because Nichols and Rostoker<sup>(179)</sup> have reported a linear relation for  $1/t_c$  ( $t_c$  = cracking time) vs.  $1/T$  for the cracking of a copper-beryllium alloy in ammonia and in mercury, although they did not offer an explanation for such a linear dependence. It is likely that the apparent linear dependence is fortuitous; a more reasonable explanation for the curvature in the Arrhenius plot is that it represents a gradual transition from one



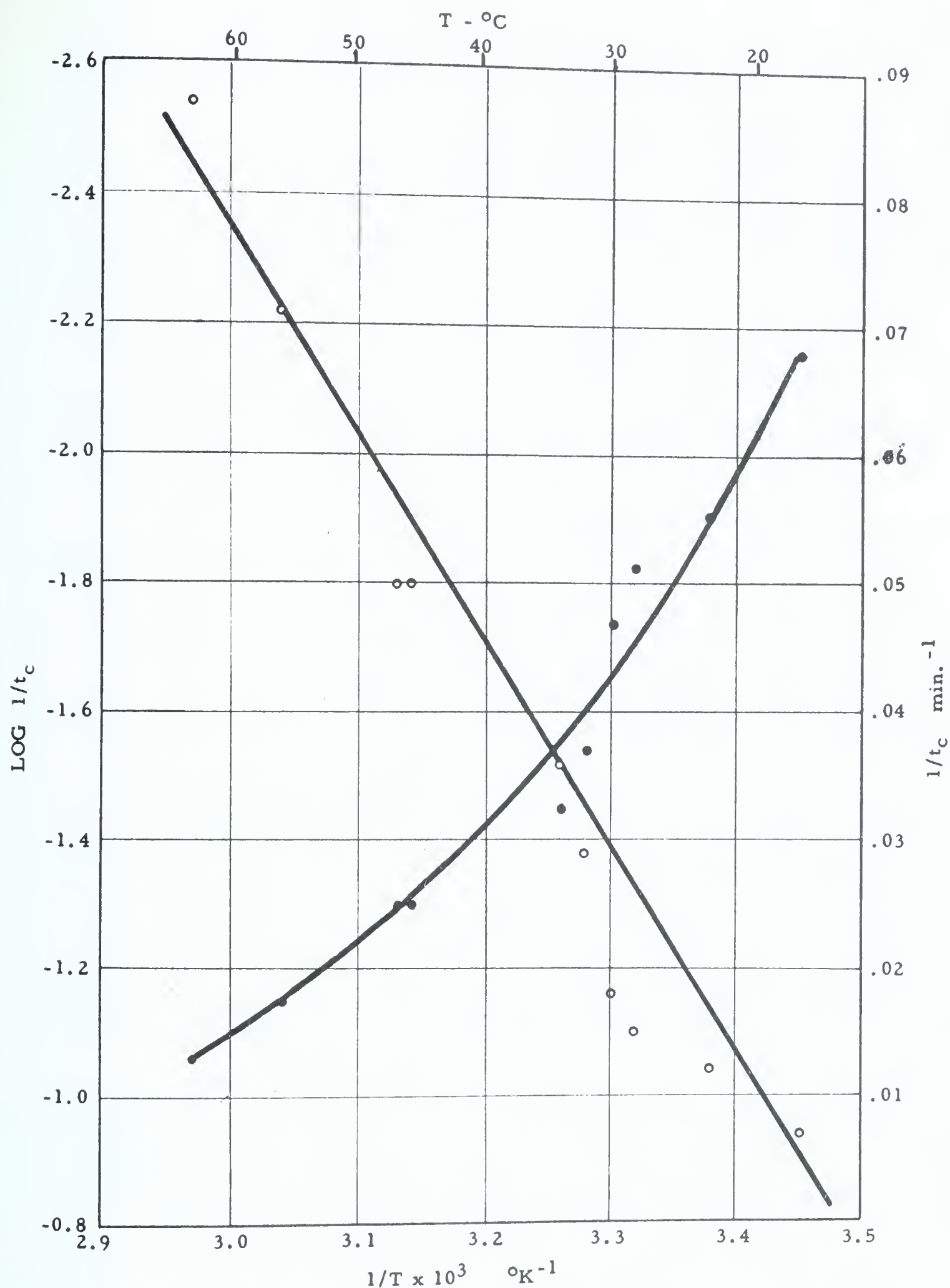


Fig. 21 Log rate ( $\log 1/t_c$ ) vs. reciprocal of absolute temperature (solid circles), and rate ( $1/t_c$ ) vs.  $1/T$  for cracking of brass in copper-ammonia solutions, pH 7.1



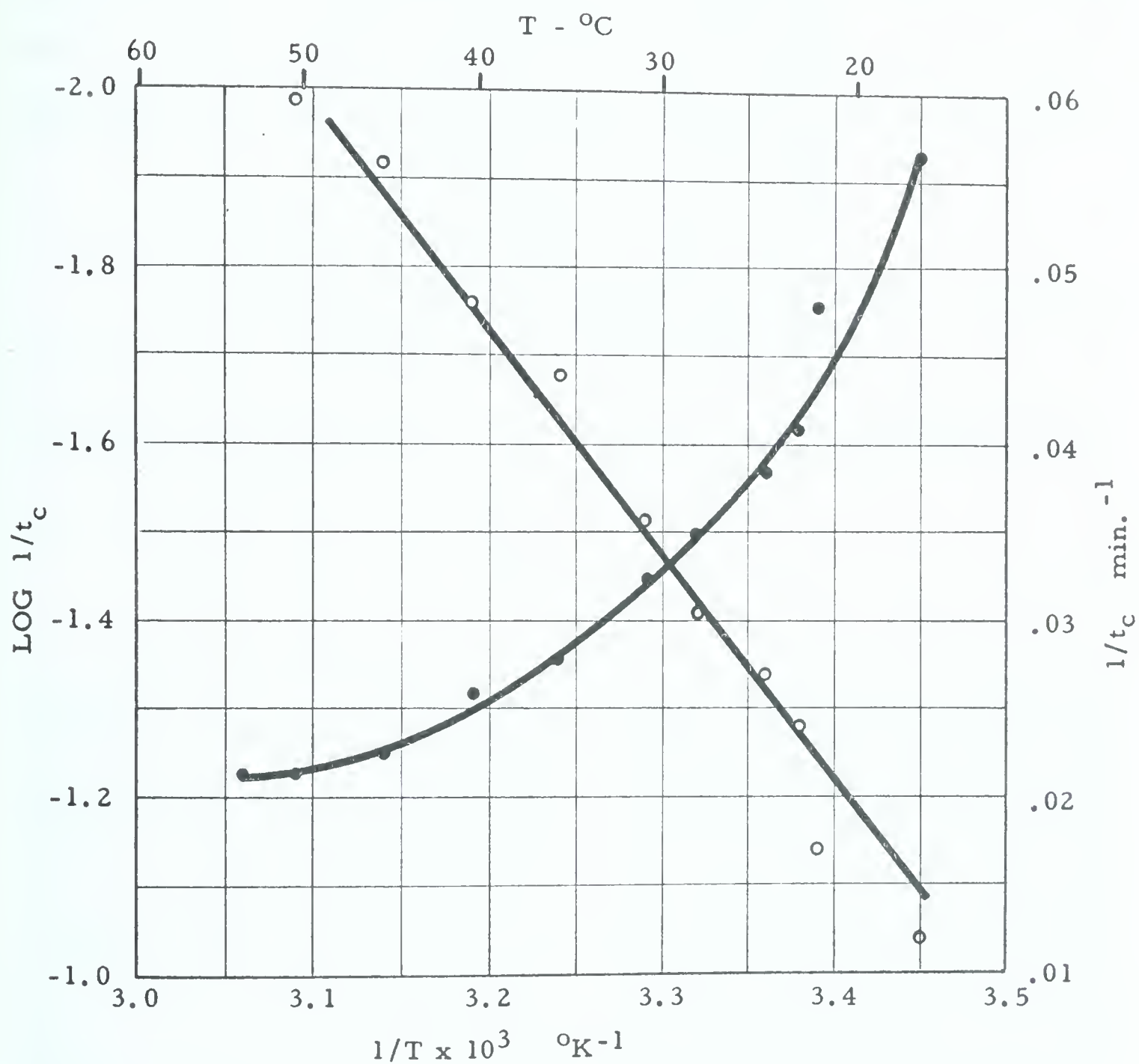


Fig. 22 Log rate ( $\log 1/t_c$ ) vs. reciprocal of absolute temperature (solid circles), and rate ( $1/t_c$ ) vs.  $1/T$  for cracking of brass in copper-ammonia solutions, pH 6.80





rate-controlling step to another; the approximate activation energies calculated by drawing tangents to the curve in Fig.22 were 11.5 kcals per mole at 20°C, dropping to about 4 kcals/mole at 45°C, which might imply a transition to diffusion control at higher temperatures, although the temperature range is too limited to draw any definite conclusions.

#### F. Other Cracking Media

The stress corrosion cracking of brass in aqueous media containing complexing reagents other than ammonia was demonstrated by immersing stressed brass strips in solutions containing tartrate ions and citrate ions, respectively.

Fig.23 shows the cracking obtained after 84 hours immersion in a solution containing 0.07M Cu and 0.6M potassium citrate adjusted to pH 10.3 with  $\text{Na}_2\text{CO}_3$ . A visible spectrum of the solution showed strong absorption at 690  $\text{m}\mu$ , corresponding to the presence of the copper(II)-citrate complex. Specimens immersed in solutions containing 0.04M Cu and 0.2M sodium citrate adjusted to pH values of 7.2, 11.0 and 12.9 with KOH did not develop cracks within 38 days. The spectra of these solutions showed no absorption peaks corresponding to the presence of the copper citrate complex.

Fig. 24a shows the intergranular stress corrosion cracking of brass after 31 days immersion in a solution containing 0.04M Cu and 0.5M potassium tartrate adjusted to pH 13.0 with KOH. The specimen







Fig. 23 Stress corrosion cracking of brass immersed in copper-citrate solution ( $\text{Cu} \approx 0.07\text{M}$ , total citrate  $\approx .6\text{M}$ ) at pH 10.3,  $25^\circ\text{C}$ . Etchant: 5% alc.  $\text{FeCl}_3$ ; X 175

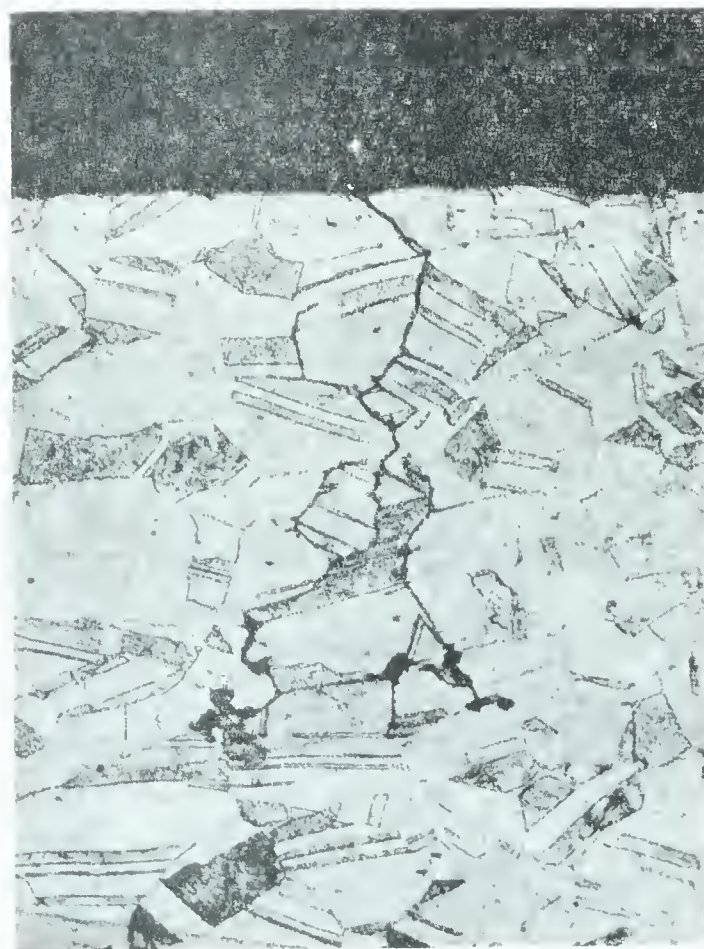
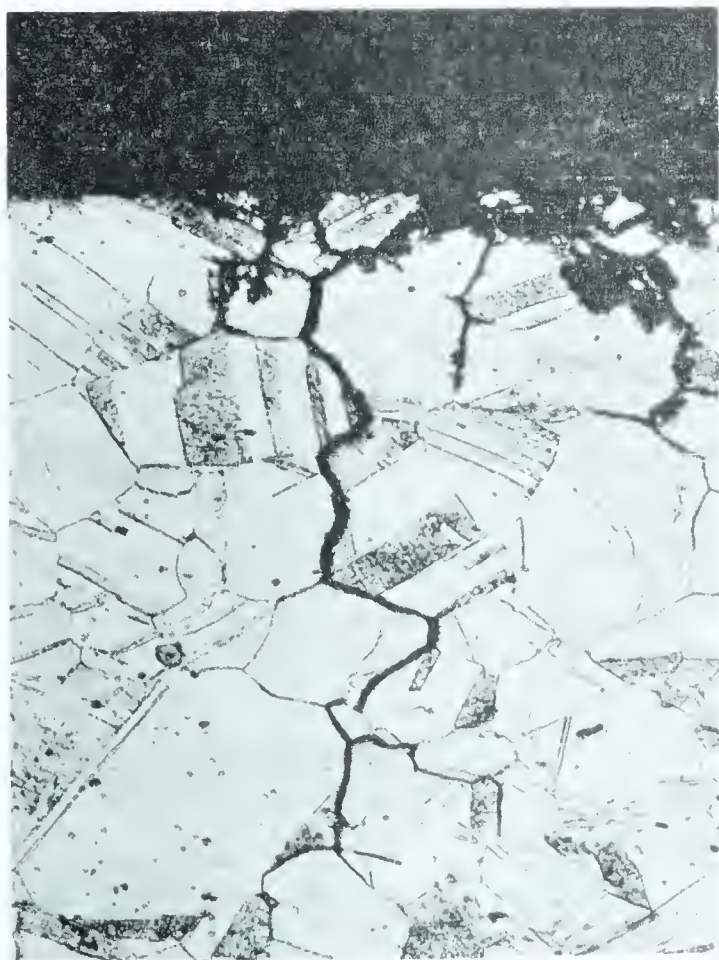


Fig. 24 Stress corrosion cracking of brass immersed in copper-tartrate solutions at  $25^\circ\text{C}$ ; a)  $\text{Cu} = 0.04\text{M}$ , total tartrate  $\approx .5\text{M}$ , pH  $\approx 13.0$ ; b)  $\text{Cu} = 0.03\text{M}$ , total tartrate  $\approx 0.4\text{M}$ , pH  $\approx 13.5$ . Etchant: 5% alc.  $\text{FeCl}_3$ ; X 175



in Fig.24b developed cracks after 500 hours immersion in a solution containing 0.03M Cu and 0.4M potassium tartrate adjusted to pH 13.0 with KOH. No cracking was observed in specimens immersed for 38 days in solutions containing 0.04M Cu and 0.6M potassium tartrate at pH values of 6.0, 9.0 and 12.6. As with the spectra of the citrate solutions, the spectra of the tartrate solutions that caused cracking showed strong absorption (in the wavelength range 600 - 640  $\mu$ ) corresponding to the formation of copper tartrate complexes.

These experiments show for the first time that citrate and tartrate reagents will induce stress corrosion cracking in brass, and demonstrate qualitatively, at least, that the cracking is associated with the copper-citrate and copper-tartrate complexes, the presence of which is controlled by the pH of the solution and concentration of the citrate and tartrate anions.

### 3. GENERAL DISCUSSION

The main features of the stress corrosion cracking of 70Cu-30Zn alloy under the testing conditions described above are:

- a) Cracking occurs in solutions containing copper-ammonia complexes of the type  $\text{Cu}(\text{NH}_3)_n^{++}$ . The most rapid (and predominantly intercrystalline) cracking occurs in the pH range 6.0 to 7.0, where  $\bar{n}$  is about 1.5 to 3.0.







- b) In solutions containing  $>0.03\text{M Cu}$ , in the pH range 6.0 - 7.0, the cracking is preceded by the formation of a  $\text{Cu}_2\text{O}$  tarnish on the specimens. This tarnish forms within a few minutes after the specimens are immersed in the testing solution, and forms **just as quickly on unstressed specimens exposed to similar solutions.** The tarnish develops within the metal, not as a deposit on the surface, and rarely exceeds one to five microns in depth. The formation of a  $\text{Cu}_2\text{O}$  tarnish (visible to the naked eye) is not a prerequisite to cracking, as is evidenced by the failure of untarnished specimens in solutions containing less than  $0.03\text{M Cu}(\text{NH}_3)_3^{++}$ , and in solutions of pH 5.0 and 5.5.
- c) The crack 'system' which leads to ultimate failure of the specimens always starts on the tension side of the specimen at a point on the U-bend where the stresses are greatest. Microscopic examination of the specimens after the tests showed smaller crack 'systems' at other points on the U-bend (e.g. Fig. 17). The main crack was usually the only one visible to the naked eye; viewed from above, it appeared to progress in short bursts, starting from one edge of the specimen and propagating towards the center, although this was only a two-dimensional observation. It was always



easily visible in tarnished specimens, since it exposed the bright yellow surface of fresh brass beneath the tarnish.

- d) In the pH range 6.0 - 7.0, the chemical reactions between the solution and the brass caused a decrease in the bulk pH of the solution, this decrease being greater in solutions containing unstressed specimens. At the same time, there was little or no general dissolution of the brass, a slight shift (  $< \text{five } \mu$ ) of the wavelength of the absorption peak towards higher wavelengths; the absorbance at this new wavelength was generally higher for the solutions containing the stressed samples.

Before outlining the proposed mechanism to account for the above observations, some attention must be given to the Pourbaix diagrams (pH/potential diagrams) which are applicable to our system. Mattsson,<sup>(168)</sup> in the original work on the pH dependence of cracking of brass, was the first to propose a correlation between certain features of the cracking and the pH/potential diagram for the copper-ammonia-water system. In his Pourbaix diagrams the stepwise formation of the copper-ammine complexes was ignored, and since one of the important features of the present investigation is the correlation of rapid cracking times with a certain ratio of ammonia ligands to dissolved copper, the Pourbaix diagrams were recalculated, using the equations



and constants listed in Appendix C. Fig. 25 shows the domains of predominance of solutes in the homogeneous system  $\text{Cu-NH}_3\text{-H}_2\text{O}$ , as calculated by Mattsson (Fig. 25a) and by us (Fig. 25b). The diagrams are essentially the same, except for the addition of the regions of stability of the intermediate copper-ammine complexes in Fig. 25b. In Fig. 26, the stability domains of the solid phases  $\text{Cu}$ ,  $\text{Cu}_2\text{O}$  and  $\text{CuO}$  have been added. The domains of  $\text{Cu}_2\text{O}$  and  $\text{CuO}$  as shown in Mattsson's diagram are incorrect; they should appear far to the right, as shown in Fig. 26b. The apparent reasons for this error are discussed in Appendix C.

It was natural that the Pourbaix diagram drawn up by Mattsson should be accepted by others<sup>(173)</sup> since the black  $\text{Cu}_2\text{O}$  tarnish appears on specimens exposed to solutions having a pH corresponding to the stability region for  $\text{Cu}_2\text{O}$  as shown by his diagram. It is important to note, however, that the diagram is calculated for copper, not brass; **pure copper does not form a tarnish in the same solutions that rapidly tarnish brass.** This was verified by simultaneously immersing brass strips and high purity copper strips (cleaned in 45%  $\text{HNO}_3$ ) in a copper-ammonia solution of pH 6.90. The brass developed the characteristic black coloration in a few minutes, while the copper remained untarnished.

The above observations do not negate the usefulness of pH/potential diagrams in interpreting the reactions accompanying cracking,





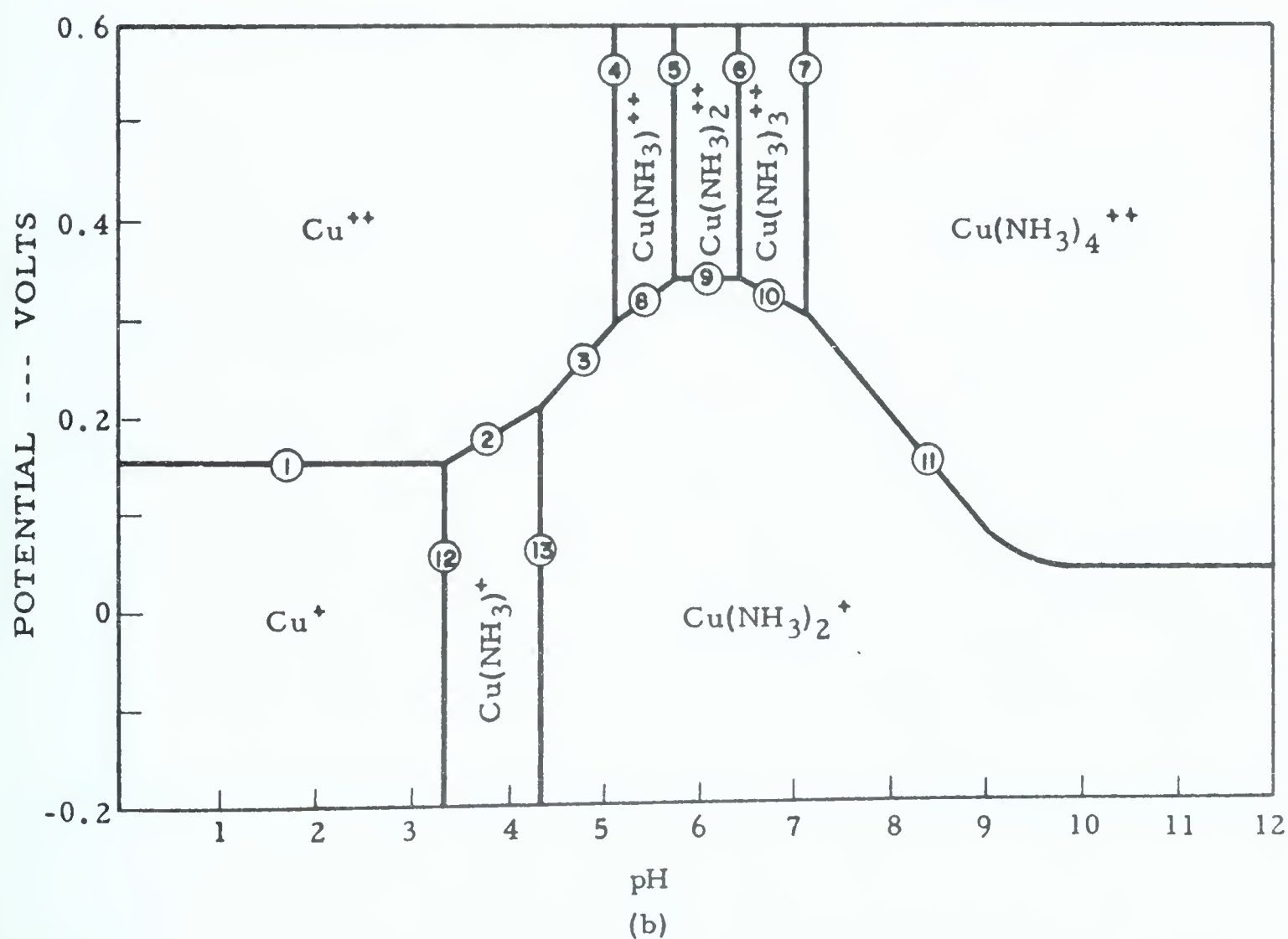
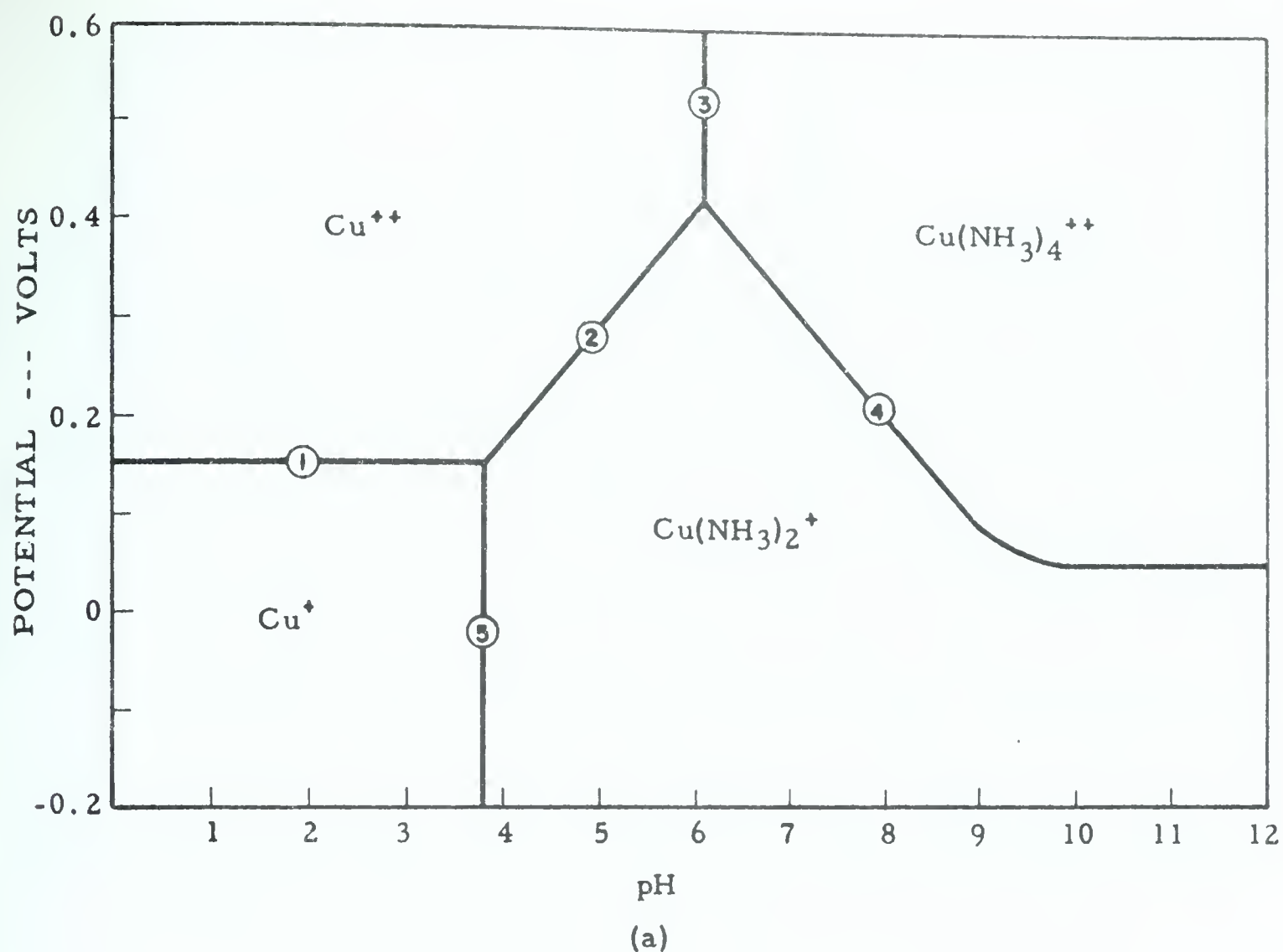


Fig. 25 pH/potential diagrams for the homogeneous system  $\text{Cu-NH}_3\text{-H}_2\text{O}$  ( $\text{Cu} = 0.05\text{M}$ , total ammonia =  $1.0\text{M}$ ) at  $25^\circ\text{C}$ , showing the domains of predominance of solutes. a) after Mattsson<sup>(168)</sup>, b) present work. The numbers correspond to each author's equations, as described in Appendix C



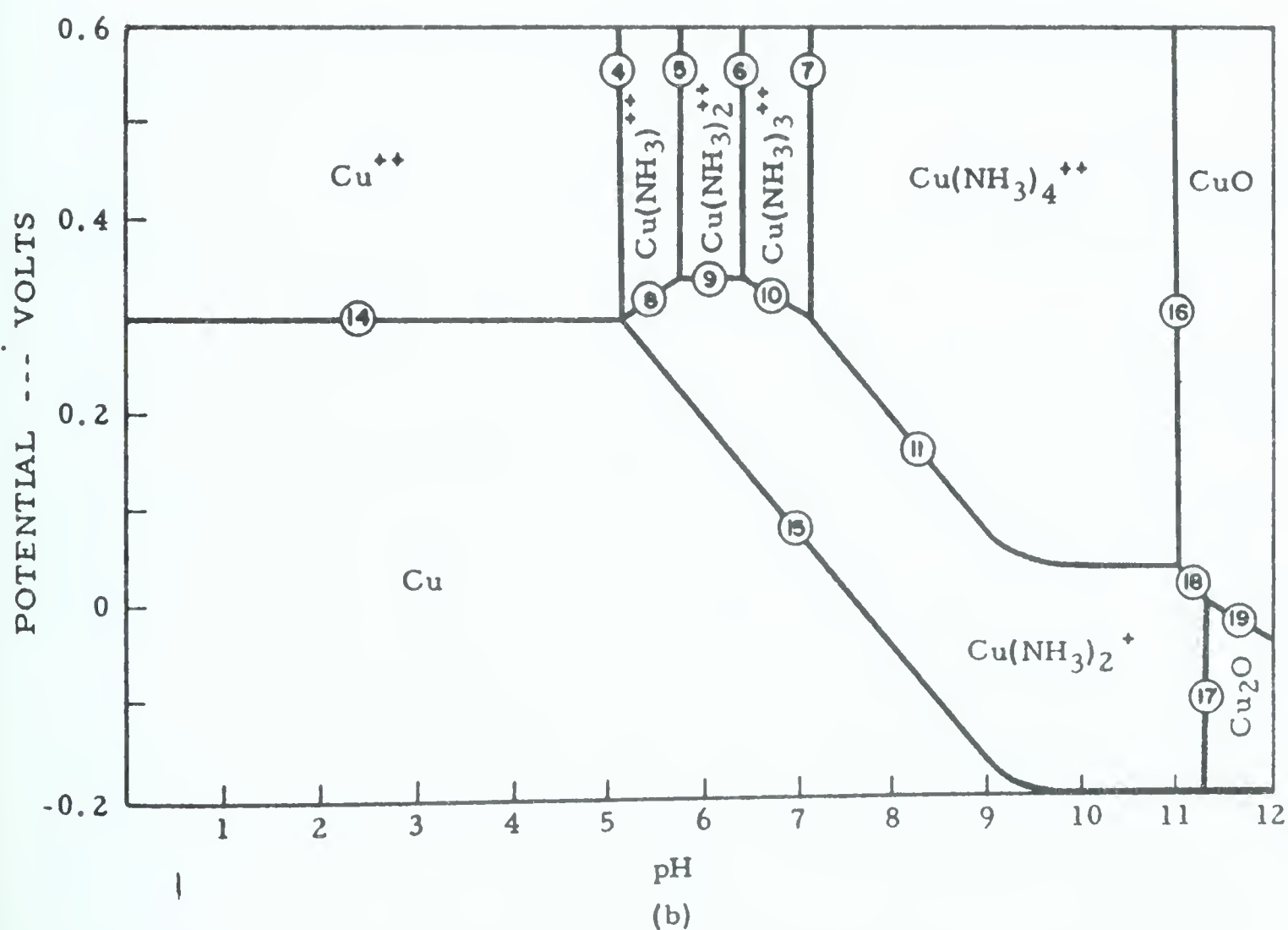
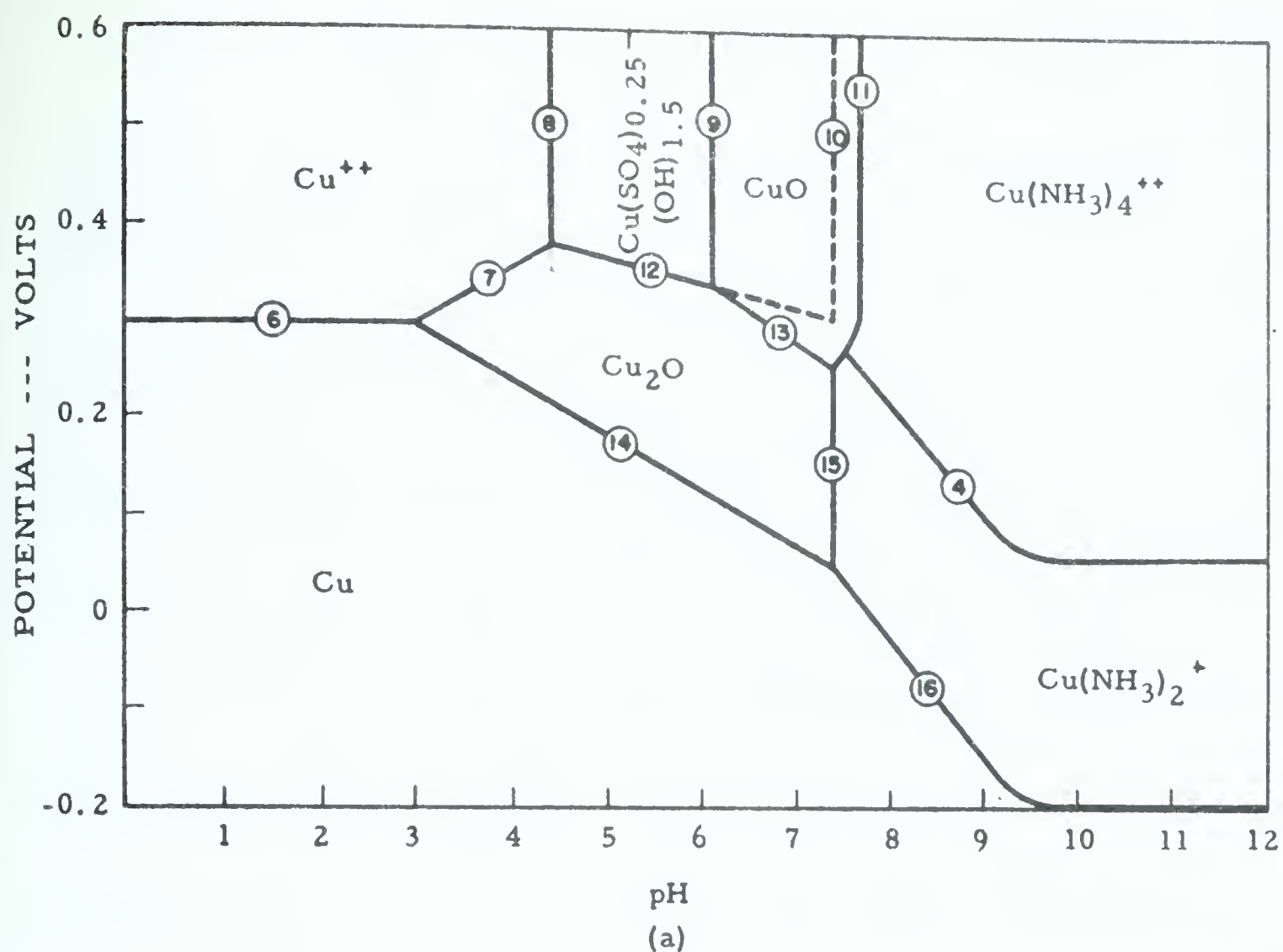


Fig. 26 pH/potential diagrams for the heterogeneous system Cu-NH<sub>3</sub>-H<sub>2</sub>O as in previous figure, with the addition of the stability domains of solid phases. a) after Mattsson<sup>(168)</sup>, b) present work



but they point out the fact that Pourbaix diagrams are calculated from thermodynamic data, on the basis that equilibrium conditions exist between the solids and solutes involved in the reaction, and so must be used with caution when applied to situations where equilibrium conditions are not established, either because of kinetic limitations or the occurrence of irreversible processes.

The fact that the pH/potential diagram for the  $\text{Zn-NH}_3\text{-H}_2\text{O}$  system must also be considered was appreciated by Mattsson, but here too his diagram appears incorrect, as can be seen by comparing Fig. 27a with Fig. 27b.

The theoretical considerations involved in constructing a pH/potential diagram for an alloy- $\text{NH}_3\text{-H}_2\text{O}$  system have not been fully developed, although a Pourbaix diagram for the system brass- $\text{H}_2\text{O}$ , showing the approximate corrosion domains, has been published.<sup>(169)</sup> In the present discussion, as in Mattsson's work, the copper and zinc diagrams (Figs. 25 - 27) will be considered simultaneously, keeping in mind the limitations imposed by not knowing the precise diagram for the system brass- $\text{NH}_3\text{-H}_2\text{O}$ .

The main theories invoked for the mechanisms of stress corrosion cracking have already been described as falling into two groups, viz. those involving a purely electrochemical dissolution which proceeds rapidly along susceptible paths, and those in which the electrochemical





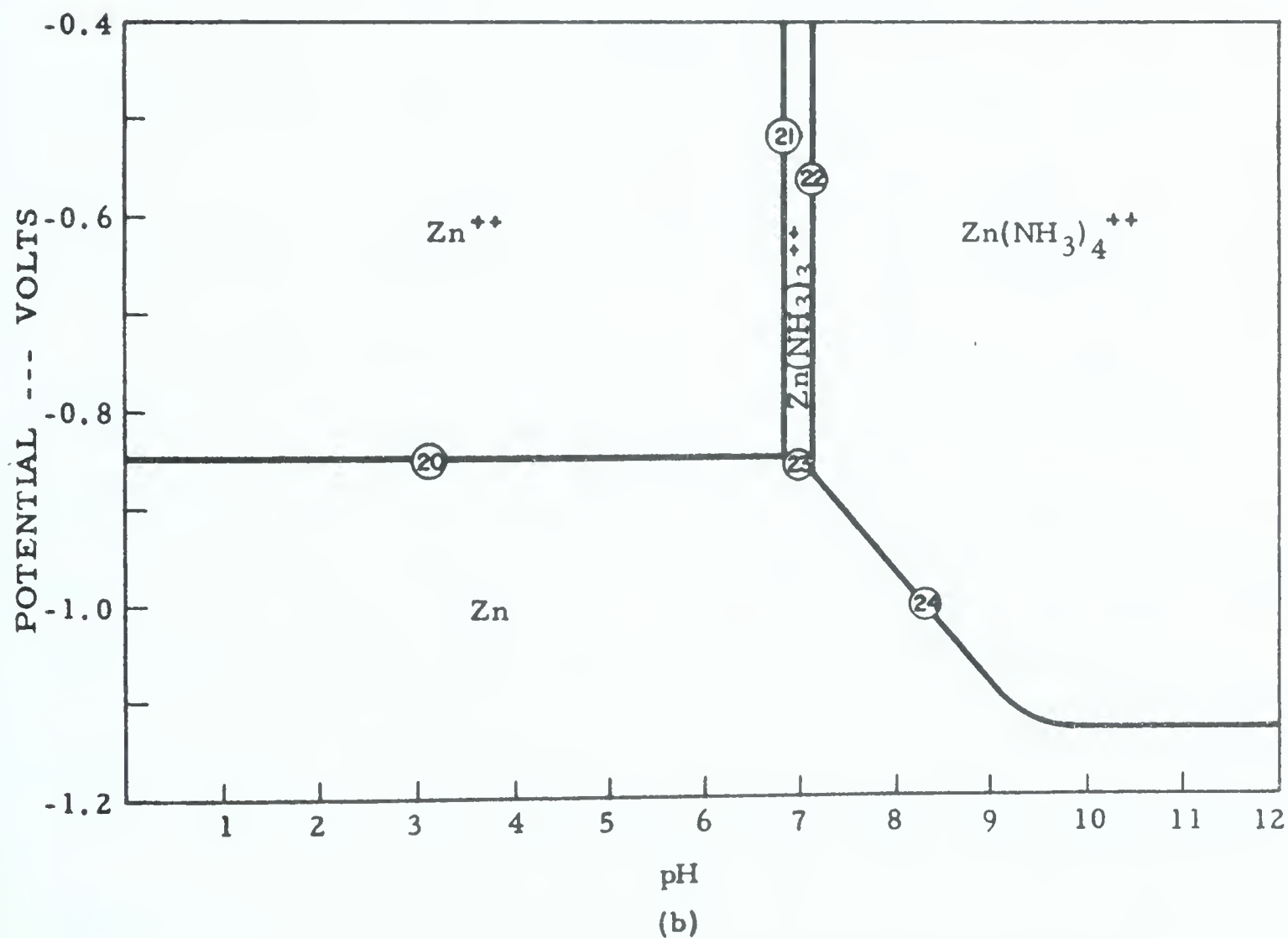
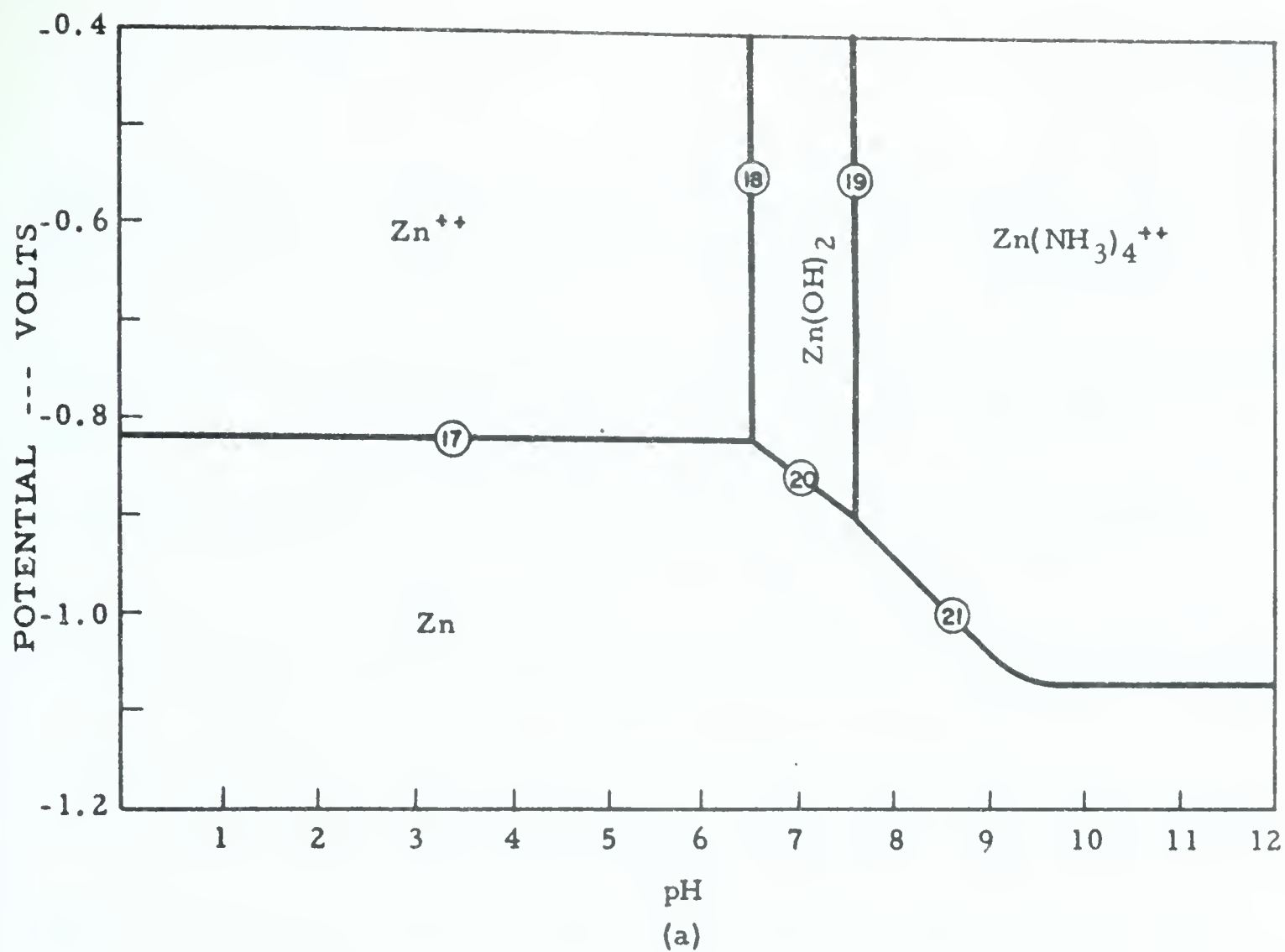


Fig. 27. pH/potential diagrams for the heterogeneous system Zn-NH<sub>3</sub>-H<sub>2</sub>O (total ammonia = 1.0M) at 25°C.  
 a) Zn = 0.01M, after Mattsson,<sup>(168)</sup> b) Zn = 0.001M, present work



stage alternates with a purely mechanical propagation of the crack through metal that is locally embrittled by chemical means, or because of short range ordering. However, the surface energy mechanism, which has been tentatively proposed in recent work,<sup>(184-187)</sup> seems to fit the present observations much better than either of the above theories. As a result of the present work, and from a re-evaluation of the extensive research done by others, it is proposed that a surface energy mechanism accounts for the intergranular stress corrosion cracking of alpha brass in aqueous ammonia solutions, and that the agent responsible for the pronounced surface energy lowering is the copper(I)-diammine complex  $\text{Cu}(\text{NH}_3)_2^+$ ; the cracking time represents the time needed to build up a concentration of  $\text{Cu}(\text{NH}_3)_2^+$  (at micro-crack sites) sufficient to provide the surface energy lowering necessary to satisfy the brittle fracture criterion.

In the following discussion, evidence will be presented to support this hypothesis, although at the outset it is admitted that such evidence is necessarily indirect, since there exists as yet no method capable of quantitatively measuring the surface tension lowering produced by the adsorption of ionic species such as  $\text{Cu}(\text{NH}_3)_2^+$  on a polycrystalline solid alloy.

The most obvious problem is the identity of the surfactant responsible for the surface energy lowering, and it is here that the



pH/potential diagrams provide significant information. From Mattsson's work it is known that cracking (in a solution initially containing copper and ammonia) occurs over the pH range 3.9 to 11.2; examination of Fig. 25 shows that the only solute capable of existing over this entire range is the monovalent copper-ammine complex. From our own closer examination of the pH range 5 - 8, it appears that 'true' stress corrosion cracking occurs over the limited pH range 6.0 - 7.5; again, from examination of the pH/potential diagrams we see that this corresponds to a region where divalent copper-ammine complexes having less than four  $\text{NH}_3$  ligands are stable (Fig. 25b), and also roughly corresponds to the region where soluble zinc is not yet appreciably converted to a zinc-ammine complex.

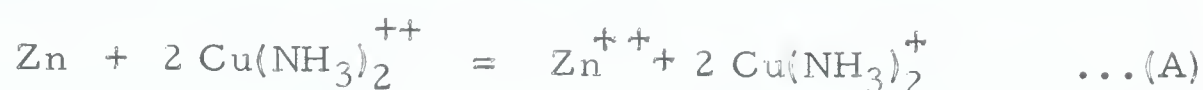
If we consider a copper-ammonia solution at a pH of 6.4, for example, we know that initially all of the dissolved copper is present as  $\text{Cu}(\text{NH}_3)_2^{++}$ ; if pure copper or pure zinc were immersed in this solution, each metal would tend to establish the equilibrium conditions shown in Figs. 26b and 27b, respectively. However, because we have a polycrystalline material consisting of a solid solution of these two elements, the situation represents a compromise between the two diagrams; further complications arise if we consider that the surface of the metal presents a heterogeneous array of point defects, emergent dislocation lines, stacking faults and grain boundaries, in





addition to the copper and zinc atoms; and finally, we must consider the fact that the activities of the two elements are not equal; in fact, the activity of zinc in 70Cu-30Zn alloy is very low.

The initial reactions at the brass/solution interface in the solution of pH 6.4 are



If enough free ammonia were present at the interface, the cuprous ion produced in reaction (B) would also be expected to form a complex; however, in the presence of water the solubility product of  $\text{Cu}_2\text{O}$  is soon exceeded, and  $\text{Cu}_2\text{O}$  is formed in the brass according to the reaction



This reaction accounts for the pH decrease observed in the test solutions, and also accounts for the tarnish formation; however, the stability of the  $\text{Cu}_2\text{O}$  is not predicted by Fig. 26b. This apparent anomaly can be explained if one remembers that the tarnish does not form on pure copper and that the tarnish does not build up on the surface of the brass (both of which are in agreement with the pH/potential diagram). Now consider the line separating the regions of stability of  $\text{Cu}(\text{NH}_3)_2^+$  and  $\text{Cu}_2\text{O}$  as shown in Fig. 26b. The equation for this line (Equation 17, Appendix C) is:



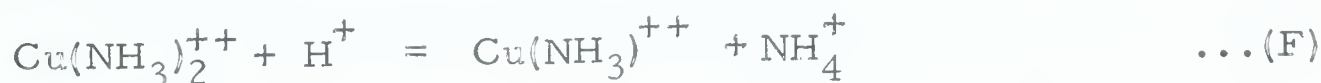
$$\text{pH} = 10.03 - \log \frac{[\text{Cu}(\text{NH}_3)_2^+]}{[\text{NH}_3]^2} \quad \dots (\text{D})$$

It can be seen that the ratio in the log term must be greater than  $10^4$  if  $\text{Cu}_2\text{O}$  is to exist (under equilibrium conditions) at pH 6.4. Since the bulk concentration of free  $\text{NH}_3$  is about  $10^{-4}\text{M}$  at this pH, either the concentration of  $\text{Cu}(\text{NH}_3)_2^+$  at the metal/solution interface must be greater than  $10^{-4}\text{M}$ , or the concentration of free  $\text{NH}_3$  must be reduced correspondingly to make the ratio greater than  $10^4$ .

Since the black tarnish develops rapidly in brass, but not in copper, it is assumed that reaction (A) contributes primarily to a local increase in the concentration of  $\text{Cu}(\text{NH}_3)_2^+$ . In fact, subsequent considerations show that the formation of the black  $\text{Cu}_2\text{O}$  tarnish is a side reaction only, which affects the cracking time only insofar as reaction (C) produces a local concentration of  $\text{H}^+$  that can 'strip' the complexes of their  $\text{NH}_3$  groups to form  $\text{NH}_4^+$



by such reactions as



The overall reaction (B) + (C) + (E) is





which shows the  $\text{Cu}_2\text{O}$  formation, without production of  $\text{Cu}(\text{NH}_3)_2^+$  complexes. The latter complex must be formed primarily by reaction (A) in order to satisfy the conditions for the stability of the  $\text{Cu}_2\text{O}$  as set out in equation (D).

The source of oxygen for the  $\text{Cu}_2\text{O}$  may be either a strongly adsorbed water layer or the solvation sheath of the complex ions; the tarnishing reaction appeared to be independent of dissolved oxygen concentration during the tests listed in Table III; also, Miller and Lawless<sup>(175)</sup> found the oxidation of pure copper in copper sulfate solutions to be independent of the dissolved oxygen content, and proposed a reaction similar to reaction (C).

The mode of cracking in the pH range 6.0 - 7.5 is predominantly intergranular; in order to explain the apparent affinity of the adsorbing species for the grain boundaries, or more correctly, to explain why the reaction leading to the production of the adsorbing species occurs more readily at the grain boundaries, we must consider the alloy composition there.

The surface energies of solid copper and solid zinc are not known precisely (Taylor<sup>(188)</sup> gives values of 580 ergs/cm<sup>2</sup> and 365 ergs/cm<sup>2</sup> respectively) but it is generally known that the surface energy of copper is much greater than zinc. Speiser and Spretnak<sup>(189)</sup> have shown theoretically that in a binary alloy the component with the





lower surface tension will be positively adsorbed at the grain boundary, i.e., in 70Cu-30Zn there should be an excess of zinc at the grain boundary interfaces.

Considering reactions (A) and (B), we note that from Figs. 26b and 27b, the potential for the oxidation of zinc lies well below the potential for the oxidation of copper; this is equivalent to saying that the free energy of formation of the zinc ion is much greater than the free energy of formation of the  $\text{Cu}(\text{NH}_3)_2^+$  complex i.e.,  $\Delta G_{\text{Zn}^{++}}^0 = -35.18$  kcal/mole,  $\Delta G_{\text{Cu}(\text{NH}_3)_2^+}^0 = -15.54$  kcal/mole ( $\Delta G_{\text{Cu}(\text{NH}_3)_2^{++}}^0 = -7.71$  kcal/mole); so that we would expect reaction (A) to be favored; in addition, if an excess of zinc were present at the grain boundaries, one would expect the reaction to proceed more rapidly there. However, the low activity of zinc in brass would have a counterbalancing effect; these two facts taken together explain the reason for the dependence of cracking time on zinc content (as originally suggested by Speiser and Spretnak<sup>(189)</sup>).

One additional factor considered important in the explanation of the rapidity of the production of  $\text{Cu}(\text{NH}_3)_2^+$  ions in the pH range 6.0 - 7.0 is the relative configuration of the reactant and product molecules involved. Reaction (A) involves only an electron transfer from the zinc atoms to the copper complexes, and no addition or transfer of  $\text{NH}_3$  ligands; however, at higher pH values, the reacting



complex will contain more  $\text{NH}_3$  ligands which it must lose in converting to the monovalent complex; it is intuitive that the activation energy will be lower for the reaction where the configurations of the reactants and products are most nearly similar, since the formation of an intermediate activated complex (complex, in this sense, refers to the 'activated state' which is a fundamental postulate of the theory of absolute reaction rates) will be facilitated.

The kinetics of the reaction leading to the formation of  $\text{Cu}(\text{NH}_3)_2^+$  at grain boundaries is definitely related to the initial concentration of  $\text{Cu}(\text{NH}_3)_n^{++}$ , as shown in Fig. 19 ; a quantitative determination of the rate of buildup of  $\text{Cu}(\text{NH}_3)_2^+$  is difficult, if not impossible, because

- a) it is the concentration of  $\text{Cu}(\text{NH}_3)_2^+$  at the grain boundaries, not in the bulk solution, that is important
- b) some dissolution of copper from the brass occurs; this means that the observed change in total dissolved copper concentration is not quantitatively related to the production of  $\text{Cu}(\text{NH}_3)_2^+$  by reaction with zinc atoms
- c) the change in bulk zinc concentration is at or below the limit of sensitivity of the analytical method.

In spite of these difficulties, we can get some idea of the order of the reaction if we consider that the cracking time represents



the time needed for the development of a critical concentration of  $\text{Cu}(\text{NH}_3)_2^+$ , or in other words, represents the time  $t_c$  needed for a certain fraction,  $c$ , of the initial  $\text{Cu}(\text{NH}_3)_n^{++}$  to react to produce a critical concentration  $(1-c)$  of  $\text{Cu}(\text{NH}_3)_2^+$ . If we then assume that the rate expression is of the simple form

$$dx/dt = k(a - x)^n \quad \dots (H)$$

(where  $n$  = order of reaction,  $a$  = initial concentration of reactant,  $x$  = amount of reactant decomposed at time  $t$ ,  $k$  = rate constant), the dependence of the fractional life period on the initial concentration is given by:<sup>(190)</sup>

$$t_c = f(n, k) / a^{n-1} \quad \dots (J)$$

where  $f$  is some function of  $n$ ,  $k$ , and is constant for a given reaction at constant temperature. In logarithmic form, equation (J) becomes

$$\log t_c = \log f - (n - 1) \log a \quad \dots (K)$$

so a plot of  $\log t_c$  vs.  $\log a$  should be linear (if the rate expression conforms to equation (H)) with a slope of  $1-n$ . Fig. 28 is a plot of  $\log t_c$  ( $t_c$  is cracking time) vs.  $\log a$  (where  $a$  = initial dissolved copper concentration), using the data of Fig. 19. Over the concentration range 0.002M to 0.05M, the points correspond fairly well to a line with a slope of minus one, which suggests a second order reaction. Reaction (A) is termolecular as written, but if the concentration of zinc were assumed to be constant, the reaction could be considered





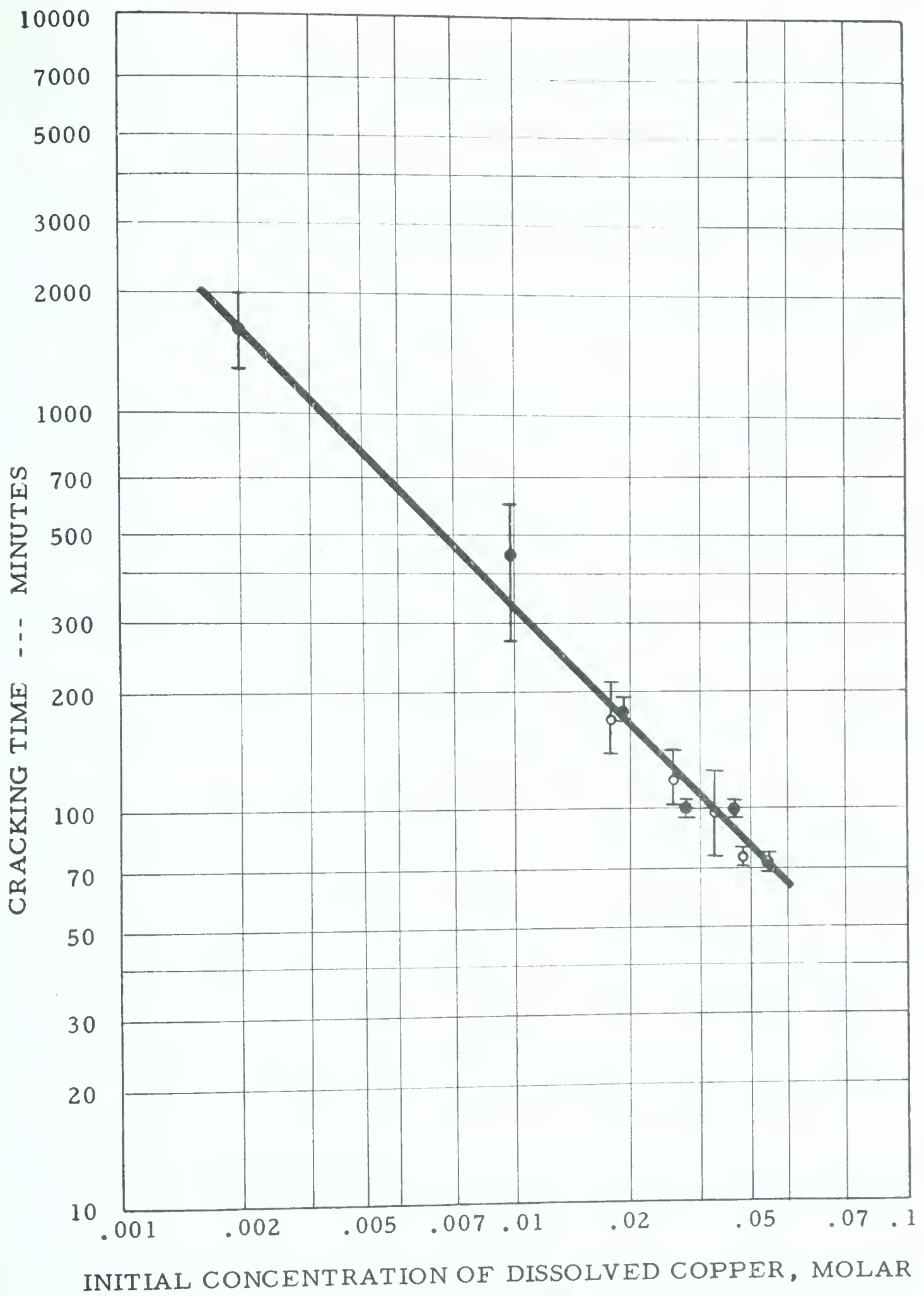


Fig. 28 Effect of initial concentration of dissolved copper on cracking of brass in 1.5M ammonia solutions, pH 7.1, at 22.5°C. Solid circles, single specimens; open circles, average of duplicate runs



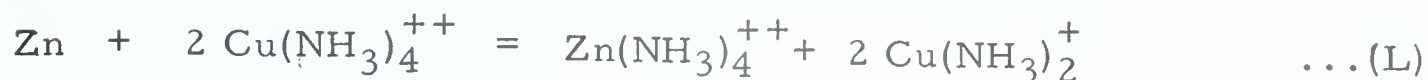
to be pseudo-bimolecular, in agreement with the observed apparent order. Although many reactions involving solid surfaces exhibit pseudo-molecularity because of the high activity of surface sites, the assumption of constant zinc concentration may be unwarranted in view of the generally low activity of zinc in brass, and also in view of the fact that zinc atoms at grain boundaries will present a non-uniform distribution of 'active sites' for the reacting molecules. But even with these limitations in mind, the strong concentration dependence of the cracking time certainly agrees qualitatively with the proposed theory.

Implicit in the discussion of kinetics is the assumption that the observed cracking time is made up of two stages, a slow initiation period during which the necessary concentration of surfactant is produced, and a very rapid (compared with the initiation period) crack propagation step. This assumption finds precedence in other stress corrosion systems (as was pointed out in the literature review) and has been recently verified for the brass-ammonia system by Booker.<sup>(191)</sup>

So far we have limited the discussion to the rapid intergranular cracking exemplified by a solution of pH 6.4; now let us consider two other pH 'regions', choosing solutions of pH 8.0 and 5.0 as examples:

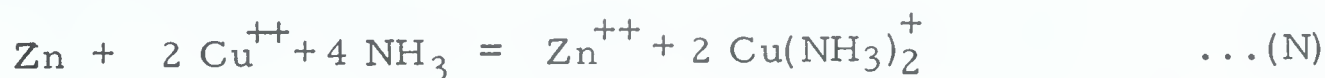


At pH 8.0, the initial possible reactions are



The free energy of formation of  $\text{Zn}(\text{NH}_3)_4^{++}$  is -73.45 kcal/mole, so that the dissolution of zinc is clearly favored; however, because of the higher concentration of free  $\text{NH}_3$  at this pH, reaction (M) also takes place, resulting in the added dissolution of copper, and the overall result is an increase in the general corrosion rate, with localized intergranular attack, as shown by the photomicrograph in Fig. 16c, and by the polarographic analyses in Table IV. It is proposed that this generally intensified corrosion in the presence of stress reduces the probability of any one grain boundary site becoming the site for crack initiation. Consequently, the distinction between intergranular corrosion and intergranular stress corrosion cracking is not straightforward at this pH, so that failure of the specimen could occur by either mechanism.

At pH 5.0, consideration of the Pourbaix diagrams shows that the possible reactions are



The supply of  $\text{NH}_3$  for these reactions would have to come mainly from the ionization of  $\text{NH}_4^+$ , which would result in a pH decrease in solution; however, a pH increase was actually observed, and this



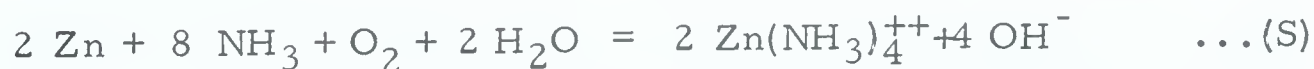
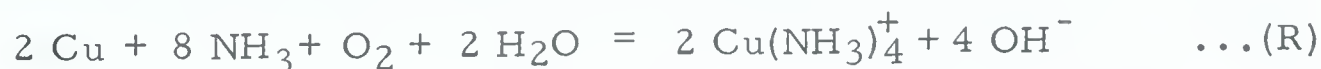


suggests that the cathodic reduction of oxygen, i.e.



might be important, especially since the oxygen could act as an electron acceptor in the oxidation of metallic copper to the cuprous state, after which it would combine with ammonia to form the  $\text{Cu}(\text{NH}_3)_2^+$  complex.

At this point we should consider another solution in which no  $\text{Cu}(\text{NH}_3)_n^{++}$  was initially present, viz. the solution at pH 7.1 with zero initial copper concentration, listed in Table VI. Here, as in the solution of pH 5.0, the cracking time is relatively long (of the order of 5000 minutes), and since no oxidizing agent (such as  $\text{Cu}(\text{NH}_3)_n^{++}$ ) is present initially, the first steps of the reaction are undoubtedly influenced by the oxygen concentration. Lu and Graydon<sup>(182)</sup> have shown that the dissolution of pure copper in air-saturated ammonia solutions is autocatalytic, and apparently of zero order in the early stages, which means that the reduction of oxygen is important only insofar as it produces the initial amount of  $\text{Cu}(\text{NH}_3)_2^+$  or  $\text{Cu}(\text{NH}_3)_n^{++}$ . The overall reaction, therefore, cannot be represented by the equations



as has been suggested by several authors,<sup>(189)(191)(193)(194)</sup> since according to these reactions an increase in solution pH should be observed, and in actual fact a slight decrease was found. The sequence of



reactions under conditions of zero initial dissolved copper could be:

- a) general dissolution of copper and zinc, and subsequent combination with  $\text{NH}_3$  to form the divalent copper and zinc complexes appropriate to the pH of the solution;
- b) reaction of the  $\text{Cu}(\text{NH}_3)_n^{++}$  complex with the zinc at suitable reaction sites to produce  $\text{Cu}(\text{NH}_3)_2^+$ .

Alternately, the sequence could be:

- a) general dissolution of copper and zinc, producing divalent zinc-ammine complexes and monovalent copper-ammine complexes at the brass-solution interface;
- b) surface diffusion of the monovalent copper complexes to suitable adsorption sites.

The available evidence does not distinguish between these sequences, but either one will produce the same end result.

In the preceding discussion we have made reference to the polarographic and pH measurements given in Tables IV and VI; there are two other items in these tables (and Table V) that should be discussed:

The first concerns the results of the absorbance measurements on test solutions. The chief value of the spectra was the unequivocal correlation of the number of  $\text{NH}_3$  ligands per copper atom (initially present in solution) with the cracking time. The spectra run on solutions at the conclusion of each test provided corroboration for the observed pH



and/or concentration changes, only if such changes were very pronounced. For example, the absorption peak wavelengths in Table V did not show any significant shift because the bulk properties of the solutions did not change appreciably during the reaction, whereas in Table VI there are definite wavelength shifts of 5 - 10  $m\mu$  (corresponding to a 0.1 - 0.2 decrease in  $\bar{n}$ , according to Fig. 15). A decrease in  $\bar{n}$  can be caused by

- a) an increase in dissolved copper concentration, i.e., more copper atoms are present to share the same number of  $NH_3$  ligands;
- b) an increase in dissolved zinc concentration (if the pH is greater than 6.8), i.e., zinc atoms must also share the available  $NH_3$  ligands;
- c) a decrease in pH which means less  $NH_3$  is available for complexing;
- d) less  $NH_3$  being available for divalent complex formation because of a transfer of  $NH_3$  ligands to the colorless monovalent copper -ammine complex.

With these four possibilities in mind, one can see that the wavelength changes for each test must be considered individually; if this is done, there is a general qualitative agreement with the pH and/or concentration changes.





The other item in the analytical results is the difference between final measurements on solutions containing stressed and unstressed specimens. There are two general conclusions that can be made: First, the overall effect of stress is to increase any general dissolution which may occur. This effect is clearly shown in the solution of pH 8.0 (Table IV) and in the solution with zero initial copper concentration (Table VI). Second, any effect which stress may have on the specific dissolution of one species (e.g., zinc at grain boundaries) is not revealed by a change in the bulk properties of the solution (under our testing conditions), within the limits of the analytical methods used. Therefore it is assumed that the observed differences (between stressed and unstressed samples) in pH and absorbance (amounting to only 1 - 2%) for solutions in the pH range 6.0 - 7.3 (Tables IV and V) are caused by the generally increased activity of the stressed specimen.

In proposing the surface energy mechanism for the cracking of brass, we have used the term 'micro-crack' sites when referring to the initiation of cracks. This was used for convenience only, and is not meant to imply the existence of wedge-shaped defects in the unstressed metal, but was meant to describe those locations on the surface of a metal where locally intensified corrosion can provide a 'notch' or 'slot' in which the surfactant molecules are particularly effective. For alpha brass exposed to copper-ammonia solutions in the pH range 6-7,



reaction (A) satisfies both conditions, i.e., it can produce a notch at the grain boundaries by chemical dissolution of zinc atoms, and at the same time produce the adsorbing species,  $\text{Cu}(\text{NH}_3)_2^+$ .

One of the chief shortcomings of the many proposed mechanisms for the cracking of brass is the lack of an explanation for the nature of the reagents which cause cracking. If the surface energy mechanism is operative, then there should be other reagents which could satisfy the two conditions mentioned in the previous paragraph. The meagre information given by Bobylev<sup>(131)</sup>, described in the literature review, Section 3B, suggests that there are other complexing reagents that will produce cracking. Our own results have shown that cracking can be produced in citrate and tartrate solutions, and that the cracking time shows some pH dependence.



## SUMMARY AND CONCLUSIONS

A study of the surface chemistry of the stress corrosion cracking of alpha brass in gaseous and aqueous environments gave the following main results:

- 1) The reaction involved aqueous ionic species, and therefore was not amenable to study in the gas phase.
- 2) In aqueous copper-ammonia solutions, the type of cracking and cracking time were strongly pH dependent; 'true', rapid intergranular stress corrosion cracking occurred over the pH range 6.0 - 7.0.
- 3) The cracking in the pH range 6.0 - 7.0 was correlated with  $\bar{n}$ , the average number of ammonia ligands per copper atom originally present in solution as the divalent copper-ammine complex  $\text{Cu}(\text{NH}_3)_n^{++}$ . Cracking was most rapid for  $\bar{n} = 1.5 - 3.0$ .
- 4) The intergranular cracking time was independent of dissolved oxygen in copper-ammonia solutions at  $\text{pH} \approx 7.1$ .
- 5) The cracking time in copper-ammonia solutions initially containing 0.002 - 0.05M dissolved copper increased exponentially with decreasing copper concentration.





- 6) The black tarnish, characteristic of many specimens undergoing stress corrosion cracking, was definitely identified as  $\text{Cu}_2\text{O}$ . Its occurrence was not a pre-requisite for cracking.
- 7) The temperature dependence of the cracking of brass in copper-ammonia solutions of pH 6.8 and 7.1 did not conform to the Arrhenius equation.
- 8) Intergranular stress corrosion cracking of brass was produced in solutions containing copper-citrate complexes and copper-tartrate complexes.

The pH/potential diagrams for the systems  $\text{Cu-NH}_3\text{-H}_2\text{O}$  and  $\text{Zn-NH}_3\text{-H}_2\text{O}$  were recalculated, showing the errors in previously published diagrams for these systems.

As a result of this work, a surface energy mechanism for the stress corrosion cracking of alpha brass has been postulated. In summary, it is proposed that the specific adsorption of the copper(I)-diamine complex at grain boundaries produces a lowering of surface energy, which, in combination with the applied tensile stress, allows the propagation of a brittle crack which continues until the stress is relieved by relaxation. The initiation and re-initiation of the cracks are caused by the reduction of copper(II)-ammonia complexes (and the concomitant oxidation of zinc) at grain boundaries. The reaction



is especially favored over the pH range 6.0 - 7.0 because of the ease of formation of the monovalent complex.

Wherever possible, the relevant observations of previous authors have been commented on, in the light of the proposed mechanism. A complete discussion of all of the ramifications of the theory (particularly those related to metallurgical factors) is beyond the scope of this thesis; the main outcome of the present work was the proposal of the surface energy mechanism in order to account for the effect of the chemical variables under the described testing conditions.



## BIBLIOGRAPHY

1. Diegel, C., Z. Ver. Bef. Gewerbefleiss, 85, 177 (1906).
2. Sperry, E. S., Brass World 2, 39 (1906).
3. Heyn, E., J. Inst. Metals 12, 3 (1914).
4. Flinn, A. D., Engineering Record 68, 527 (1913).
5. Jonson, E., Trans. Am. Inst. Metals 8, 135 (1914).
6. Jonson, E., Proc. A.S.T.M. 15, II, 101 (1915).
7. Merica, P. D., and Woodward, R.W., Nat. Bur. Standards (U.S.) Technol. Paper No. 82 (1917).
8. Merica, P.D., and Woodward, R.W., Trans. Am. Inst. Metals 9, 298 (1915).
9. White, A.E., Proc. A.S.T.M. 16, II, 151 (1916).
10. Proc. A.S.T.M. 18, II, 147 (1918).
11. Symposium on Stress-Corrosion Cracking of Metals, A.S.T.M. - A.I.M.E., New York (1945).
12. Stress Corrosion Cracking and Embrittlement, Robertson, W.D., ed., Wiley, New York (1956).
13. Physical Metallurgy of Stress Corrosion Fracture, Rhodin, T.N., ed., Interscience, New York (1959).
14. Teknisk-Vetenskaplig Forskning 32, 94 (1961).
15. Proc. First Int. Congr. Metallic Corrosion, Butterworths, London (1962).
16. Proc. Second Int. Congr. Metallic Corrosion, in press.
17. Waber, J.T., and McDonald, H.J., Stress Corrosion Cracking of Mild Steel, Corrosion Publishing Co., Pittsburgh (1947).





18. Report on Stress-Corrosion Cracking of Austenitic Chromium-Nickel Stainless Steels, A.S.T.M., Philadelphia (1960).
19. Shvartz, G.L., and Kristal, M.M., Corrosion of Chemical Apparatus, Consultants Bureau, New York (1959).
20. Intercrystalline Corrosion and Corrosion of Metals Under Stress, Levin, I.A., ed., Consultants Bureau, New York (1962).
21. Glikman, L.A., Corrosion-Mechanical Strength of Metals, Butterworths, London (1962).
22. Romanov, V.V., Stress-Corrosion Cracking of Metals, Israel Program for Scientific Translations, Jerusalem(1961).
23. Bailey, A.R., Metals Rev. 6, 101 (1961).
24. Mears, R.B., Brown, R.H., and Dix, E.H., Jr., Ref. (11), p. 323.
25. Cohn, L.M., Elektrotechnik u. Machinebau 31, 415 (1913).
26. Dix, E.H., Jr., Trans. A.I.M.E. 137, 11 (1940).
27. Althoff, F., Luftfahrt-Forsch. 15, 60 (1938).
28. Bungardt, W., and Schaitberger, G., Z. Metallk. 35, 47 (1943).
29. Colner, W.H., and Francis, H.T., J. Electrochem. Soc. 105, 377(1958).
30. Loose, W.S., and Barbian, H.A., Ref. (11), p. 273.
31. Timonova, M.A., Ref. (20), p. 263.
32. Morris, A., Trans. A.I.M.E. 89, 256 (1930).
33. Moore, H., Beckinsdale, S., and Mallinson, C.E., J. Inst. Metals 25, 35 (1921).
34. Rosenthal, H., and Jamieson, A.L., Trans. A.I.M.E. 156, 212 (1944).
35. Bassett, W.H., Ref. (10), p. 153.
36. Arnott, J., Trans. Faraday Soc. 17, 202 (1921).



37. Pinkerton, A., and Tait, W.H., J. Inst. Metals 36, 233 (1926).
38. Thompson, D.H., and Tracy, A.W., Trans. A.I.M.E. 185, 100 (1949).
39. Burghoff, H.L., and Mitchell, N.W., A.S.M. Metals Handbook, p. 1468 (1939).
40. Merica, P.D., and Woodward, R.W., Proc. A.S.T.M. 19, 278 (1919).
41. Graf, L., and Budke, J., Z. Metallk. 46, 378 (1955).
42. Wilson, T.C., Edmunds, G., Anderson, E.A., and Pierce, W.M., Ref. (11), p. 173.
43. Schroeder, W.C., and Berk, A.A., Trans. A.I.M.E. 120, 387 (1936).
44. Jones, J.A., Trans. Faraday Soc. 17, 102 (1921).
45. Portevin, A., Rev. Met. 22, 179 (1925).
46. Schroeder, W.C., and Partridge, E.P., Trans. A.S.M.E. 58, 223 (1936).
47. Desch, C.H., Engineer(London) 167, 418 (1939).
48. Schmidt, H.W., Gegner, P.J., Heinemann, C., Pogacar, C.F., and Wyche, E.H., Corrosion 7, 295 (1951).
49. Houdremont, E., Benneck, H., and Wentrup, H., Stahl u. Eisen 60, 757 (1940).
50. Ref.(19), p. 69.
51. Dawson, T.J., Welding J. (N.Y.) 35, 568 (1956).
52. Parkins, R.N., J. Iron Steel Inst.(London) 174, 317 (1953).
53. Vollmer, L.V., Corrosion 8, 326 (1952).
54. Herzog, E., Corrosion et Anti-Corrosion 2, 3 (1954).
55. Ref.(19), pps. 87, 88.
56. Robertson, W.D., Grenier, E.G., Davenport, W.H., and Nole, V.F., Ref. (13), p. 273.



57. Azhogin, F.F., Ref. (20), p. 211.
58. Ref.(22), p. 86.
59. Hoyt, S.L., and Scheil, M.A., Trans. Am. Soc. Metals 27, 191 (1939).
60. Scheil, M.A., Zmeskal, O., Waber, J., and Stockhausen, F., Welding J. (N.Y.) 22, 493s (1943).
61. Hodge, J.C., and Miller, J.L., Trans. Am. Soc. Metals 28, 25 (1940).
62. Franks, R., Binder, W.O., and Brown, C.M., Ref. (11), p. 411.
63. Mackay, J.S., Ref. (11), p. 429.
64. Klement, J.F., Maersch, R.E., and Tully, P.A., Metal Progr. 75, No. 2, 82 (1959).
65. Perryman, E.C.W., J. Inst. Metals 78, 621 (1951).
66. Farmery, H.K., and Evans, U.R., J. Inst. Metals 84, 413 (1955-56).
67. Phelps, E.H., and Mears, R.B., Ref. (15), p. 319.
68. Rideout, S.P., Ref. (16).
69. Davis, F.W., Trans. Am. Soc. Metals 42, 1233 (1950).
70. Logan, H.L., and Sherman, R.J., Jr., Welding J. (N.Y.) 35, 389s (1956).
71. Bowers, C.N., McGuire, W.J., and Wiehe, A.E., Corrosion 8, 333 (1952).
72. Fraser, J.P., and Treseder, R.S., Corrosion 8, 342 (1952).
73. Fraser, O.B.J., Ref. (11), p. 458.
74. Copson, H.R., and Cheng, C.F., Corrosion 12, 647t (1956).
75. Roberts-Austen, W.C., Proc. Roy. Inst. G.B. 11, 395 (1886).
76. Graf, L., Ref. (12), p. 48.





77. Schneider, A., and Esch, U., Z. Elektrochem. 49, 72 (1943).
78. Cohen, E., and Helderman, W.D., Proc. Acad. Sci. Amsterdam 17, 822 (1914).
79. Archbutt, S.L., Trans. Faraday Soc. 17, 22 (1921).
80. Dunham, J.T., and Kato, H., U.S. Bur. Mines, Rep. Invest. 5784 (1961).
81. Ref. (11), p. 330.
82. Ref. (17), p. 66.
83. Sobolev, N.D., J. Tech. Phys. (U.S.S.R.) 22, 1630 (1952).
84. Ref. (22), p. 36.
85. Merica, P.D., and Woodward, R.W., Ref. (10), p. 165.
86. Symposium on Internal Stresses in Metals and Alloys, Institute of Metals, London (1947).
87. Ref. (21), p. 4.
88. Harwood, J.J., Corrosion 6, 249 (1950).
89. George, C.W., and Chalmers, B., Ref. (11), p. 345.
90. Ref. (21), p. 7.
91. Hoar, T.P., and Hines, J.G., J. Iron Steel Inst. (London) 182, 124 (1956).
92. Hoar, T.P., and Hines, J.G., Ref. (12), p. 107.
93. Yang, L., Horne, G.T., and Pound, G.M., Ref. (13), p. 29.
94. Fryxell, R.E., and Nachtrieb, N.H., J. Electrochem. Soc. 99, 495 (1952).
95. Nobe, K., and Tan, S., Corrosion 18, 391t (1962).



96. Tan, S., and Nobe, K., Can. J. Chem. 41, 495 (1963).
97. Nobe, K., Baum, E., and Seyer, W.F., J. Electrochem. Soc. 108, 97 (1961).
98. Evans, U.R., The Corrosion and Oxidation of Metals, Edward Arnold, London (1960), p. 386.
99. Uhlig, H.H., Ref. (13), p. 1.
100. Barnartt, S., Corrosion 18, 322t (1962).
101. Parkins, R.N., Ref. (12), p. 140.
102. Parkins, R.N., and Usher, R., J. Appl. Chem.(London) 9, 445 (1959).
103. Parkins, R.N., J. Iron Steel Inst. (London) 172, 149 (1952).
104. Schroeder, W.C., discussion, Trans. A.S.M.E. 66, 117 (1944).
105. Ref. (17), p. 3.
106. Logan, H.L., Ref. (13), p. 295.
107. Parkins, R.N., and Brown, A., J. Iron Steel Inst. (London) 193, 45 (1959).
108. Uhlig, H.H., and White, R.A., Trans. Am. Soc. Metals 52, 830 (1960).
109. Van Rooyen, D., Ref. (15), p. 309.
110. Nielsen, N.A., Ref. (13), p. 121.
111. Lang, F.S., Corrosion 18, 378t (1962).
112. Copson, H.R., Ref. (13), p. 247.
113. Copson, H.R., Ref. (15), p. 328.
114. Gulbransen, E.A., and Copan, T.P., Ref. (13), p. 155.
115. Phelps, E.H., and Loginow, A.W., Corrosion 16, 325t (1960).



116. McGlasson, R.L., and Greathouse, W.D., Corrosion 15, 437t (1959).
117. Fraser, J.P., and Eldredge, G.G., Corrosion 14, 524t (1958).
118. Fraser, J.P., Eldredge, G.G., and Treseder, R.S., Corrosion 14, 517t (1958).
119. Rocha, H.J., Tech. Mitt. Krupp A. Forschungsber. 5, 1 (1942).
120. Pickering, H.W., Beck, F.H., and Fontana, M.G., Corrosion 18, 230t (1962).
121. Williams, W.L., and Eckel, J.F., J. Am. Soc. Naval Engrs. 68, 93 (1956).
122. Edeleanu, C., J. Iron Steel Inst. (London) 175, 390 (1953).
123. Leu, K.W., and Helle, J.N., Corrosion 14, 249 (1958).
124. Graf, L., Z. Metallk. 38, 193 (1947).
125. Bobylev, A.V., Corrosion Cracking of Brass, Metallurgizdat, Moscow (1955).
126. Rodda, J.L., and Edmunds, G., Metal Progr. 47, 505 (1945).
127. Cook, M., Ref. (86), p. 73.
128. Edmunds, G., Ref. (11), p. 67.
129. Lynes, W., Proc. A.S.T.M. 41, 859 (1941).
130. Price, W.B., Ref. (11), p. 194.
131. Bobylev, A.V., Ref. (20), p. 298.
132. Crampton, D.K., Trans. A.I.M.E. 89, 233 (1930).
133. Ref. (22), p. 72.
134. Wasserman, G., Z. Metallk. 39, 66 (1948).
135. Heidenreich, R.D., Gerould, G.H., and McNulty, R.E., Trans. A.I.M.E. 166, 15 (1946).





136. Pardue, W.M., Beck, F.H., and Fontana, M.G., Trans. Am. Soc. Metals 54, 539 (1961).
137. Priest, D.K., Beck, F.H., and Fontana, M.G., Trans. Am. Soc. Metals 47, 473 (1955).
138. Priest, D.K., Ref. (12), p. 81.
139. Matthaes, K., Z. Metallk. 47, 37 (1946).
140. Grogan, J.D., and Pleasance, R.J., J. Inst. Metals 64, 57 (1939).
141. Chaudron, G., Herenguel, J., and Lacombe, P., Compt. Rend. 218, 404 (1944).
142. Perryman, E.C.W., and Blade, J.C., J. Inst. Metals 77, 263 (1950).
143. Yannaquis, N., and Lacombe, P., Compt. Rend. 226, 498 (1948).
144. Perryman, E.C.W., Ref. (12), p. 61.
145. Champion, F.A., J. Inst. Metals 83, 385 (1954-55).
146. Chadwick, R., Muir, N.B., and Grainger, H.B., J. Inst. Metals 85, 161 (1956-57).
147. Edeleanu, C., J. Inst. Metals 80, 187 (1951-52).
148. Brenner, P., and Roth, W., J. Inst. Metals 74, 159 (1948).
149. Perryman E.C.W., and Hadden, S. E., J. Inst. Metals 77, 207 (1950).
150. Ref. (22), p. 74.
151. Herenguel, J., Rev. Met. 44, 77 (1947).
152. Brenner, P., Z. Metallk. 44, 85 (1953).
153. Gilbert, P.T., and Hadden, S.E., J. Inst. Metals 77, 237 (1950).
154. Gruhl, W., Z. Metallk. 53, 670 (1962).
155. Johnston, R.G., Sheet Metal Inds. 14, 1197 (1940).



156. Thompson, D.H., Corrosion 15, 433t (1959).
157. Jevons, J.D., The Metallurgy of Deep Drawing and Pressing, Wiley, New York (1940), pps. 161-177.
158. Morris, A., Ref. (34), p. 212.
159. Grimston, F.S., J. Inst. Metals 39, 255 (1928).
160. Shreider, A.V., J. Appl. Chem. (U.S.S.R.) 30, 836 (1957).
161. Loginow, A.W., and Phelps, E.H., Corrosion 18, 299t (1962).
162. Ref. (22), p. 104.
163. Rostoker, W., McCaughey, J.M., and Markus, H., Embrittlement by Liquid Metals, Reinhold, New York (1960).
164. Edmunds, G., Anderson, E.A., and Waring, R.K., Ref. (11), p. 7.
165. Skorchelletti, V.V., and Titova, V.A., J. Appl. Chem. (U.S.S.R.) 26, 37 (1953).
166. Rask, S., Recent Advances in Stress Corrosion, A. Bresle, ed., Bulletin No. 25 of the Corrosion Committee of the Royal Swedish Academy of Engineering Sciences, Stockholm (1961), p. 81.
167. Mattsson, E., Ref.(14), p. 132.
168. Mattsson, E., Electrochimica Acta 3, 279 (1961).
169. Mukaibo, T., and Fueki, K., J. Electrochem. Soc. Japan 22 11, 59 (1954).
170. Forty, A.J., and Humble, P., Phil. Mag. 8, 247 (1963).
171. Tyler, W.P., and Brown, W.E., Anal. Chem. 15, 520 (1943).
172. Bjerrum, J., Ballhausen, C.J., and Jorgensen, C.K., Acta Chem. Scand. 8, 1275 (1954).
173. Hoar, T.P., Corrosion 19, 331t (1963).



174. Kubaschewski, O., and Hopkins, B.E., Oxidation of Metals and Alloys, Butterworths, London (1962), p. 252.
175. Miller, G.T., Jr., and Lawless, K.R., J. Electrochem. Soc. 106, 854 (1959).
176. Kruger, J., J. Electrochem. Soc. 106, 847 (1959).
177. Takahashi, N., and Trillat, J.J., Acta Met. 4, 201 (1956).
178. Bjerrum, J., Metal Ammine Formation in Aqueous Solution, P. Haase, Copenhagen (1957), pps. 114 - 127.
179. Nichols, H., and Rostoker, W., Trans. Am. Soc. Metals 56, 494 (1963).
180. Halpern, J., Trans. A.I.M.E. 9, 280 (1957).
181. Dix, E.H., Jr., Proc. A.S.T.M. 41, 928 (1941).
182. Lu, B. C.-Y., and Graydon, W.F., J. Am. Chem. Soc. 77, 6136 (1955).
183. Ref. (22), p. 94.
184. Coleman, E.G., Weinstein, D., and Rostoker, W., Acta Met. 9, 491 (1961).
185. Hopkins, B.E., Precipitation Processes in Steels, Iron and Steel Institute, London (1959), p. 137.
186. McLean, D., Mechanical Properties of Metals, Wiley, New York (1962), p. 383.
187. Uhlig, H.H., Corrosion and Corrosion Control, Wiley, New York, (1963), p. 119.
188. Taylor, J.W., J. Inst. Metals 86, 456 (1957-58).
189. Speiser, R., and Spretnak, J.W., Ref. (12), p. 92.
190. Frost, A. A., and Pearson, R.G., Kinetics and Mechanism, Wiley, New York (1961), p. 42.





191. Booker, C.J.L., unpublished work.
192. Kondrat'ev, A.N., Metalloved. i Obrabotka Metal. No. 12, 45 (1958).
193. Read, T.A., Reed, J.B., and Rosenthal, H., Ref. (11), p. 90.
194. Graf, L., and Lacour, H.R., Z. Metallk. 51, 152 (1960).
195. Pourbaix, M.J.N., Thermodynamics of Dilute Aqueous Solutions, Edward Arnold, London (1949).
196. Pourbaix, M.J.N., Atlas of Potential/pH Diagrams, Pergamon, Oxford (1962).
197. Latimer, W.M., Oxidation Potentials, 2nd. ed., Prentice-Hall, Englewood Cliffs (1952).
198. Stability Constants, Part II: Inorganic Ligands, The Chemical Society, London (1958).
199. Sager, G.F., Brown, R.H., and Mears, R.B., Ref. (11), p. 255.
200. Sidorov, V.P., and Ryabchenkov, A.V., Metalloved. i Obrabotka Metal. No. 6, 25 (1958).
201. Bakish, R., and Robertson, W.D., J. Electrochem. Soc. 103, 320 (1956).
202. Logan, H.L., and Perryman, E.C.W., separate private communications to Bakish and Robertson, Ref. (201).
203. Hoar, T.P., and Hines, J.G., Proc. 8th Meeting C.I.T.C.E. Madrid 1956, Butterworths, London (1958), p. 273.
204. Hines, J.G., Corrosion Science 1, 2 (1961).
205. Barnartt, S., and van Rooyen, D., J. Electrochem. Soc. 108, 222 (1961).
206. Barnartt, S., Stickler, R., and van Rooyen, D., Corrosion Science 3, 9 (1963).
207. Engell, H.-J., and Baumel, A., Ref. (13), p. 341.



208. Szklarska-Smialowska, Z., Ref. (16).
209. Winterstein, M.G., McDonald, H.J., and Waber, J.T.,  
Welding J. (N.Y.) 26, 723s (1947).
210. Logan, H.L., J. Research N.B.S. 66C, 347 (1962).
211. Logan, H.L., J. Research N.B.S. 61, 503 (1958).
212. Hines, J.G., and Hoar, T.P., J. Appl. Chem. (London) 8,  
764 (1958).
213. Bhatt, H.J., and Phelps, H., Corrosion 17, 430t (1961).
214. Logan, H.L., Welding J. (N.Y.) 37, 463s (1958).
215. Romanov, V.V., and Dobrolyubov, V.V., Metalloved. i  
Obrabotka Metal., No. 7, 19 (1958).
216. Uhlig, H.H., and Lincoln, J., Jr., J. Electrochem. Soc.  
105, 325 (1958).
217. Ryabchenkov, A.V., and Nikiforova, V. M., Ref. (20), p. 161.
218. Parkins, R.N., and Usher, R., Ref. (15), p. 289.
219. Berk, A.A., and Waldek, W.F., Chem. Eng. 57, No. 6, 235 (1950).
220. McGlasson, R.L., Greathouse, W.D., and Hudgins, C.M.,  
Corrosion 16, 557t (1961).
221. Strauss, M.B., and Bloom, M.C., Corrosion 16, 553t (1961).
222. Radeker, W., and Grafen, H., Stahl u. Eisen 76, 1616 (1956).
223. Hudgins, C.M., McGlasson, R.L., and Rosborough, W.M., Ref. (16).
224. Loginow, A.W., and Phelps, E.H., Corrosion 18, 299t (1962).
225. Berg, S., and Henrikson, S., Jernkont. Ann. 144, 392 (1960).
226. Brennert, S., and Nathorst, H., Jernkont. Ann. 140, 839 (1956).



- 227. Scharfstein, L.R., and Brindley, W.F., Corrosion 14, 588t (1958).
- 228. Logan, H.L., McBee, M.J., and Romanoff, M., Mat. Res. and Standards 3, 635 (1963).
- 229. Staehle, R.W., Beck, F.H., and Fontana, M.G., Corrosion 15, 373t (1959).
- 230. Bhatt, H.J., and Phelps, E.H., Corrosion 17, 430t (1961).
- 231. Edeleanu, C., J. Iron Steel Inst. (London) 173, 140 (1953).
- 232. Hines, J.G., and Jones, E.R.W., Corrosion Science 1, 88 (1961).
- 233. Scheil, M.A., Ref. (11), p. 395.
- 234. Hawkes, H.P., Beck, F.H., and Fontana, M.G., Corrosion 19, 249t (1963).
- 235. Van Rooyen, D., Corrosion 17, 421t (1961).
- 236. Reed, R.E., and Paxton, H.W., Ref. (15), p. 301.
- 237. Wassermann, G., Z. Metallk. 34, 297 (1942).
- 238. Edeleanu, C., and Forty, A.J., Phil. Mag. 5, 1029 (1960).
- 239. Bakish, R., and Robertson, W.D., Acta Met. 4, 342 (1956).
- 240. Logan, H.L., J. Research N.B.S. 56, 159 (1956).
- 241. Kirk, W.W., Beck, F.H., and Fontana, M.G., Ref. (13), p. 227.
- 242. Hoar, T.P., and West, J.M., Nature 181, 835 (1958).
- 243. West, J.M., Nature 185, 92 (1960).
- 244. Forty, A.J., Teknisk-Vetenskaplig Forskning 32, 104 (1961).
- 245. Logan, H.L., J. Research N.B.S. 48, 99 (1961).
- 246. Uhlig, H.H., and Sava, J., Trans. Am. Soc. Metals 56, 361 (1963).





- 247. Pickering, H.W., and Swann, P.R., Corrosion 19, 373t (1963).
- 248. Swann, P.R., and Nutting, J., J. Inst. Metals 88, 478 (1959-60).
- 249. Robertson, W.D., and Tetelman, A.S., Strengthening Mechanisms in Solids, A.S.M., Metals Park (1962), p. 217.
- 250. Swann, P.R., Corrosion 19, 102t (1963).
- 251. Douglass, D.L., Thomas, G., and Roser, W.R., Corrosion 20, 15t (1964).
- 252. Swann, P.R., and Pickering, H.W., Corrosion 19, 369t (1963).
- 253. Likhtman, V.I., Rehbinder, P.A., and Karpenko, G.V., Effect of a Surface-Active Medium on the Deformation of Metals, Her Majesty's Stationery Office, London (1958).
- 254. Backensto, E.B., and Yurick, A.N., Corrosion 18, 169t (1962).
- 255. Nichols, H., and Rostoker, W., Acta Met. 8, 788, 848 (1960).
- 256. Orowan, E., Welding J. (N.Y.) 34, 157s (1955).



## APPENDIX A

## DESCRIPTION OF MAJOR VACUUM SYSTEM COMPONENTS

(Notation refers to Figs. 4 and 8)

|  |                             |  |
|--|-----------------------------|--|
| $P_1$                                    | Rotary Vacuum Pump          | - Cenco Hyvac, Model 14<br>- 1.05 liters/sec capacity at<br>1 micron Hg  |
| $P_2$                                    | Oil Fractionation Pump      | - Consolidated Vacuum Corp.,<br>Model GF-25<br>- three-stage, all-glass, water-<br>cooled fractionation type, using<br>Octoil-S<br>- 25 liters/sec pumping speed |
| $P_3$                                    | Rotary Vacuum Pump          | - Cenco Hyvac, Model 7<br>- .525 liters/sec capacity<br>at 1 micron Hg   |
| $G_1$ and $G_3$                          | Thermocouple<br>Gauge Tubes | - Veeco Type DV-1M   |
| $G_2$                                    | Ionization Gauge Tube       | - Veeco Type RG-75<br>- inverted Bayard-Alpert gauge<br>with thoria-coated iridium filament  |
| Control Unit for $G_1$ , $G_2$ and $G_3$ |                             | - Veeco Type RG31-A  |
| L.D. Leak Detector                       |                             | - Edwards Palladium Barrier<br>Leak Detector, Model LT4A<br>- Type P.L.2 gauge head  |



## APPENDIX B

CALCULATION OF  $\bar{n}$ , THE AVERAGE LIGAND NUMBER

The stepwise formation of a complex species  $ML_n$  formed in solution from a metal ion  $M$  and a ligand  $L$  is represented by the equilibrium reaction



One of the methods for the determination of the equilibrium constants for such reactions makes use of the average ligand number  $\bar{n}$ , which is given by

$$\bar{n} = \frac{C_L - [L]}{C_M} \quad \dots(B)$$

where  $C_L$  and  $C_M$  are the total concentrations of ligand and metal ion in the system, and  $[L]$  is the concentration of free ligand. The calculation of  $\bar{n}$  in metal- $NH_3$ - $H_2O$  systems is taken from Bjerrum:<sup>(178)</sup>

For a solution of copper ions in an ammoniacal salt solution, equation (B) becomes

$$\bar{n} = \frac{C_{NH_3} - [NH_3]}{C_{Cu}} \quad \dots(C)$$

Here,  $C_{Cu}$  = stoichiometric concentration of dissolved copper,  $C_{NH_3}$  = stoichiometric concentration of  $NH_3$  added as ammonium hydroxide, and  $NH_3$  = concentration of free ammonia, which can be calculated from the equation

$$[NH_3] = k_{NH_4^+} \cdot \frac{[NH_4^+]}{[H^+]} \quad \dots(D)$$





where  $k_{\text{NH}_4^+} = 2.43 \times 10^{-10}$ , is the acid dissociation constant of the ammonium ion,  $[\text{NH}_4^+]$  is the stoichiometric concentration of the ammonium salt, and  $[\text{H}^+]$  is the hydrogen ion concentration. In the solutions used in the present work, known amounts of copper sulfate solution and ammonium sulfate solution were mixed together, and the pH adjusted to the desired value by additions of a standardized  $\text{NH}_4\text{OH}$  solution from a burette. The value of  $\bar{n}$  was then calculated by substituting the proper values in equations (C) and (D) above.



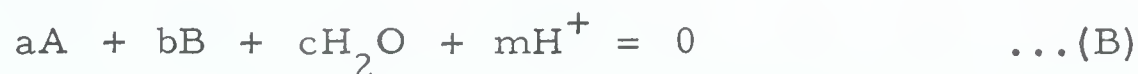
## APPENDIX C

## CONSTRUCTION OF pH/POTENTIAL DIAGRAMS

The principles involved in the construction of pH/potential diagrams for metal/water systems and some ternary systems have been developed by Pourbaix and co-workers.<sup>(195)(196)</sup> Briefly, all the various equilibria which occur in aqueous solution are written to conform to the general equation



For reactions without oxidation, reaction (A) is written (with all terms collected to one side) as



For this reaction, the relation between pH and concentration of reactants and products is given by

$$a \log [A] + b \log [B] = \log K + m \text{ pH} \quad \dots(C)$$

where the square brackets denote concentration (more exactly, activity) of A and B, and the equilibrium constant K is given by

$$\log K = - \frac{\sum \nu \mu^\circ}{1363} \quad \dots(D)$$

$$\text{or } \log K = - \frac{a\mu^\circ_A + b\mu^\circ_B + c\mu^\circ_{H_2O} + m\mu^\circ_{H^+}}{1363} \quad \dots(D)$$

where  $\nu$  = stoichiometric coefficient (given the proper sign) and

$\mu^\circ$  = standard molar chemical potential at 25°C.



For reactions with oxidation, reaction (A) is written as



and the relationship between pH, potential and concentration of substances is given by

$$E = E^\circ - \frac{0.0591}{n} \text{ pH} + \frac{0.0591}{n} (a \log [A] + b \log [B]) \quad \dots(F)$$

where the standard potential  $E^\circ$  is

$$E^\circ = \frac{\sum v\mu^\circ}{23,060 n} \quad \dots(G)$$

$$\text{or } E^\circ = \frac{a\mu^\circ_A + b\mu^\circ_B + c\mu^\circ_{H_2O} + m\mu^\circ_{H^+}}{23,060 n} \quad \dots(G')$$

The following conventions are observed when plotting K vs. pH and

E vs. pH for equations (C) and (F):

- 1) For reactions without oxidation, the coefficients a and m are taken as positive, making b and c negative. The substance A is thus the more basic of the compounds involved, and appears to the right in the diagram.
- 2) For reactions with oxidation, a and n are taken as being positive, so that substance A is the more highly oxidized of the compounds involved, and thus appears above substance B in the diagram.

The values of  $E^\circ$ ,  $\mu^\circ$  and the equilibrium constants used in the construction of our diagrams are given in Table VII; they do not differ significantly from those used by Mattsson<sup>(168)</sup>.





Table VII

Constants used in pH/Potential Equations

1) Oxidation Potentials (IUPAC Convention)

|  | <u>Reference</u>  |
|--|---|
| $\text{Cu}^{++} + 2\text{e}^- = \text{Cu} \quad E^0 = +0.337\text{V}$  | $\left. \begin{array}{l} \\ \\ \\ \end{array} \right\} (197)$ |
| $\text{Cu}^+ + \text{e}^- = \text{Cu} \quad E^0 = +0.521\text{V}$      |   |
| $\text{Cu}^{++} + \text{e}^- = \text{Cu}^+ \quad E^0 = +0.153\text{V}$ |   |
| $\text{Zn}^{++} + 2\text{e}^- = \text{Zn} \quad E^0 = -0.763\text{V}$  |   |

2) Equilibrium Constants

$$\beta_n = \frac{[\text{ML}_n]}{[\text{M}] [\text{L}]^n}$$

| <u>Complex</u>                  | <u>log <math>\beta_n</math></u> |  |
|---------------------------------|---------------------------------|--|
| $\text{Cu}(\text{NH}_3)^+$      | 5.93                            | $\left. \begin{array}{l} \\ \end{array} \right\} (198)$          |
| $\text{Cu}(\text{NH}_3)_2^+$    | 10.86                           |  |
| $\text{Cu}(\text{NH}_3)^{++}$   | 4.18                            | $\left. \begin{array}{l} \\ \\ \\ \\ \end{array} \right\} (178)$ |
| $\text{Cu}(\text{NH}_3)_2^{++}$ | 7.71                            |  |
| $\text{Cu}(\text{NH}_3)_3^{++}$ | 10.63                           |  |
| $\text{Cu}(\text{NH}_3)_4^{++}$ | 12.79                           |  |
| $\text{Zn}(\text{NH}_3)_3^{++}$ | 7.28                            |  |
| $\text{Zn}(\text{NH}_3)_4^{++}$ | 9.42                            |  |

$$\text{pK}_{\text{NH}_4^+} = 9.164 \quad @ \quad 22^\circ\text{C} \quad (2\text{MNH}_4\text{NO}_3)$$

Table 1

Summary of the data for the first part of the study

Table 1 shows the results of the first part of the study

Table 1

|         |      |     |       |
|---------|------|-----|-------|
| Group   | Mean | SD  | Range |
| Group 1 | 10.5 | 2.5 | 8-15  |
| Group 2 | 12.0 | 3.0 | 9-18  |
| Group 3 | 11.0 | 2.0 | 9-16  |
| Group 4 | 10.0 | 1.5 | 8-14  |

Table 1 shows the results of the first part of the study

|         |      |     |       |
|---------|------|-----|-------|
| Group   | Mean | SD  | Range |
| Group 1 | 10.5 | 2.5 | 8-15  |
| Group 2 | 12.0 | 3.0 | 9-18  |
| Group 3 | 11.0 | 2.0 | 9-16  |
| Group 4 | 10.0 | 1.5 | 8-14  |
| Group 5 | 11.5 | 2.2 | 9-17  |
| Group 6 | 10.8 | 1.8 | 8-15  |
| Group 7 | 11.2 | 2.1 | 9-16  |
| Group 8 | 10.3 | 1.6 | 8-14  |

Table 1 shows the results of the first part of the study

Table 1 shows the results of the first part of the study

Table VII (cont'd)

3) Molar standard chemical potentials, kcals @ 25°C.

| <u>Substance</u>                                | <u>State</u> | <u><math>\mu^\circ</math></u> | <u>Reference</u>                         |
|---|--------------|-------------------------------|--|
| H <sup>+</sup>                                  | aq           | 0                             | (197)                                    |
| NH <sub>3</sub>                                 | aq           | -6.36                         |  |
| NH <sub>4</sub> <sup>+</sup>                    | aq           | -19.00                        |  |
| Cu <sup>+</sup>                                 | aq           | +12.01                        |  |
| Cu <sup>++</sup>                                | aq           | +15.53                        |  |
| Cu  | Solid        | -30.4                         |  |
| Cu <sub>2</sub> O                               | Solid        | -34.98                        |  |
| Cu  | Solid        | 0                             |  |
| Zn  | Solid        | 0                             |  |
| Zn <sup>++</sup>                                | aq           | -35.184                       |  |
| ZnO   | Solid        | -76.05                        | Calculated from<br>equilibrium constants |
| Cu(NH <sub>3</sub> ) <sup>+</sup>               | aq           | - 2.45                        |  |
| Cu(NH <sub>3</sub> ) <sub>2</sub> <sup>+</sup>  | aq           | -15.54                        |  |
| Cu(NH <sub>3</sub> ) <sup>++</sup>              | aq           | + 3.47                        |  |
| Cu(NH <sub>3</sub> ) <sub>2</sub> <sup>++</sup> | aq           | - 7.71                        |  |
| Cu(NH <sub>3</sub> ) <sub>3</sub> <sup>++</sup> | aq           | -18.05                        |  |
| Cu(NH <sub>3</sub> ) <sub>4</sub> <sup>++</sup> | aq           | -27.36                        |  |
| Zn(NH <sub>3</sub> ) <sub>3</sub> <sup>++</sup> | aq           | -64.20                        |  |
| Zn(NH <sub>3</sub> ) <sub>4</sub> <sup>++</sup> | aq           | -73.48                        |  |



The following chemical reactions and corresponding pH/potential equations were used in constructing Figs. 25b, 26b and 27b. (The equation numbers correspond to the numbers on the lines in the "b" diagrams):



$$E = 0.153 + 0.0591 \log [\text{Cu}^{++}]/[\text{Cu}^{+}]$$



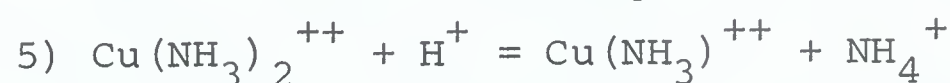
$$E = -0.044 + 0.0591 \text{ pH} + 0.0591 \log [\text{NH}_4^{+}] + 0.0591 \log \frac{[\text{Cu}^{++}]}{[\text{Cu}(\text{NH}_3)^{+}]}$$



$$E = -0.301 + 0.118 \text{ pH} + 0.118 \log [\text{NH}_4^{+}] + 0.0591 \log \frac{[\text{Cu}^{++}]}{[\text{Cu}(\text{NH}_3)_2^{+}]}$$



$$\text{pH} = 5.09 - \log [\text{NH}_4^{+}] + \log [\text{Cu}(\text{NH}_3)^{++}]/[\text{Cu}^{++}]$$



$$\text{pH} = 5.74 - \log [\text{NH}_4^{+}] + \log [\text{Cu}(\text{NH}_3)_2^{++}]/[\text{Cu}(\text{NH}_3)^{++}]$$



$$\text{pH} = 6.35 - \log [\text{NH}_4^{+}] + \log [\text{Cu}(\text{NH}_3)_3^{++}]/[\text{Cu}(\text{NH}_3)_2^{++}]$$



$$\text{pH} = 7.11 - \log [\text{NH}_4^{+}] + \log [\text{Cu}(\text{NH}_3)_4^{++}]/[\text{Cu}(\text{NH}_3)_3^{++}]$$



$$E = 0.0591 \text{ pH} + 0.0591 \log [\text{NH}_4^{+}] + 0.0591 \log \frac{[\text{Cu}(\text{NH}_3)^{++}]}{[\text{Cu}(\text{NH}_3)_2^{+}]}$$



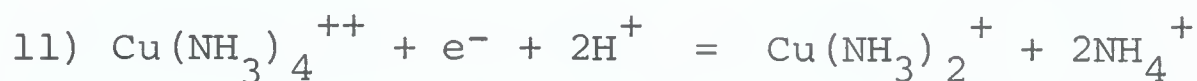




$$E = 0.340 + 0.0591 \log [\text{Cu}(\text{NH}_3)_2^{++}] / [\text{Cu}(\text{NH}_3)_2^+]$$



$$E = 0.715 - 0.0591 \text{ pH} - 0.0591 \log [\text{NH}_4^+] + 0.0591 \log [\text{Cu}(\text{NH}_3)_3^{++}] / [\text{Cu}(\text{NH}_3)_2^+]$$



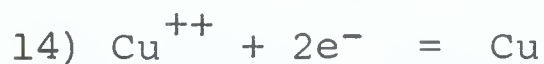
$$E = 1.135 - 0.118 \text{ pH} - 0.118 \log [\text{NH}_4^+] + 0.0591 \log [\text{Cu}(\text{NH}_3)_4^{++}] / [\text{Cu}(\text{NH}_3)_2^+]$$



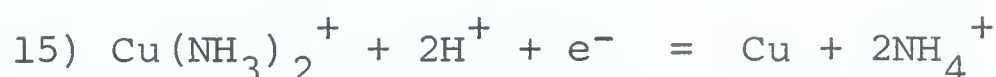
$$\text{pH} = 3.33 + \log [\text{Cu}(\text{NH}_3)^+] / [\text{Cu}^+] - \log [\text{NH}_4^+]$$



$$\text{pH} = 4.34 - \log [\text{NH}_4^+] + \log [\text{Cu}(\text{NH}_3)_2^+] / [\text{Cu}(\text{NH}_3)^+]$$



$$E = 0.337 + 0.0295 \log [\text{Cu}^{++}]$$



$$E = 0.972 - 0.118 \text{ pH} - 0.118 \log [\text{NH}_4^+] + 0.0591 \log [\text{Cu}(\text{NH}_3)_2^+]$$



$$\text{pH} = 10.35 + 2 \log [\text{NH}_3] - 0.5 \log [\text{Cu}(\text{NH}_3)_4^{++}]$$



$$\text{pH} = 10.03 + 2 \log [\text{NH}_3] - \log [\text{Cu}(\text{NH}_3)_2^+]$$



$$E = 1.262 - 0.118 \text{ pH} + 0.118 \log [\text{NH}_3] - 0.0591 \log [\text{Cu}(\text{NH}_3)_2^+]$$

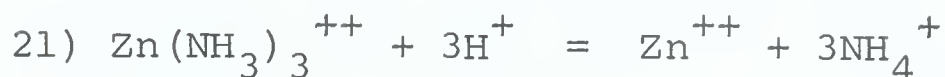




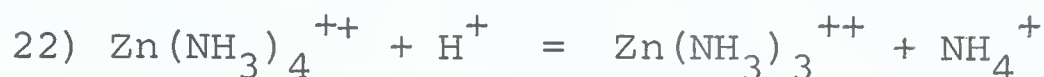
$$E = 0.669 - 0.0591 \text{ pH}$$



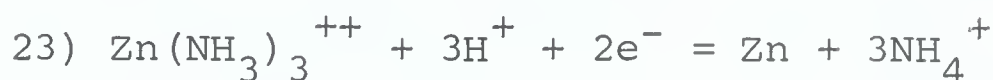
$$E = -0.763 + 0.0295 \log [\text{Zn}^{++}]$$



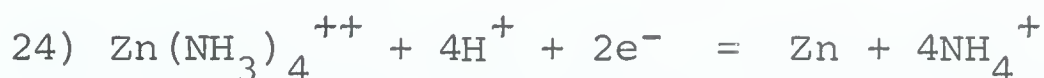
$$\text{pH} = 6.83 + 0.333 \log [\text{Zn}(\text{NH}_3)_3^{++}] / [\text{Zn}^{++}] - \log [\text{NH}_4^+]$$



$$\text{pH} = 7.13 - \log [\text{NH}_4^+] + \log [\text{Zn}(\text{NH}_3)_4^{++}] / [\text{Zn}(\text{NH}_3)_3^{++}]$$



$$E = -0.156 - 0.089 \text{ pH} - 0.089 \log [\text{NH}_4^+] + 0.0295 \log [\text{Zn}(\text{NH}_3)_3^{++}]$$



$$E = 0.055 - 0.118 \text{ pH} - 0.118 \log [\text{NH}_4^+] + 0.0295 \log [\text{Zn}(\text{NH}_3)_4^{++}]$$

The lines represented by equations (1) - (24) were plotted by substituting the following concentrations in the appropriate equations: 0.05M total dissolved copper, 0.001M total dissolved zinc, and 1.0M total dissolved ammonia ( $\text{NH}_3$  plus  $\text{NH}_4^+$ ). Figs. 25a, 26a and 27a are taken from Mattsson's paper; the numbered lines correspond to his equations. The important differences between his and our diagrams are:

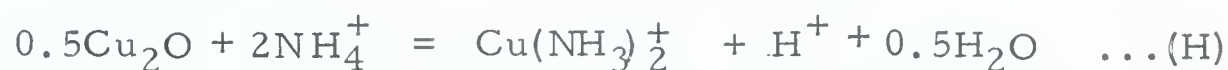
- a) We have modified Fig. 25a to show the stepwise addition of  $\text{NH}_3$  ligands (our equations 4, 5, 6, 7, 12 and 13); Mattsson's diagram is not



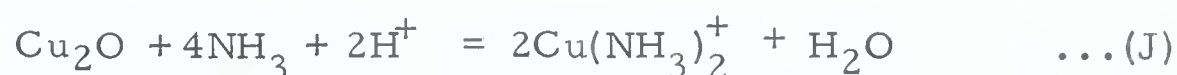
incorrect in this respect, but does not clearly show the important regions where intermediate complexes are stable.

b) In Fig. 26a, Mattsson shows a region of stability for the solid phase  $\text{Cu}(\text{SO}_4)_{0.25}(\text{OH})_{1.5}$ . This precipitate did not form in our test solutions, so it is not included in Fig. 26b.

c) Fig. 26a shows a stability region for  $\text{Cu}_2\text{O}$  which is incorrectly located. Mattsson's equation 15 was written as



It is clear from the general equation (A) given at the beginning of this appendix that his equation does not conform to the conventions used in constructing these diagrams, since his equation has both hydrogen ions and water on the same side of the equation, when they should appear on opposite sides, i.e. with stoichiometric coefficients of opposite sign. The equation is properly written as



which is our equation (17). Then, according to convention,  $\text{Cu}_2\text{O}$  is more basic than  $\text{Cu}(\text{NH}_3)_2^+$  and should appear to the right of  $\text{Cu}(\text{NH}_3)_2^+$  as shown in Fig. 26b. Reaction (J) can also be justified as taking precedence over reaction (H) on thermodynamic grounds, since the free energy change for reaction (J) is -27.4 kcals/mole compared with -23.2 kcals/mole for reaction (H). This latter figure is calculated after rewriting (H) as

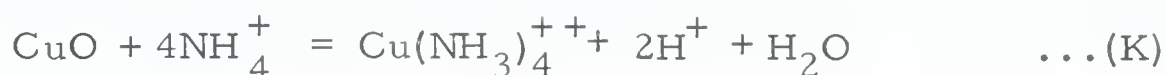




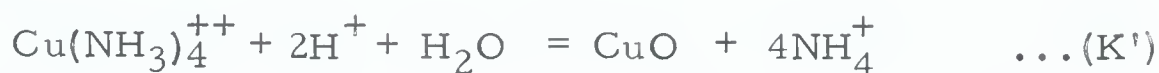


in order to make the stoichiometry equal to (J), and to conform with the convention in which the coefficient of the hydrogen ion is taken as being positive (reaction (H) as written has a positive free energy change).

- d) The region shown for the stability of CuO in Fig. 26a is also incorrect, for the same reasons as discussed above. Mattsson's equation (11) is



and, if written in the reverse order to give it a negative free energy change, becomes,



The correct equation, shown as line 16 in Fig. 26b is

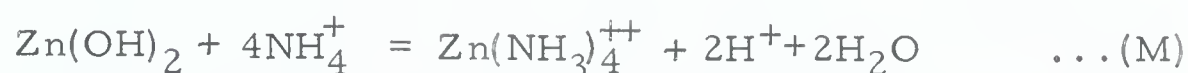


Here, too, a comparison of the free energies of the reactions shows that (L) is favored over (K') (-28.2 kcals/mole vs -22.4 kcals/mole, respectively). Halpern<sup>(180)</sup> has published a diagram of the Cu-NH<sub>3</sub>-H<sub>2</sub>O system in which the CuO region is located far to the right as we have shown in Fig. 26b; his diagram is calculated for dissolved copper concentrations of 10<sup>-6</sup>M, so the absolute positions of the lines are different from ours, but the relative position of the CuO and Cu(NH<sub>3</sub>)<sub>4</sub><sup>++</sup> is in accordance with our calculations.

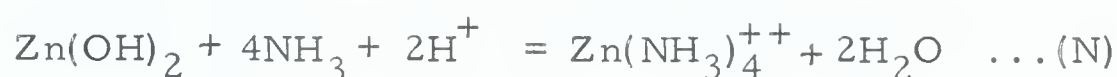


e) Finally, in Fig. 27a , the region of stability of  $\text{Zn(OH)}_2$  is incorrectly predicted, again for the same reasons as discussed before.

Mattsson's equation (19) is



which has a free energy change of 21.74 kcal/mole; the correct equation is



which is not shown in Fig. 27b because the line separating the

$\text{Zn(OH)}_2 / \text{Zn(NH}_3)_4^{++}$  regions occurs at a pH of 13.

Incidentally it should be pointed out that the stepwise formation of the zinc-ammine complexes is not ignored in Fig. 27b , but the uptake of the first three  $\text{NH}_3$  ligands occurs over such a narrow pH range that the separate regions could not be shown on the pH scale used. For this reason, only line 21 is included in the diagram.







**B29820**